

**University of Alberta**

*Thaw Induced Axle Load Limitations*

by

*Guðjón Örn Björnsson*

A thesis submitted to the Faculty of Graduate Studies and Research in partial fulfillment of  
the of the requirements for the degree of *Master of Science*

in

*Geotechnical Engineering*

Department of *Civil and Environmental Engineering*

Edmonton, Alberta

*Fall 2006*

# University of Alberta

## Library Release Form

**Name of Author:** *Guðjón Örn Björnsson*

**Title of Thesis:** *Thaw Induced Axle Load Limitations*

**Degree:** *Master of Science*

**Year this Degree Granted:** *2006*

Permission is hereby granted to the University of Alberta Library to reproduce single copies of this thesis and to lend or sell such copies for private, scholarly or scientific research purposes only.

The author reserves all other publication and other rights in association with the copyright in the thesis, and except as herein before provided, neither the thesis nor any substantial portion thereof may be printed or otherwise reproduced in any material form whatsoever without the author's prior written permission.

---

*Signature*

# University of Alberta

## Faculty of Graduate Studies and Research

The undersigned certify that they have read, and recommend to the Faculty of Graduate Studies and Research for acceptance, a thesis entitled **Thaw Induced Axle Load Limitations** submitted by Guðjón Örn Björnsson in partial fulfillment of the requirements for the degree of Master of Science in Geotechnical Engineering.

---

Dr. David Segó

---

Dr. Sigurður Erlingsson

---

Dr. Kevin Biggar

---

Dr. Hamid Soleymani

---

Dr. Douglas Schmitt

*June 1<sup>st</sup>, 2006*

## **ABSTRACT**

This thesis analyzed road conditions during spring thaw and considered how these conditions affect axle load limitations for roads in Iceland. The data for this project relied on information collected by the Icelandic Road Administration (ICERA). ICERA provided measurements for air temperatures, and profiles for roadbed moisture content, road temperatures and electrical conductivity. Because the road conditions were known, it offered an opportunity to evaluate the suitability of methodologies to impose and/or remove spring load restrictions (SLR) developed by various road administration agencies. A comparative analysis of moisture content and electrical conductivity supported the idea of using the latter to guide the decision of imposing SLR

Comparing measured and predicted temperature profiles determined the thermal properties of a road section, which were then analyzed by Temp/W and refined and re-analyzed until predictions reproduced measured temperature profiles. The thermal properties used in this process were consistent with published or calculated values. Although this approach could be improved, it effectively predicted temperature profiles.

**Key words:** axle load limitations, spring thaw, road, electrical conductivity, moisture content, falling weight deflection test.

**University of Alberta**

*Thaw Induced Axle Load Limitations*

by

*Guðjón Örn Björnsson*

A thesis submitted to the Faculty of Graduate Studies and Research in partial fulfillment of  
the of the requirements for the degree of *Master of Science*

in

*Geotechnical Engineering*

Department of *Civil and Environmental Engineering*

Edmonton, Alberta

*Fall 2006*

# University of Alberta

## Library Release Form

**Name of Author:** *Guðjón Örn Björnsson*

**Title of Thesis:** *Thaw Induced Axle Load Limitations*

**Degree:** *Master of Science*

**Year this Degree Granted:** *2006*

Permission is hereby granted to the University of Alberta Library to reproduce single copies of this thesis and to lend or sell such copies for private, scholarly or scientific research purposes only.

The author reserves all other publication and other rights in association with the copyright in the thesis, and except as herein before provided, neither the thesis nor any substantial portion thereof may be printed or otherwise reproduced in any material form whatsoever without the author's prior written permission.

---

*Signature*

# University of Alberta

## Faculty of Graduate Studies and Research

The undersigned certify that they have read, and recommend to the Faculty of Graduate Studies and Research for acceptance, a thesis entitled **Thaw Induced Axle Load Limitations** submitted by Guðjón Örn Björnsson in partial fulfillment of the requirements for the degree of Master of Science in Geotechnical Engineering.

---

Dr. David Segó

---

Dr. Sigurður Erlingsson

---

Dr. Kevin Biggar

---

Dr. Hamid Soleymani

---

Dr. Douglas Schmitt

*June 1<sup>st</sup>, 2006*

## **ACKNOWLEDGEMENTS**

I am grateful to my supervisors Dr. David C. Segó and Dr. Sigurður Erlingsson for their guidance, expertise and support throughout this project.

The Icelandic Road Administration generously supported this thesis by giving me access to the information they collected about Icelandic road conditions and providing me with financial support. Samskip provided additional funding for the duration of my study and for that I am thankful.

I thank all the professors, staff, and colleagues in the University of Alberta Geotechnical Group for a challenging, outstanding, and interesting graduate program that I have been fortunate to participate in for the last two years.

I want to offer thanks to the people who helped me editing and proof-reading the thesis in the final stages of its preparation.

I would like to thank my fiancé, Þorbjörg María, for her support, patience, encouragement and for constantly believing in me.

Finally I want to thank all my friends in Edmonton who made the last two years enjoyable and unforgettable.

# TABLE OF CONTENTS

<b>1.</b>	<b><u>INTRODUCTION</u></b>	<b>1</b>
1.1.	Background	1
1.2.	Examples of similar work	2
1.3.	Objectives	4
1.4.	Methodology	6
1.5.	The Organization of the thesis	7
1.6.	References	9
<b>2.</b>	<b><u>LITERATURE REVIEW</u></b>	<b>11</b>
2.1.	Introduction	11
2.2.	Measurement techniques	12
2.2.1.	Temperature profiles and air temperature	12
2.2.2.	Moisture content	13
2.2.3.	The electrical conductivity probe	14
2.2.4.	Falling Weight Deflectometer	15
2.2.5.	Frost Tubes	16
2.2.6.	Visual inspection	17
2.3.	Determining onset and removal times for SLR	17
2.3.1.	The Cost of axle load limitations compared to repair costs	20
2.4.	Material properties of frozen soil and asphalt	21
2.5.	Status reports from the project	23
2.5.1.	Southwest Iceland	24
2.5.2.	Northern Iceland	24
2.6.	Comparable projects	25
2.6.1.	Estimation of damage during spring thaw	27
2.6.2.	Calibration of FWD tests and moisture content	27
2.6.3.	SLR determined by temperature in the road section	28
2.6.4.	Determination of maximum allowable load	29
2.7.	Other literature related to the project	29
2.8.	References	32
2.9.	Figures	38
<b>3.</b>	<b><u>THEORY</u></b>	<b>39</b>
3.1.	Seasonal frozen pavements	39
3.1.1.	Variations from conventional geotechnical engineering	39
3.1.2.	Classification of frozen soil	42
3.1.3.	Frost susceptibility	43
3.1.4.	Thermal properties	44
3.1.4.1.	Heat flow - differential equation	44
3.1.4.2.	Heat capacity	46
3.1.4.3.	Latent heat of fusion	46
3.1.4.4.	Thermal expansion	47
3.2.	Freezing and thawing of a road section	47
3.2.1.	Heat flow in road sections	48
3.2.2.	Air temperature	49
3.2.3.	Freezing and thawing indices	50
3.2.4.	Insulation	52
3.2.5.	Frost penetration	52
3.3.	Icelandic weather conditions	54
3.4.	Axle load limitations	55
3.4.1.	The onset and removal of spring load restrictions	57
3.5.	Back calculated layer moduli	60

3.6.	<b>References</b>	<b>63</b>
3.7.	<b>Tables</b>	<b>66</b>
3.8.	<b>Figures</b>	<b>67</b>
<b>4.</b>	<b><u>DATA COLLECTED</u></b>	<b>70</b>
4.1.	<b>Monitoring data from Icelandic road sections</b>	<b>70</b>
4.2.	<b>Monitoring stations and description of test sites</b>	<b>71</b>
4.2.1.	Sections 1.4.1 and 1.4.2 in southwest Iceland	71
4.2.2.	Section 3.2.3.1 in southwest Iceland	72
4.2.3.	Dyrastadir in northern Iceland	72
4.2.4.	Vatnsskard in northern Iceland	73
4.2.5.	Blonduos in northern Iceland	73
4.2.6.	Saudarkrokur in northern Iceland	73
4.2.7.	Recently installed test sections at various locations	73
4.3.	<b>Data available</b>	<b>74</b>
4.3.1.	Data from test sections in southwest Iceland	74
4.3.2.	Data from test sections in northern Iceland	74
4.3.3.	Data from new test sections at various locations in Iceland	76
4.3.4.	Falling weight deflection	76
4.3.5.	Frost tubes	76
4.4.	<b>Description of testing equipment</b>	<b>77</b>
4.4.1.	TDR moisture content probes	77
4.4.2.	Campell scientific moisture content probes	79
4.4.3.	Electrical conductivity probe	80
4.4.4.	Calibration of the electrical conductivity probe	85
4.4.5.	Falling weight deflectometer test	86
4.4.6.	Frost tubes	86
4.5.	<b>The road cross-section</b>	<b>87</b>
4.6.	<b>Summary</b>	<b>89</b>
4.7.	<b>References</b>	<b>90</b>
4.8.	<b>Tables</b>	<b>92</b>
4.9.	<b>Figures</b>	<b>95</b>
<b>5.</b>	<b><u>IMPORTANT PARAMETERS</u></b>	<b>101</b>
5.1.	<b>Introduction</b>	<b>101</b>
5.2.	<b>Air temperature</b>	<b>102</b>
5.2.1.	Onset of spring load restrictions.	105
5.2.1.1.	Duration of Spring Load Restrictions	105
5.2.1.2.	Applicability of formulas	107
5.2.1.3.	Dyrastadir (2001-2002)	107
5.2.1.4.	Thingvellir (1998-1999)	109
5.2.2.	Air - and road temperature	111
5.2.3.	Heat distribution with depth	112
5.3.	<b>Moisture content</b>	<b>113</b>
5.3.1.	Moisture content compared to electrical conductivity	114
5.3.2.	Moisture content compared to temperature	118
5.4.	<b>Falling weight deflection tests.</b>	<b>121</b>
5.5.	<b>Summary</b>	<b>126</b>
5.6.	<b>References</b>	<b>127</b>
5.7.	<b>Tables</b>	<b>129</b>
5.8.	<b>Figures</b>	<b>130</b>
<b>6.</b>	<b><u>MODELING OF HEAT FLOW IN A ROAD SECTION</u></b>	<b>143</b>
6.1.	<b>Introduction</b>	<b>143</b>
6.2.	<b>Description of cases</b>	<b>146</b>
6.2.1.	Case 1	146
6.2.2.	Case 2	146

6.2.3.	Case 3	147
<b>6.3.</b>	<b>Variables</b>	<b>147</b>
6.3.1.	Assumptions used during model runs	148
6.3.2.	Thermal conductivity	149
6.3.3.	Function of unfrozen water content versus temperature	149
6.3.4.	Volumetric heat capacity	150
6.3.5.	Volumetric water content	150
6.3.6.	The thermal modifier function	151
<b>6.4.</b>	<b>Results</b>	<b>152</b>
6.4.1.	Estimation of error	152
6.4.2.	Thermal modifier function	153
6.4.3.	Thermal conductivity	154
6.4.4.	Function of unfrozen water content versus temperature	157
6.4.5.	Volumetric heat capacity	157
6.4.6.	Volumetric moisture content	159
<b>6.5.</b>	<b>Comparison of measured and predicted values</b>	<b>159</b>
<b>6.6.</b>	<b>Possible improvement</b>	<b>162</b>
<b>6.7.</b>	<b>Practical implications</b>	<b>163</b>
<b>6.8.</b>	<b>Reference</b>	<b>165</b>
<b>6.9.</b>	<b>Tables</b>	<b>166</b>
<b>6.10.</b>	<b>Figures</b>	<b>167</b>
<b>7.</b>	<b><u>SUMMARY AND CONCLUSIONS</u></b>	<b>176</b>
7.1.	Modeling	179
7.2.	Improvements and recommendations	181
7.3.	References	185
	<b>APPENDIX A - CLASSIFICATION OF FROZEN SOIL</b>	<b>186</b>
	<b>APPENDIX B - GRAIN SIZE DISTRIBUTIONS</b>	<b>187</b>
	<b>APPENDIX C - DYRASTADIR FREEZING AND THAWING INDICES</b>	<b>190</b>
	<b>APPENDIX D, THINGVELLIR FREEZING AND THAWING INDICES</b>	<b>195</b>
	<b>APPENDIX E - COMPARISON OF PREDICTED AND MEASURED TEMPERATURE PROFILES</b>	<b>201</b>
	<b>APPENDIX F – VARIOUS FORMULAS</b>	<b>203</b>

## LIST OF TABLES

Table 3- 1: Example of n-factors after Andersland and Ladanyi (2004).	66
Table 3- 2: Typical sensor configuration for FWD	66
Table 4- 1: Thickness and classification of layers in sections 1.4.1. and 1.4.2. [Bjarnason et al. 1999]	92
Table 4- 2: Thickness and classification of layers in section 3.2.3.1 [Bjarnason et al. 1999]	92
Table 4- 3: Thickness and classification of layers in the section at Dyrastadir [Erlingsson 2002a]	92
Table 4- 4: Thickness and classification of layers in the section at Vatnskard [Erlingsson 2002a]	93
Table 4- 5: Overview of available data from test sections in southwest Iceland.	93
Table 4- 6: Overview of available data from test sections in northern Iceland.	93
Table 4- 7: Overview of available data from recently installed sections at various locations in Iceland.	94
Table 4- 8: Resistivity/conductivity and appropriate units	94
Table 5- 1: Duration of SLR for Dyrastadir determined using various relationships reported in the literature	129
Table 5- 2: Duration of SLR for Thingvellir determined using various relationships reported in the literature	129
Table 6- 1: Summary of the material properties used for the prediction in Temp/W	166
Table 6- 2: Depth to 0°C isotherm in the sections modeled in case 2 and 3	166
Table A- 1: Classification of frozen soil, modified from Andersland and Ladanyi (2004)	186
Table E- 1: Calculations for average error in case 1 at Dyrastadir	201
Table E- 2: Calculations for average error in case 2 at Dyrastadir	201
Table E- 3: Calculations for average error in case 3 at Vatnskard	202

## LIST OF FIGURES

Figure 2- 1: How decisions are taken regarding to onset (a) or removal (b) of SLR.	38
Figure 3-1: Mass/volume relationship for unfrozen and partially frozen soil.	67
Figure 3-2: Frozen core sample showing ice lens formation, (Photograph taken by Bale, B.)	67
Figure 3-3: Limits of frost susceptibility of soils according to Chamberlain (1981)	68
Figure 3-4: Schematic drawing of heat flow after Andersland and Ladanyi (2004).	68
Figure 3-5: Schematic drawing of the ocean currents around Iceland from Calvin (1998)	69
Figure 3-6: Typical deflection basin from Erlingsson (2004)	69
Figure 4- 1: Map of test sections in southwest Iceland and nearby weather stations [Bjarnason et al. 1999]	95
Figure 4- 2: Map of test locations in northern Iceland [Erlingsson 2004b]	95
Figure 4- 3: Screen-capture from a monitoring program for the Icelandic test sections shows the approximate location.	96
Figure 4- 4: Data logger and transmitting device [Erlingsson 2002a].	96
Figure 4- 5: IMKO (right) and CAMPELL (left) moisture content probes [Erlingsson 2002a]	97
Figure 4- 6: Pictures taken from the installation of one of the conductivity probes. [Erlingsson 2004b]	97
Figure 4- 7: Resistivity of various materials changing with temperature [Hoekstra and McNeill 1973]	98
Figure 4- 8: Conductivity measurements from Vatnsskard winter/spring 2003-2004, at 45 cm depth in the road section	98
Figure 4- 9: Conductivity measurements from Dyrastadir 2003-2005, at 37cm depth in the road section.	99
Figure 4- 10: Conductivity measurements from Vatnsskard 2002-2005, at 45cm depth in the road.	99
Figure 4- 11: Two options for a road sections according to Icelandic design guidelines. [Erlingsson 2002b]	100
Figure 5- 1: Moisture content measurements from TDR during spring 2002, Dyrastadir.	130
Figure 5- 2: Air temperature measurements during spring 2002 Dyrastadir.	130
Figure 5- 3: Comparison of observed and predicted thaw durations from WSDOT and Mn/Road, modified from van Deusen et al. (1998)	131
Figure 5- 4: Measured volumetric moisture content vs. time, and evaluation of various methods determining onset and removal of axle load limitations, Dyrastadir spring 2002.	131
Figure 5- 5: Evaluation of various methods determining onset and removal of axle load limitations, Thingvellir spring 1999.	132
Figure 5- 6: Comparison between air temperature and temperature at 7cm depth in the road section at Vatnsskard 2003-2004.	132
Figure 5- 7: Heat distribution in the road during spring thaw at Dyrastadir January and February 2004	133
Figure 5- 8: Measurements of moisture content at Kjos during 1998-1999 (modified from Bjarnason et al. 1999)	134

Figure 5- 9: Comparison of relative conductivity and volumetric moisture content at Dyrastadir 2003-2004, 12 cm depth	135
Figure 5- 10: Comparison of relative conductivity and volumetric moisture content at Dyrastadir 2003-2004, approximately at 30 cm depth	135
Figure 5- 11: Comparison of relative conductivity and volumetric moisture content at Dyrastadir 2003-2004, approximately at 55 cm depth	136
Figure 5- 12: Comparison of relative conductivity and volumetric moisture content at Dyrastadir 2003-2004, approximately at 90 cm depth	136
Figure 5- 13: Moisture content and temperature at 12 cm depth during thaw at Dyrastodum 2003-2004	137
Figure 5- 14: Moisture content and temperature at 30 cm depth during thaw at Dyrastodum 2003-2004	137
Figure 5- 15: Moisture content and temperature at 55 cm depth during thaw at Dyrastodum 2003-2004	138
Figure 5- 16: Moisture content profile compared to deflection data during the 2001-2002 season at Dýrastöðum, a) Moisture content profile and onset/removal of SLR, b) Data from FWD-tests	139
Figure 5- 17: Moisture content profile compared to deflection data during the 2001-2002 season at Vatnskarði a) Moisture content profile, b) Data from FWD-tests	140
Figure 5- 18: Moisture content profile and onset/removal of SLR for the spring thaw 2002 at Dýrastöðum	141
Figure 5- 19: Measurements of deflection of the road section during spring thaw 2002 at Dýrastöðum	141
Figure 5- 20: Measurements of the surface curvature index during spring thaw 2002 at Dyrastodum	142
Figure 5- 21: Measurements of the base damage index during spring thaw 2002 at Dyrastodum	142
Figure 6- 1: Air temperature during the period of Case 1	167
Figure 6- 2: Air temperature during the period of Case 2	167
Figure 6- 3: Air temperature during the period of Case 3	168
Figure 6- 4: Picture taken from the section at Vatnskard (photograph taken by ICERA)	168
Figure 6- 5: Thermal conductivity versus temperature for gravel, graph from Temp/W	169
Figure 6- 6: The relationship between unfrozen water content and temperature, Coarse material was used in case 3 and rock in case 1 and 2.	169
Figure 6- 7: Schematic drawing of measured temperatures at a road section.	170
Figure 6- 8: The thermal modifier function versus temperature, graph from Temp/W.	170
Figure 6- 9: Sensitivity analysis, showing how thermal conductivity is dependant on the porosity.	171
Figure 6- 10: Comparison of measured and predicted temperature profiles for case 1	172
Figure 6- 11: Comparison of measured and predicted temperature profiles for case 2	173
Figure 6- 12: Comparison of measured and predicted temperature profiles for case 3	174
Figure 6- 13: The mesh used in the analysis, the section is 1.5m wide and the height is 6m.	175

Figure B- 1: Grain size distribution from Dyrastadir test section.....	187
Figure B- 2: Grain size distribution from Vatnskard test section .....	188
Figure B- 3: Grain size distribution of the material used with the electrical conductivity probe. ....	189

## LIST OF SYMBOLS

Symbol	Definition
$w_u$	unfrozen water content [-]
$w_i$	ice content [-]
$V_w$	volume of water [m <sup>3</sup> ]
$V_v$	volume of voids[m <sup>3</sup> ]
$G_s$	specific gravity [-]
$e$	void ratio [-]
$n$	porosity [-]
$S_{ru}$	degree of saturation with respect to the unfrozen water [-]
$S_{ri}$	degree of saturation with respect to the ice content [-]
$\rho_w$	density of water [kg/m <sup>3</sup> ]
$\rho_i$	density of ice [kg/m <sup>3</sup> ]
$Q$	heat flow [J s]
$A$	area [m <sup>2</sup> ]
$k$	thermal conductivity [J/s m °C]
$\delta T / \delta x$	thermal gradient [°C/m]
$c$	mass heat capacity [(J/g)/°C]
$c_v$	volumetric heat capacity [MJ/m <sup>3</sup> °C]
$\rho_d$	dry density of sample [kg/m <sup>3</sup> ]
$\rho_f$	bulk density of a frozen sample [kg/m <sup>3</sup> ]
$\rho_{df}$	dry density of a frozen sample [kg/m <sup>3</sup> ]
$L$	latent heat [kJ/kg]
$w_{vol}$	volumetric moisture content [-]
$w_{grav}$	gravimetric moisture content [-]
$T_{mean}$	daily average temperature [°C]
$T_{ref}$	reference freezing temperature at which pavement thaws [°C]
$k_{frozen}$	frozen thermal conductivity [J/s m °C]
$k_{unfrozen}$	unfrozen thermal conductivity [J/s m °C]
$k_{sat}$	saturated thermal conductivity. [J/s m °C]
$k_{dry}$	dry thermal conductivity [J/s m °C]
$k_s$	thermal conductivity of solid particles [J/s m °C]
$K_e$	Kersten number

## List of Abbreviations

AADT	Average Annual Day Traffic
BDI	Base Damage Index
CRREL	Cold weather Regional Research Engineering Laboratory
EASL	Equivalent Axle Single Load
FI	Freezing Index [degree days]
FHwA	Federal Highway Administration
FWD test	Falling weight deflection test
ICERA	Icelandic Road Administration
masl	Meters Above Sea Level
MnDOT	Minnesota Department of Transportation
SCI	Surface Curvature Index
SLR	Spring load restrictions
TI	Thawing Index [degree days]
TDR	Time Domain Reflectometry
USCS	Unified Soil Classification System
USFS	US Department of Agriculture Forest Service
WsDOT	Washington State Department of Transportation

# **1. INTRODUCTION**

A road system is one of the most valuable pieces of infrastructure of any society. In Iceland, considerable amounts of money are spent yearly to repair or carry out preventive maintenance on the road system. Kestler et al. (1999) report that 40% of the total yearly damage on road sections occurs during spring thaw. Janoo and Shepherd (2000) indicate that up to 90% of the damage on pavements occurs during spring thaw. Limiting the allowable axle load during spring thaw can significantly increase the durability of the roads. Ovik et al. (2000) state that the lifetime of a road system can be increased by 10% by applying load restrictions during spring thaw. The Icelandic Road Administration (ICERA) solely determines when to apply and remove axle load limitations on the Icelandic road system. Recently, the agency has developed and installed electrical conductivity probes that improves the agency's capabilities to decide when to impose axle load limitations when roads are at weakened states during spring thaw.

## **1.1. Background**

Every year, during spring thaw, axle load limitations have to be applied to road systems at various locations in the world to reduce the deterioration of roads. Limitations also have to be temporarily applied during short thawing periods in the winter. The decision of when to apply and remove the limitations is regional; no general guidelines regarding axle load limitations are available for the Icelandic road system or for most other jurisdictions.

The research conducted in this study focused on analysing data collected by the Icelandic Road Administration. Several sections have been monitored for the last few years, and information has been gathered about moisture content, road bed temperature, air temperature, and electrical conductivity at various depths in road sections. Some falling weight deflection tests (FWD) have also been conducted at test sites. This available information offers a unique opportunity to analyze the behaviour of road sections during spring thaw, as well as to verify the applicability of guidelines developed by other road administration agencies to Icelandic road conditions.

Recently designed electrical conductivity probes are being used to determine variation in conductivity with depth in the road sections. By measuring the conductivity, an estimation of the moisture content in the road can be achieved. However, this is a rather unconventional method for determining the state of roads, but it is simpler and less costly<sup>1</sup> than the more conventional Time Domain Reflectometry (TDR) measurements. Measuring electrical conductivity in a road section to evaluate the moisture content to determine axle load limitations has not been reported in the literature.

## **1.2. Examples of similar work**

From 1998 to 1999, the Icelandic Road Administration was experimenting with an automatic monitoring system of test sections in southwest Iceland. Two sections were monitored with temperature sensors and moisture content probes. Falling weight deflection tests were conducted during spring thaw. Bjarnason et al. (1999) published a comprehensive description of the experiment. A description of the installed equipment,

---

<sup>1</sup> Erlingsson, S. (personal communication 2006)

installation techniques, road cross section, material properties of the road, and graphical presentations of the measurements can be found in the report. The report was a part of a cooperative study between 10 institutions in Europe that were seeking a better understanding of road construction and maintenance. The data gathered from the Icelandic test sections were available for this thesis.

Two progress reports [Erlingsson (2002), and (2004)] have been written about the project that this thesis is mainly based on. The Icelandic Road Administration installed two new sections in 2001 (Dyrastadir and Vatnskard), in northern Iceland where colder winters than in southwest Iceland can be expected. A prototype of the electrical conductivity probe was installed at the new test sites. Erlingsson (2002) describes the cross section at the test site, the equipment installed, and the falling weight deflection tests carried out at both locations. Numerous photographs from the installation are presented in Erlingsson (2002).

An improved version of the electrical probe was installed at two new test sections in 2002 and 2003, and the old probes at the previously installed sections were replaced. Erlingsson (2004) describes the improved probe as well as the installation technique. The sites at Dyrastodum and Vatnskard had been collecting data hourly for two years when the status report was prepared. The available data were presented in the status report by Erlingsson (2004), mainly to make sure that the installed equipment was functioning properly. Falling weight deflection tests were carried out on the sections at Dyrastodum and Vatnskard, and the results were introduced in the status report. No decisive

conclusions are drawn in Erlingsson (2004); the presentation of data is mainly to explain the opportunity to use these measurements to significantly improve the decisions about imposing or removing axle load limitations on the Icelandic road system.

The Minnesota Department of Transportation (MnDOT) [Ovik et al. 2000] summarized various techniques and guidelines used by road administration agencies at various locations in the world. This summary and the methodology used by the MnDOT in evaluating various guidelines proved to be very useful when working on this thesis. The MnDOT uses air temperature, moisture content, and temperature profiles in road sections to evaluate spring load restrictions (SLR). Ovik et al. (2000) also discuss the applicability of falling weight deflection tests when estimating the conditions of a road section.

### **1.3. Objectives**

The objectives of this thesis are:

- To present the data that has been gathered by the Icelandic Road Administration for the last few years. Special attention will be paid to spring thaw and the behaviour of road sections while thawing. The presentation of the data will provide an understanding of what properties of road sections govern the bearing capacity and durability of the section.
- To verify and test applications used by road agencies that apply or remove axle load limitations. Most of these agencies use methods that are highly dependent on regional conditions such as material properties of road sections, weather patterns, or traffic conditions. The intention is to gather this experience and apply it to

Icelandic conditions. In some cases, changes have to be made to regulations to account for differences in local conditions.

- To be able to predict temperatures in the road section by solving the differential equation for heat flow and estimating the thermal properties of the section as well as know the air temperature. The development of this function will allow agencies similar to the ICERA to predict temperature profiles in road sections based solely on air temperatures from long-term weather forecasts. The software Temp/W from GEOSLOPE is used to solve the heat flow differential equations.
- To add to the knowledge and experience of the applicability of the equipment used. Values from the electrical conductivity probe that is being developed by the ICERA will be compared to measurements from more conventional TDR equipment. Correlations between temperature profiles, moisture content, and electrical conductivity with depth in the road section will be examined. The objective of the ICERA is to make the monitoring of the sections as automated as possible; hourly measurements of temperature and electrical conductivity with depth are to be taken and should be accessible via the Internet.
- To examine the relationship between moisture content and temperature in the road sections and how it affects the stiffness and bearing capacity of the sections, especially how the phase of the water in the sections, whether liquid or frozen, affects the bearing capacity.
- To provide a basis for further work done on the determination of axle load limitations in Iceland. It should benefit the ICERA and transportation companies to have guidelines concerning when to apply or remove spring load restrictions.

## 1.4. Methodology

The data collected by the ICERA are summarized and presented in this study. Hourly measurements of the conditions of the road section, collected for several years are presented in figures. During the experiment, improvements on the equipment and installation resulted in more reliable data being collected. Comparisons of electrical conductivity, moisture content, and temperature in the road section aided in establishing a relationship between these measured variables. Comparing these variables to measurements of stiffness of the road section indicated the significance of each of them to bearing capacity. Based on this study, a better understanding of the behaviour of the test sections installed by the ICERA has been established.

The datasets collected made it possible to verify various approaches used by other road administration agencies to determine when to apply spring load restrictions. Methods and guidelines summarized in Ovik et al. (2000) were compared to Icelandic conditions. The methodology used by Ovik et al. (2000) when evaluating the applicability of various methods to conditions in Minnesota proved to be helpful when evaluating similar methods for Icelandic conditions, in particular when using empirical equations that involve the relationship of air temperature and conditions of a road section.

The differential equation for heat flow was solved for the road section with the software Temp/W from Geoslope. A comparison of measured and predicted values made it possible to iteratively back calculate previously unknown material (thermal) parameters of the road section.

## 1.5. The Organization of the thesis

The thesis was written in paper format, and as a result some sections may be repetitive from chapter to chapter. General guidelines from the Canadian Geotechnical Journal<sup>2</sup> regarding the format of articles were followed.

- Chapter 1 explains why this study was conducted and introduces the structure of the thesis.
- Chapter 2 provides a literature review of previous research concerning various implications of axle load limitations. Equipment and methods used by various road administration agencies are introduced.
- Chapter 3 discusses the theory necessary to understand the behaviour of a frozen road section. The difference between conventional non-frozen and slightly more complicated partly thawed/frozen geotechnical engineering is summarized. Thermal properties of soil are discussed as well as the heat flow differential equation. Equations to estimate the stiffness of a road section from falling weight deflection tests are introduced.
- Chapter 4 introduces the completed and ongoing projects that evaluate the application of spring load restrictions. The chapter describes the equipment used, and samples of the collected data are presented graphically.
- Chapter 5 analyzes and presents the data that has been collected for the test sections by ICERA for the last 8 years. The objective is to evaluate which parameters are of importance in determining the bearing capacity of roads during

---

<sup>2</sup> [http://pubs.nrc-cnrc.gc.ca/rp/rppdf/cgj\\_instruct\\_e.pdf](http://pubs.nrc-cnrc.gc.ca/rp/rppdf/cgj_instruct_e.pdf)

thaw. The relationship between electrical conductivity, moisture content, and temperature is explored

- Chapter 6 models the heat flow in a road section. Measured temperature profiles are compared with predicted temperature profiles to determine the thermal properties of a road section. The differential equation simulating heat flow was solved in Temp/W from Geoslope.
- Chapter 7 provides the final summary, conclusions, and recommendations.

## 1.6. References

- Bjarnason, G., Erlingsson, S., Petursson, P., and Thorisson, V. 1999. Constructed Unbound Road Aggregates in Europe (COURAGE) Icelandic Final report. Public Road Administration Iceland.
- Erlingsson, S. 2004. Mælitækni til strýringar á þungatakmörkunum, Áfangaskýrsla 2, Icelandic Road Administration/University of Iceland. [in Icelandic]
- Erlingsson, S. 2002. Mælitækni til strýringar á þungatakmörkunum, Áfangaskýrsla 1, Icelandic Road Administration/University of Iceland [in Icelandic]
- Janoo, V., and Shepherd, K. 2000. Seasonal Variation of Moisture and Subsurface Layer Moduli. U.S. Army Cold Regions Research and Engineering Laboratory Transportation Research Record 1709. pages 98-107
- Kestler, M. A., Hanek, G., Truebe, M. and Bolander, P. 1999. Removing spring thaw load restrictions from low-volume roads: development of a reliable, cost-effective method. In Proceedings, 7th International Conference on Low-Volume Roads, May 23-26, Baton Rouge, LA. In: Transportation Research Record, no. 1652, v. 2. Washington, D.C.: National Academy Press, 188-197.

Ovik, J.M., Siekmeier, J. A., and van Deusen D. 2000. Improved load restrictions guidelines using mechanistic analysis. Minnesota Road Research Project (Mn/RoadProject)

Available from: <http://www.lrrb.gen.mn.us/pdf/200018.pdf> [accessed 27th March 2006]

## **2. LITERATURE REVIEW**

### **2.1. Introduction**

Material that addresses the study of axle load limitations is widely available. However, the determination of spring load restrictions (SLR) is regional, and therefore it is not feasible to develop guidelines that can be applied everywhere. A considerable contradiction in the literature thus exists due to these regional methods: what may work at one location may not work at all in another. The intention of this review is to go through the available literature and determine which methods can be applied in the determination of axle load limitations during spring thaw in Iceland.

SLR (spring load restrictions) are used as a method of preventing premature pavement deterioration on highway structures resulting from heavy loads during the critical spring thaw period when the pavement structure is at a weakened state [Ovik et al. 2000].

A theoretical description of the problem resulting in load restrictions being necessary during spring thaw could be as follows: during freezing of a road section, negative pore pressures develop at the freezing front. Moisture migrates to this freezing front from water sources below, and ice lenses form perpendicular to the direction of heat flow from the embankment. During spring, thawing occurs predominately from the surface downward. Water released due to melting ice lenses cannot drain because of the frozen layers below, resulting in the soil being less stiff than is generally required to carry loads imposed by heavily loaded trucks [Kestler et al. 1999].

According to Kestler et al. (2000), there are three conditions necessary for ice segregation:

- The soil must be frost susceptible
- Freezing temperatures must penetrate into the soil
- A water source must be available at the advancing freezing front

## **2.2. Measurement techniques**

Evaluating whether a road section is frozen or not can be done in several ways. Various measurement techniques have been developed, and this section will cover the most widely used approaches. The most commonly used techniques to evaluate the conditions of roads are the following:

- Temperatures at various depths in the road section.
- Measurements of air temperature.
- Measurements of moisture content.
- Electrical conductivity or resistivity.
- Falling weight deflection tests (FWD).
- Frost tubes.
- Visual inspection.

### ***2.2.1. Temperature profiles and air temperature***

Kestler et al. (1999) recommend using the temperature profile of the road to determine the onset of SLR (Spring Load Restrictions) and TDR (Time Domain Reflectometry) to determine when any limitations should be removed. When a road reaches 0°C during

thaw, the limitations should be applied. However, the limitations should be removed when the moisture content in the road reaches drained values. This combination is reported to work well. Radio frequency moisture sensors were also tested in Kestler's et al. study and proved to be accurate and reliable.

A temperature profile with depth is quite useful; however, it is expensive to install thermistors at various depths in the road profile; it is easier to measure the air temperature. Various relationships have been derived from cumulative air temperature measurements during both the freezing and thawing seasons. Freezing and thawing indices use the air temperature over a season. Ovik et al. (2000) summarize various formulas applied to conditions in Minnesota. In general, freezing and thawing indices give a good indication of the state of a road, but the formulas/guidelines available in the literature as mentioned are highly regional.

Saarelainen (in press) highlights the importance of using the temperature in the road instead of using the air temperature. The difference can be quite significant, especially when the sun's radiation warms the black asphalt and the road beneath even at below 0°C air temperatures.

### ***2.2.2. Moisture content***

It is common to measure the moisture content with TDR (Time Domain Reflectometer), a device that measures the unfrozen volumetric moisture content based on electromagnetic technology. When the water in the soil freezes it is considered to be a solid material with a typical solid electromagnetic signature. The measurements from the TDR are a measure of the unfrozen moisture content which has a significantly different electromagnetic

signature. A TDR was used by Janoo and Shepherd (2000) with good results. On a plot that shows moisture content versus time, it is very obvious when a road thaws and moisture drains. Therefore, TDR measurements are very useful when decisions about when to apply and remove limitations are required. Janoo and Shepherd (2000) discussed ways to find a value that can be used as an indicator of drained conditions for the moisture content in a road section. They compared the stiffness of a road section to its moisture content during drainage after spring thaw and found an approximate moisture content value that represented sufficient stiffness.

Kestler et al. (1999) described how the USFS (US Department of Agriculture Forest Service) uses the TDR to determine when to remove axle load limitations (USFS uses temperature for onset). Falling weight deflection tests were carried out simultaneously with the moisture content measurements and an approximate value of moisture content for drained conditions was developed.

It should be noted, though, that this approach tends to be expensive and time consuming requiring installation and monitoring of the TDR equipment to acquire moisture content profiles in a road section. It is less expensive to install and run an electrical conductivity probe to estimate moisture content, especially when observing existing road.<sup>1</sup>

### ***2.2.3. The electrical conductivity probe***

The electrical conductivity probe is a relatively new invention, and few articles have been published about it. The research program evaluating its use is still under development at the ICERA (Icelandic Road Administration), and researchers are working to patent the

---

<sup>1</sup> Erlingsson, S. (personal communication 2006)

probe. Therefore, little information is available regarding details of the design. A considerable amount of work has been reported on measurements of the electrical resistivity of various soils, such as that by Harada et al. (1994) and Hoekstra and McNeill (1973), especially for permafrost soils. To the author's knowledge, the electrical conductivity of a road section has not yet been used to evaluate SLR. However, electrical resistivity has been used, for example, by Watson and Rajapakse (2000).

Doré and Duplain (2002) describe a project carried out by the Quebec Ministry of Transportation and Laval University. A technique involving monitoring the moisture content was tested using fibre optic sensors to approximate insitu moisture content. This approach is quite similar to the one used by the electrical conductivity probe and was reported to work as well. A strain gage and TDR equipment were installed in a roadway section to assist with calibration of the fibre optic equipment and to measure deformations.

#### ***2.2.4. Falling Weight Deflectometer***

Ovik et al. (2000) and other references discuss the use of FWD to determine appropriate times for both the onset and removal of SLR. The deflection was measured at fixed distances on a road while a standardized load (500 kg) was dropped from a certain height (further details are provided in Chapter 3.5). It is very expensive to repeatedly test a road system with the FWD because the equipment and labour are costly, especially for agencies that must deal with long roads with low traffic volume roads. When deflections of a road surface are observed with the FWD-test, the road has already reached critical conditions and damage associated with thawing is in progress. However, the FWD is

useful to estimate the integrity and conditions of a road, especially when comparing conditions from one year to another. The FWD is most useful, to monitor how the road regains its strength after the spring thaw when a road is draining. Through an examination of the deflections at various locations, it is possible to estimate where in the section the deformations are occurring. The uppermost layers thaw first, and then as the thaw penetrates deeper into the section, more significant deflections occur and are recorded deeper in the road section. Later during thaw, these deformations deep in the road section become significant, creating deflections of the road surface and pavement. FWD is in general not suitable for determination of the onset of SLR but can be used, with caution, to determine the removal of SLR [Ovik et al. 2000]. FWD test data are especially useful when measurements of moisture content are also available.

### ***2.2.5. Frost Tubes***

Ingólfsson and Bjarnason (1985), describe a frost tube used by the ICERA. The frost tubes were made of two pipes. An approximately 4 cm diameter transparent pipe was put into an approximately 5 cm diameter pipe. The inner pipe was sealed off and filled with a liquid that is blue when unfrozen but turns white when it freezes. The coloring material does not change the freezing point of the water in the tubes. The pipes were installed in the center of a road by drilling a hole and then fastening the larger diameter pipe to the asphalt. The inner pipe could slide in and out of the bigger diameter pipe, allowing monitoring personnel to lift the inner tube and measure the frost depth. The pipes were approximately 1.5 m long and the thermal properties of the pipes are not believed to affect the heat flow.

Over 90 of these tubes have been installed in the Icelandic road system, and for several years the Icelandic Road Administration primarily used information from these frost tubes to decide when to apply and remove load restrictions on the road system.

### **2.2.6. Visual inspection**

The least reliable method, but still the most widely used by road administration agencies, is to visually inspect a road and determine the onset and removal times for SLR according to this visual inspection. The process is difficult, and requires extensive experience to properly evaluate the state of a road as it thaws. Observers look for water filled cracks in the asphalt as well as signs of thaw in the shoulder of the road

## **2.3. Determining onset and removal times for SLR**

In 1997, a survey of SLR was sent out to 45 of 50 Departments of Transportation (DOT) in the USA. The US Department of Agriculture Forest Service was contacted as well. The charts in Figure 1 a and b are the results of the study [Kestler et al. 2000] and show how decisions are made to determine onset and removal of SLR by different agencies.

### **To determine the onset of SLR:**

- 24% of DOT in the US uses quantitative methods (FWD, frost tubes or FI/TI)
- 24% of DOT uses fixed date
- 52% of DOT uses observation and inspection of the roads

### **To determine the removal of SLR:**

- 14% of DOT in the US uses quantitative methods (FWD, frost tubes or FI&TI)
- 29% of DOT uses fixed date
- 57% of DOT uses observation/inspection of the roads

It is a fact that load restrictions during spring save money related to reduced maintenance and road replacement. Whether the savings are sufficient when compared to the negative economic impact that the restrictions impose on the local companies affected by the restrictions is, however, open to debate [Kestler et al. 2000]. The Norwegians argue for not imposing any SLR on their road system. The costs of the load restrictions to society are judged to be higher than the estimated repair costs, and therefore no load restrictions are applied in Norway [Ovik et al 2000]. This is the only case, to the author's knowledge, where load restrictions are judged not to be cost effective.

Van Deusen et al. (1997) summarize the methods used by the Minnesota Department of Transportation (MnDOT) to evaluate both the onset and removal of SLR. Ovik et al. (2000) also discuss the methods used by the MnDOT three years later. To improve its SLR guidelines, the department summarized most of the techniques used by similar agencies around the world and discussed the benefits and drawbacks of each approach. When appropriate, the MnDOT modified these methods to suit regional conditions. For example, the regulations put in place by the Washington State Department of Transportation (WsDOT) were modified for local conditions in Minnesota. The goal was to include as many of the important factors as possible, including pavement structures, soil types, traffic patterns, frost depth, air temperatures and drainage conditions, in the evaluation of imposing and removing SLR while keeping the regulations relatively simple.

Determining the duration of SLR was problematic. The MnDOT could not develop reliable and cost effective methods for determining when to remove the SLR, and

therefore a fixed restriction duration of 7-9 weeks is used, depending on roadway conditions. The MnDOT has been one of the leading research organizations focused on understanding spring load restrictions. Hence, it is surprising that it has not applied a more rigorous evaluation method to determine when to remove these load restrictions. The MnDOT is probably conservative when setting dates for removing the restrictions and the local economy would benefit if more accurate criteria to remove the SLR were developed.

The onset of SLR in Minnesota is usually specified when the top 15 cm of a road section thaws. However, maximum deflection and damage occur when thaw depth reaches roughly 1 m. Spring load restrictions are usually not applied unless the forecasted weather conditions are favourable for continued thawing. However, a 7 day notice has to be given in Minnesota before the SLR generally can begin [Ovik et al. 2000]. Therefore, a thawing index using long-term weather forecasts can be useful in establishing the start date for SLR.

The MnDOT has focused on developing empirical formulas that use freezing (FI) and thawing (TI) indices (cumulative air temperature) to determine the onset of SLR since air temperature is simple and inexpensive to measure. The majority of the roads in Minnesota are constructed using a similar design with respect to thickness of layers and material used, so the most variable factor is the air temperature.

The beginning of the thaw is much more critical than the end; each day of delay in the onset of SLR is equivalent to 28 additional days of reduced loads at the end of the restricted period [Ovik et al. 2000]. Due to the fact that MnDOT tries to impose the SLR

as early as possible, it is more effective to place the restrictions early than to delay their removal, since MnDOT uses a fixed duration of the imposed restriction.

Freezing and thawing indices are widely used by other agencies because it is simple to measure air temperature. Instructions on how to use them can be found in Yesiller et al. (1996). The same article also discusses the accuracy of the method designed by the Federal Highway Administration (FHWA). Results from frost tube measurements are compared to the prediction of the FI and TI. Yesiller et al. (1996) conclude that the use of the method designed by the FHWA is not conservative; it predicts that thawing of roads occurs too late and freezing occurs too soon. These methods should therefore not be used alone to predict application of axle load limitations.

Because these indices are easy to use (only air temperature is required) many empirical formulas are available to predict frost penetration depths. Formulas developed from TI and FI can be applied at various locations other than where the formulas were derived because roads in general have quite similar thermal properties. Air temperature however is regional, and therefore, when considering the air temperature over the winter, the most significant unknown related to regional variation is eliminated.

### ***2.3.1. The Cost of axle load limitations compared to repair costs***

According to Eva Hlin Dereksdóttir<sup>2</sup> (2005), an operations engineer at Samskip, a transportation company with approximately 50% of the market share of road transportation in Iceland, the cost associated with imposition of spring load restrictions is approximately 1,000,000 to 2,000,000 IKr, (\$20,000-40,000 CAD) per day for Samskip.

---

<sup>2</sup> Dereksdóttir, E.H. (personal communication 2005)

In a financial report for the year 2004 from the Icelandic Road Administration published in 2005<sup>3</sup>, it is reported that the total cost of repair for the road system was approximately 1,811,000,000 IKr (\$33 million CAD<sup>4</sup>). Financial report for 2004 was the only ICERA financial report that was looked at in this study, however it seems reasonable for expenses for a typical year. The repair involved general repair and repaving of asphalt, and reconstructing road sections. In Kestler et al. (1999) the use of a damage model showed that 40% of the damage to the road system occurs during the thaw period, Janoo and Shepherd (2000) reported that up to 90% of the damage to the pavement can occur during thaw-weakening periods. The percentage of damage caused by heavy vehicles has not been studied in Iceland yet, however it is known that the damage caused by personal cars is insignificant compared to the heavy vehicles. If the duration of thaw is assumed to be 6 weeks (42 days) then the expenses due to spring thaw restrictions is around \$2,520,000 CAD (30,000 x 42 x 2) for transportation companies, however the cost of repair is \$13.2 million CAD (0.4 x 33 million). Therefore, it can be seen that the cost for transportation companies due to axle load limitations is insignificant compared to the annual cost of maintenance required for the road system.

## **2.4. Material properties of frozen soil and asphalt**

Hoekstra and McNeill (1973) carried out experiments on the electrical resistivity of permafrost. Their results, combined with those of Harada et al. (1994), provide background for the interpretation of data from electrical conductivity probes. Both reports

---

<sup>3</sup>

[http://www.vegagerdin.is/vefur2.nsf/Files/Skyrslasamgonguradherra2004/\\$file/Skyrsla%20radherra%202004.pdf](http://www.vegagerdin.is/vefur2.nsf/Files/Skyrslasamgonguradherra2004/$file/Skyrsla%20radherra%202004.pdf) (accessed the 17th januar 2006)

<sup>4</sup> 1\$ CAD is assumed to be equivalent of 55 IKr

look at electrical resistivity at temperatures between -10 and 10°C, the phase change temperature of interest. The resistivity of soils is highly dependent on the unfrozen moisture content and the type of soils (gravel, sand, clay, silt, rock).

The fluctuations in temperature at particular sites cause seasonal variations in the unfrozen moisture content. The moisture content then greatly affects the stiffness of the base and subgrade layers that make up a road's cross section. With increased amount of fines in the soil the potential volumetric moisture content can be increased, as the finer grains are more able to retain moisture in their structure than coarse material. When a road is completely frozen, it has one or two orders of magnitude greater stiffness than when it is thawed [Ovik et al. 2000]. Due to the increased stiffness of a frozen road, a 10% increase in axle load limitation is often allowed during the winter months by road authorities.

Doré (2004) tried to establish a method for estimating the weakening (loss of stiffness) of a road section. In the study, analytical techniques were used to compute stresses and strains in the road section, and from that information an estimation of the damage of the road was determined. However, the focus of the research was related to fine grained soils in the road section, limiting the applicability of these results since all the roads in Iceland studied for this thesis are constructed from coarse grained soils, which are the norm in Iceland.

Backstrom (2000) discusses the difference in ground temperatures within porous pavement (asphalt content of 5% and  $D_{10}$  value of 1.0 mm) compared to impermeable pavements (asphalt content of 6% and  $D_{10}$  value of 0.125 mm). The results indicate that

the frost penetration of porous pavement is less than for impermeable pavement. The duration of frozen conditions is also shorter for porous pavement because of its increased heat conductivity. The thawing process occurs more quickly because of infiltration of melt water into the subsurface. In general, it appears that porous pavement is better in every aspect of road design and operations.

Zaghloul et al. (2003) discussed a project carried out by the New Jersey Department of Transportation and the Federal Highway Administration. Environmental data as well as monitoring data from a road were recorded for 24 test sections. The article discusses the variations in material properties in roads as a function of the moisture content and temperature. The back calculated layer modulus shows a 20-35% decrease during spring thaw. Rain appeared to have insignificant effects on the moisture content in the road sections throughout the year.

## **2.5. Status reports from the project**

Two projects have been carried out to study the behaviour of road during spring thaw in Iceland. The first includes temperature and moisture content measurements in southwest Iceland. The second involves temperature and moisture content measurements and electrical conductivity probes at four sites in northern Iceland. The second project is still ongoing; the next steps will be to install approximately 20 electrical probes in Highway 1 (goes around Iceland) and monitor the ongoing conditions. The installation of the probes will take place in 2006, the objective being to monitor the roads during spring thaw as well as gather continuous data from future seasons on the behaviour of the roads at these selected test sections.

### ***2.5.1. Southwest Iceland***

Several reports have been written on the project in southwest Iceland. Bjarnason et al. (1999) and Erlingsson et al. (2002) both discuss the project in detail.

Two test sections were monitored with both TDR and thermistors, and FWD test measurements were occasionally carried out. Metrological data from nearby weather stations were used. The data from these measurements were analyzed and processed. Moisture content and temperature were plotted versus time, and reasonable data were acquired. Up to a 50% reduction in stiffness was observed during spring thaw from the FWD measurements when compared to measurements made during winter. The experience gained in conducting the experiments in southwest Iceland proved to be valuable in guiding the project in northern Iceland. Extensive experience has been gained on proper installation techniques of measuring equipment and data processing for these projects.

A comprehensive report [Bjarnason et al. 1999] on the findings of this project was written for the “COURAGE”, which is an abbreviation for **CO**nstruction with **Unbound Road AG**gregates in **E**urope. The contribution from the Icelandic Road Administration is a detailed description of the complete project, including details about the tests, test-sites, and the field results.

### ***2.5.2. Northern Iceland***

Two progress reports have been written about this project, mainly describing the test procedures, equipment installation techniques, and information about the road cross

sections. Neither report discusses the results of the experiment; the reports present some of the data to confirm that the installed instruments were functioning properly.

Erlingsson (2002) wrote the earlier status report for the project. At that time, only two test sites had been commissioned, and various modifications were being made to the electrical conductivity probe. The probe and the installation technique were improved after the first year (2001). The procedure to carry out the FWD measurements is outlined in details along with other measurement techniques.

Details about the two test sections including layer thickness, the grain size distribution curves of each layer, and photographs from the installation can be found in the study by Erlingsson (2002).

The second status report [Erlingsson 2004b] published in February 2004 included information on two new sites. The electrical probes reliability was improved and their production cost reduced. The status report describes the FWD tests carried out on each section and presents some of the field test results. Preliminary analysis of the data, including the moisture content and temperature measurements indicate that all the equipment was functioning properly.

## **2.6. Comparable projects**

The Manitoba Highway and Transportation Department and Federal Highway Administration carried out a study similar to the study conducted by the ICERA. The results were presented in Watson and Rajapakse (2000). TDR, temperature, and electrical resistivity probes were installed in a road section and metrological data were gathered as

well. The data collected were similar to the data available from this project. However, they were presented in a different manner. The main focus of the project was to back calculate the resilient modulus from the FWD-tests for the layers in the road section and try to find relationships with external factors. Temperature, moisture content, electrical resistivity, and thawing index were compared to the results from the FWD measurements. Watson and Rajapakse (2000) used the data from the electrical resistivity and the moisture content to determine whether the material was frozen or not. The results are presented in graphs, and the authors chose to plot the resilient modulus versus thawing index ( $^{\circ}\text{C}$ -hours) for the base and subgrade layer and then fit a third degree polynomial to the data. The polynomial fits well to the data: the correlation coefficient is around 0.99 for the base layer and 0.95 for the subgrade layer. Similarly, the surface temperature was compared to the resilient modulus for the asphalt layer. The correlation coefficient is approximately 0.95.

According to Watson and Rajapakse (2000), the deflections close to where the load is dropped represent the modulus of the upper layers, whereas the deflections of the outer sensor are more sensitive to the properties of the subgrade layers. The road section tested consisted of 111 mm asphalt concrete, 468 mm of unbound granular material, and more than 6 m of sandy silt subgrade. The layer in which the  $0^{\circ}\text{C}$  isotherm was located was divided into frozen and unfrozen layers. Therefore, the calculations<sup>5</sup> for the stiffness moduli included four layers with different material properties.

The Canadian strategic highway research program summarized financial implications of axle load limitations. Information from various road administrations in the world was

---

<sup>5</sup> Calculations were done in EVERCALC designed by Washington state Department of Transportation

gathered, and the average estimated reduction in repair cost of the road section when SLR were applied was assumed to be 79%. Different methods, regulations and guidelines from the Canadian provinces were compared; different regulations apply in each province, but most of the provinces use fixed date for both onset and removal.

### ***2.6.1. Estimation of damage during spring thaw***

The U.S. Department of Agriculture Forest Service (USFS) and CRREL (Cold Regions Research Engineering Laboratory) have been working on an approach for the removal of spring load restrictions for low-volume roads in a reliable and cost effective way [Kestler 1999]. A road section was modeled using the cumulative damage model developed by The U.S. Army Corps of Engineers and the results were quite determinative: 40% of the total yearly damage on the road section occurred between mid-March and mid-April when thawing occurred in this specific case. Janoo and Shepherd (2000) indicate that up to 90% of the damage on pavements occurs during spring thaw.

### ***2.6.2. Calibration of FWD tests and moisture content***

TDR equipment was installed at several sites monitored by the USFS, and during spring thaw FWD measurements were taken as well. A partial deflection basin based on the FWD data (correlates to the stiffness modulus of the road section) was calculated and plotted versus the moisture content from the TDR measurements. As the moisture content increased the road weakened. Through local experience, the designers knew that when the partial basin area is  $0.026 \text{ in}^2$ , the road is stiff enough to remove axle load limitations. Therefore, approximate safe moisture content can be found from the moisture content versus partial basin area plot. When the road section reaches the calculated moisture

content via draining after spring thaw, it is safe to remove the load restrictions. By calibrating the sections of the road system as described above, it is possible to get an approximate reference value for the moisture content indicating that the road section has recovered from critical conditions [Kestler 1999].

### ***2.6.3. SLR determined by temperature in the road section***

Load restrictions are imposed on roads monitored by the USFS when the temperature in the section reaches 0°C during thaw. This approach it has proven to be an excellent one to determine the onset of SLR according to the USFS [Kestler et al. 1999]. Kestler's study does not state where in the road the temperature was taken, but low-volume roads are not thick, and therefore it must have been relatively close to the surface. However, Janoo and Shepherd (2000) disagree with this approach: they argue that the stiffness of a road section depends on the moisture content within the section, and temperature is just an additional factor that affects the moisture content. The Montana Department of Transportation [Janoo and Shepherd 2000] carried out a study on ten sites where temperature and moisture content were closely monitored. The maximum moisture content in the base layer occurred when the temperature in the base layer was -2.4°C. The base layer reached 0°C 23 days later. This implies that the critical thawing period would have been missed by three weeks if the 0°C benchmark was used. The study also shows that the moisture content peaks at different times within layers in the road; the base layer could, for example, reach its peak and drain when the subbase had not even reached its maximum moisture content. Therefore, the top layers usually determine the onset of the axle load limitations and the subbase time for the removal.

The fines content of the material in the road has a determinative effect on the time it takes for the moisture content to recover to drained values. Studies on airport sections [Janoo and Shepherd 2000] show that if the base layers have more than 3% fines content, the moisture dissipation is considerably slower.

#### ***2.6.4. Determination of maximum allowable load***

The maximum allowable load during normal conditions of a road should be decided by a rigorous method. A reasonable suggestion is presented in a study by Huaizhang and Qun (1999) in which the cost of damage caused by heavy trucks is compared to the cost of limiting the axle load. The break even point is the maximum allowable axle load; this axle load must then be reduced during spring thaw due to the thaw-induced weakening. This report considered Chinese conditions but could be applied for every situation. The maximum axle load is generally between 8 and 13 tons: 10 tons is used in the UK, Germany, Japan, Brazil, and the Netherlands. However, 13 tons is used in France, Spain, and Iran. [Huaizhang and Qun 1999]. It might not seem to be a big difference whether the axle load is 10 or 11 tons, but the load significantly affects the durability of a road section. The damage caused by different axle loads is far from linear; research has shown that the relationship is to the fourth power. For example, an axle with a load of 10 tons causes 10,000 times more damage than an axle that is bearing a weight of 1 ton. [Jónsdóttir 2006]

### **2.7. Other literature related to the project**

The U.S. Army Corps of Engineers has developed a program that estimates the cumulative damage to roads [Kestler et al. 1997]. A number of input parameters are used

in the program, including: the geometry of the section, material properties of the road, section air temperature over one season, and traffic characteristics (percentage of heavy trucks, EASL [Equivalent Axle Single Load]). From this information, the program calculates the frost or thaw penetration, nodal temperatures, moisture content distribution, and strains and stresses. When all this information is available, the program calculates the cumulative damage to the road and it is then possible to estimate the damage caused by heavy vehicles. The main focus of this study was to evaluate how different tire pressures affect the durability of roads. Results showed that damage can be reduced substantially by restricting hauling or reducing the tire pressures of trucks. The computer model was used along with real data but imaginary test sections, and the cumulative damage index was also calculated. Three sections were modeled, all of them low-volume roads. As expected in thicker the roads less deformations is expected. Reducing tire pressure clearly improves the durability of roads; however, it is not clear how a reduced tire pressure would affect a well-built road consisting of granular material. Reduced tire pressure would probably not affect well built roads as much as lower quality road sections.

Failure of a road during spring thaw can result in excessive pavement rutting. Janoo and Shoop (2004) carried out an experiment examining the amount of rutting in pavement during freeze and thaw cycles. An empirical formula calculating the degree of rutting was developed as a function of EASL, pavement cross sections, thaw and frost depths and the stiffness modulus of the road.

Erlingsson (2004a) discusses the most important factors that influence the performance and durability of roads (with a focus on pavement) and how these factors should be

included in design. The factors that should be included in the design are cross section, climatic conditions, axle loading and the material properties of the layers in the road.

## 2.8. References

Bjarnason, G., Erlingsson, S., Petursson, P., and Thorisson, V. 1999. Constructed Unbound Road Aggregates in Europe (COURAGE), Icelandic Final report. Public Road Administration Iceland.

Backstrom, M. 2000. Ground temperature in porous pavement during freezing and thawing. *Journal of Transportation Engineering – American Society of Civil Engineers* 126(5) pp. 375-381.

Canadian Strategic Highway Research Program, Seasonal load restrictions in Canada and around the world, C-SHRP Technical Brief #21. Available from <http://www.cshrp.org/products/brief-21.pdf> [cited 5<sup>th</sup> June 2006]

Doré, G., and Duplain, G. 2002. Monitoring pavement response during spring thaw using fiber-optic sensors. *Proceedings 6<sup>th</sup> International Conference on the Bearing Capacity of Roads and Airfields*. Lisbon, Portugal. Edited by A.G. Correia and F.E.F. Branco, pp. 15-24

Doré, G. 2004. Development and validation of the Thaw-weakening Index. *International Journal of Pavement Engineering*, 5 (4) pp. 185-192.

- Erlingsson, S. 2004a. Mechanistic pavement design methods – A road to better understanding of pavement performance. Nordisk Vejteknisk Forbund -Via Nordica, Copenhagen, June 7-9<sup>th</sup>, 8 p.
- Erlingsson, S. 2004b. Mælitækni til strýringar á þungatakmörkunum, Áfangaskýrsla 2, Icelandic Road Administration/University of Iceland. [in Icelandic]
- Erlingsson, S. 2002. Mælitækni til strýringar á þungatakmörkunum, Áfangaskýrsla 1, Icelandic Road Administration/University of Iceland [in Icelandic]
- Erlingsson, S. Bjarnason, G., and Thorisson, V. 2002. Seasonal variation of moisture and bearing capacity in roads with a thin surface dressing wearing course, Proceedings, 9<sup>th</sup> International Conference on Asphalt Pavements. Copenhagen Denmark.
- Harada, K. Fukuda, M., and Ishizaki, T. 1994. Measurements of electrical resistivity of frozen soils. Proceedings, 7<sup>th</sup> International Symposium on Ground Freezing, Nancy, France, Oct. 24-28. Edited by M Fremond, Rotterdam, A.A. Balkema, p 157-162.
- Hoekstra, P., and McNeill, D. 1973. Electromagnetic probing of permafrost. In North Am. Contrib., 2nd Int Conf. on Permafrost, Yakutk, U.S.S.R. Washington, D.C.: National Academy of Sciences, pp 517-26.

- Huaizhang, L. and Qun Y. 1999. Study on rational maxim axis load on highway, Proceedings 99<sup>th</sup> International Conference on Agricultural Engineering, Beijing, China. pp. I-54 - I-57 Available from:  
<http://www.lib.ksu.edu/depts/issa/china/icae/part1/am54.pdf> [accessed 20<sup>th</sup> March 2006].
- Ingólfsson, G. and Bjarnason, G. 1985 (3). KUAB 50 Sænska falllóðið, Ný aðferð við mælingar á burðarþoli vega. Vegamál fréttabréf (Icelandic Road Administration) 8. árg. – 3.TBL, 12-16, [In Icelandic].
- Janoo, V., and Shepherd, K. 2000. Seasonal variation of moisture and subsurface layer moduli. U.S. Army Cold Regions Research and Engineering Laboratory Transportation Research Record 1709. pp 98-107.
- Janoo, V., and Shoop, S. 2004. Influence of spring thaw on pavement rutting; Taylor and Francis Group, London.
- Jónsdóttir, S. V. (2006, 12<sup>th</sup> February). Þrýst á Þjóðvegina. Morgunblaðið, pp 22,24 [In Icelandic]

Kestler, M. A., Hanek, G., Truebe, M., and Bolander, P. 1999. Removing spring thaw load restrictions from low-volume roads: development of a reliable, cost-effective method. Proceedings, 7<sup>th</sup> International Conference on Low-Volume Roads, May 23-26, Baton Rouge, LA. In: Transportation Research Record, no. 1652, v. 2. Washington, D.C.: National Academy Press, 188-197.

Kestler, M. A., Knight, T., and Krat A. S. 2000. Thaw weakening and load restriction practices on low volume roads. US Army Corps of Engineers, Engineer Research and Development Center and Cold Regions Research and Engineering Laboratory. Available from [http://www.crrel.usace.army.mil/techpub/CRREL\\_Reports/reports/TR00-6.pdf](http://www.crrel.usace.army.mil/techpub/CRREL_Reports/reports/TR00-6.pdf) [accessed 14<sup>th</sup> February 2006].

Kestler, M. A., Berg and R. L. and Moore T. L. 1997. Reducing damage to low-volume roads by using trucks with reduced tire pressures. Transportation Research Record, 1589: 9-18.

Ovik, J.M., Siekmeier, J. A., and van Deusen D. 2000. Improved load restrictions guidelines using mechanistic analysis. Minnesota Road Research Project (Mn/Road Project) Available from: <http://www.lrrb.gen.mn.us/pdf/200018.pdf> [accessed 27<sup>th</sup> March 2006].

Roberson, R. and Siekmeier, J. 2002. Determining material moisture characteristics for pavement drainage and mechanistic empirical design, MnDOT research Bulletin, M&RR 09, 2002 Available from [http://www.mnroad.dot.state.mn.us/research/MnROAD\\_Project/ResearchBulletins/Determining\\_Material\\_Moisture\\_Characteristics.pdf](http://www.mnroad.dot.state.mn.us/research/MnROAD_Project/ResearchBulletins/Determining_Material_Moisture_Characteristics.pdf) [accessed 16<sup>th</sup> February 2006].

Saarelainen, S. Thaw penetration, thaw weakening and permanent deformation on pavements. *In* Proceedings of the Frost committee text for ISSMGE Osaka Conference. Osaka, Japan, 11 – 15 September 2005. International Society of Soil Mechanics and Geotechnical Engineering. 5 pages [in press].

van Deusen, D., Schrader C. and Johnson. G. 1997. Evaluation of Spring Thaw Load Restriction and Deflection Interpretation Techniques, Proceedings, 8<sup>th</sup> International Conference on Asphalt Pavements, Seattle, WA.

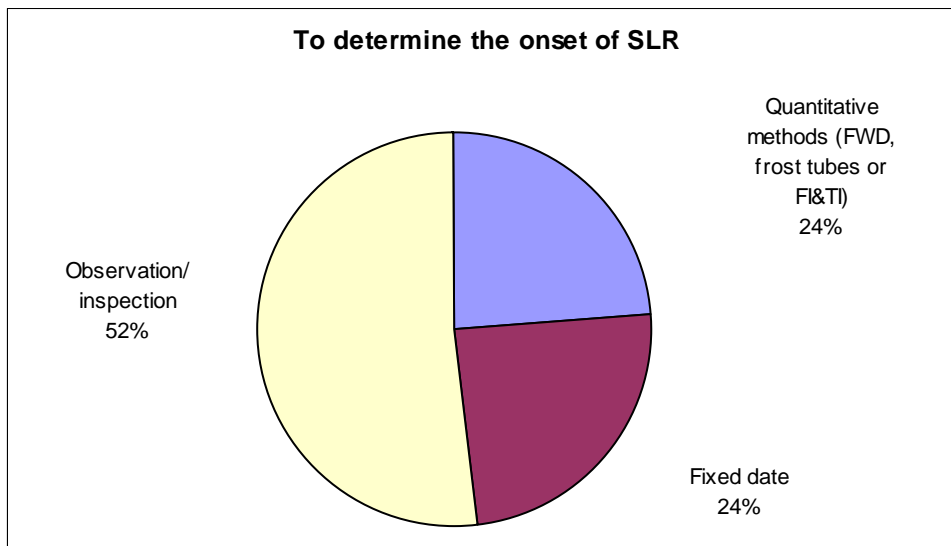
Watson, D.K., and Rajapakse, R.K.N.D. 2000. Seasonal variation in material properties of a flexible pavement. Canadian Journal of Civil Engineering, 27: 44-54. Available from [http://rpas.webp.cisti.nrc.ca/RPAS/RPViewDoc?\\_handler\\_=HandleInitialGet&journal=cjce&volume=27&calyLang=fra&articleFile=199-049.pdf](http://rpas.webp.cisti.nrc.ca/RPAS/RPViewDoc?_handler_=HandleInitialGet&journal=cjce&volume=27&calyLang=fra&articleFile=199-049.pdf) [[accessed 17<sup>th</sup> March 2006].

Yesiller, N., Benson, C. H., and Bosscher, P. J. 1996. Comparison of Load restriction timings determined using FHWA guidelines and frost tubes, Journal of Cold Regions Engineering. 10 (1) March 1996. pp 6-24.

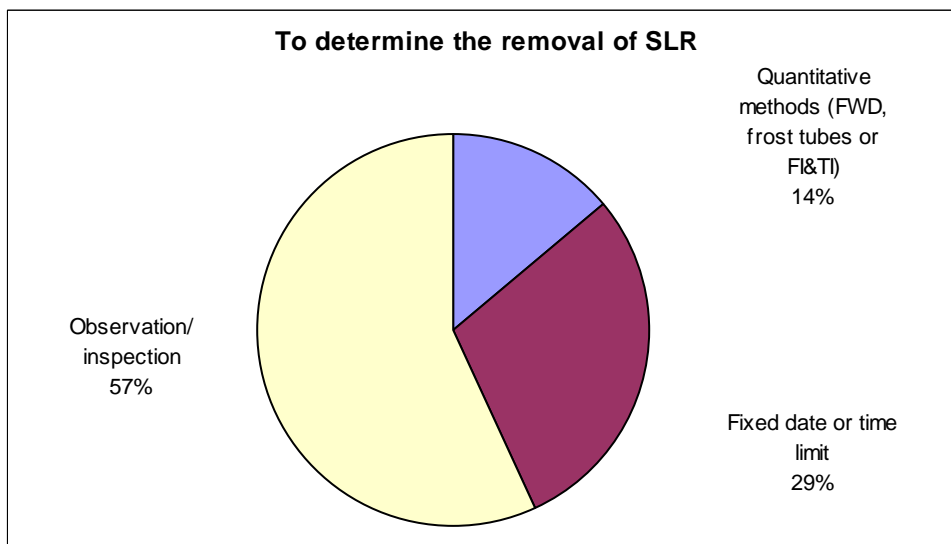
Zaghloul, S., Vitillo N., Gucunski, N. and Ayed, A. 2003. Seasonal variation in material properties. Paper presented at 82<sup>nd</sup> annual meeting of the Transportation Research Board, Washington , DC.

Available from: [http://www.ltrc.lsu.edu/TRB\\_82/TRB2003-001282.pdf](http://www.ltrc.lsu.edu/TRB_82/TRB2003-001282.pdf) [[accessed 17<sup>th</sup> March 2006].

## 2.9. Figures



a) Onset of SLR



b) Removal of SLR

**Figure 2- 1: How decisions are taken regarding to onset (a) or removal (b) of SLR.**

### **3. THEORY**

#### **3.1. Seasonal frozen pavements**

Freeze and thaw in general is a well-studied phenomenon in physics. The theory, however, under natural conditions with unknown material properties and with variable climatic conditions becomes complicated. In this chapter the basic formulation will be introduced. Formulas that can be applied to analyze freezing and thawing of a section of a highway are discussed in this chapter.

Andersland and Ladanyi (2004) define frozen ground as: “soil or rock at subzero temperature” without any implication about water or ice content.

##### ***3.1.1. Variations from conventional geotechnical engineering***

Most of the basic geotechnical engineering theory can be applied to frozen soil, with a few exceptions. The strength of the material is increased if the sample is frozen due to added cohesion from the bonding between the ice and soil particles. The variation that has the greatest influence on the behaviour of a partly frozen soil is the fact that water can exist in two phases (liquid and solid). A partly frozen sample is shown in the fundamental diagram related to mass-volume relationship, illustrated in Figure 3-1.

The definition of gravimetric moisture content, the ratio between the mass of water and the mass of solids in the sample, must be altered for application to frozen soils. The mass

of water consists of the combined mass of water in liquid state and ice (water in solid state).

The moisture content in the partially frozen sample will therefore consist of frozen and unfrozen water:

$$w = w_u + w_i \quad [3-1]$$

Where:

$w_u$  is the unfrozen water content ( $m_{\text{water}}/m_{\text{solids}}$ )

$w_i$  is the ice content ( $m_{\text{ice}}/m_{\text{solids}}$ )

All the formulas that contain moisture content will require the use of the modified definition of moisture content shown in Equation 3-1.

Ice does not necessarily have to be inside the pores of the material; it can form ice lenses that separate the soil into layered system as illustrated in Figure 3-2. The volume of voids ( $V_v$ ) from Figure 3-1 is usually greater for a frozen sample than a non-frozen one. Most of the classical geotechnical formulas are unchanged; however, the formula for the degree of saturation has to be redefined.

The degree of saturation is a ratio of the volume of voids and the volume of water in the sample. The conventional formula for the degree of saturation ( $S_{ru}$ ) is:

$$S_{ru} = \frac{V_w}{V_v} \text{ or } S_{ru} = \frac{w_u G_s}{e} \quad [3-2]$$

Where:

$V_w$  is volume of water

$V_v$  is volume of voids

$w_u$  is moisture content

$G_s$  is the specific gravity

$e$  is the void ratio

The subscript  $u$  denotes unfrozen state.

When there is ice in the sample, the volume of water consists of water both in liquid and solid state. Therefore, the formula for degree of saturation for partially frozen sample is:

$$S_{rf} = S_{ri} + S_{ru} = \left( \frac{w_i \rho_w}{\rho_i} + w_u \right) \frac{G_s}{e} \quad [3-3]$$

Where:

$S_{ri}$  is the degree of saturation with respect to the ice content

$S_{ru}$  is the degree of saturation with respect to the unfrozen water

$\rho_w$  density of water (1000 kg/m<sup>3</sup>)

$\rho_i$  density of ice (916.8 kg/m<sup>3</sup>)

The ice content in a sample is calculated as:

$$i_r = \frac{M_i}{M_w} = \frac{w - w_u}{w} \quad [3-4]$$

Where:

$M_i$  is the mass of ice

$M_w$  is the total mass of water ( $M_w = M_i + M_{uw}$ )

### **3.1.2. Classification of frozen soil**

Classification of a soil is commonly carried out using the Unified Soil Classification System (USCS) developed by Casagrande in 1948. The system divides soils into granular, cohesive, or highly organic categories depending on grain size distribution, liquid, and plastic limit. The sample is assigned a group symbol and a name in the USCS. When frozen soil needs to be classified, the USCS system is used with two additional steps added to the classification to provide additional information about the state and appearance of the sample. First the soil is classified according to USCS, and then the characteristics between the ice-formation are examined. The ice crystal structure is studied to determine if the ice is in the voids of the grains, or is coating the particles. Size and shape of the ice formation is included in the classification. Some of the classification cannot be done only by eye, therefore microscopes or magnifying glasses should be used. The third part of the classification is a study of the ice strata, such as its thickness. The classification considers soil inclusions in the ice, the hardness, structure, and colour of the ice within the frozen sample.

The stratification of a sample depends on the freezing process. A saturated sample contains its moisture in the pores of the soil. When water freezes, the volume increases by about 9%, if the rate at which the temperature decreases in the soil is low, the ice gradually pushes the unfrozen water out of the pores. That water then freezes and may form ice lenses. If the freezing process is rapid, the water freezes in the pores, often trapping unfrozen water in the pores. The slow freezing process with the formation of ice lenses is more common in nature below about 1m.

In Appendix A, Table A-1 presents the classification system for frozen soil. The table is modified from Andersland and Ladanyi (2004).

### ***3.1.3. Frost susceptibility***

Frost susceptibility focuses on the soils ability to attract water to ice lenses, which generally result in thaw weakening and strain due to excess water during thaw. Freezing affects soils in different ways. Fine grained soils tend to weaken when thawed. Soils with large amounts of fine grained material of silt size tend to frost heave. Poorly graded, coarse soils can frost heave, if the grain size distribution curve consists of considerable amount of silt size particles. Figure 3-3 [Chamberlain 1981] presents a classification of frost susceptibility based on grain size distribution. Well-graded, coarse grained soils tend to increase its bearing capacity with added cohesion due to freezing. Very few materials are not affected as they freeze and thaw.

Determination of frost susceptibility relying on the USCS-classification was developed by the U.S. Army Corps of Engineers [Johnson et al. 1986]. Classification of the sample

using the USCS and determination of the amount passing sieve with and opening of 0.02mm is used to determine the frost susceptibility. The method divides soils into six categories<sup>1</sup> of frost susceptibility. The method recommends that if precise frost susceptibility information for design is required, a detailed freezing test should be carried out. Many classifications are available to determine frost susceptibility, and Chamberlain (1981) summarizes various tests to determine frost susceptibility. Most of them are based on grain size distribution, plastic and liquid limit, and the USCS-classification. Classifications that would be considered more advanced include frost heave rates and segregation potential.

### ***3.1.4. Thermal properties***

When soil freezes and thaws in situ, there is an interaction between the air temperature and the soil surface. The top part of the soil in which the temperature fluctuates above and below 0°C is called the active layer. For this definition it does not matter whether the soil beneath the active layer is frozen (permafrost) or not.

#### **3.1.4.1. Heat flow - differential equation**

It is possible to apply classical physics (thermodynamics) to the active layer. To predict the temperature distribution and these fluctuations in a particular section, for example in a road, the basic one dimensional partial differential heatflow equation can be used [Strauss 1992]. See Equation 3-5 [Andersland and Ladanyi 2004]

---

<sup>1</sup> Negligible, very low, low, medium high and very high.

$$Q = -k_u A \frac{\delta T}{\delta x} \quad [3-5]$$

Where :

$Q$  is heat flow [J s] often used with area then  $Q/A$  [J s/m<sup>2</sup>]

$A$  is area [m<sup>2</sup>]

$k$  is thermal conductivity [J/s m °C]

$\delta T/\delta x$  is the thermal gradient [°C/m]

The thermal conductivity is a measure of the ability of material to conduct heat [Benson 1996]. It depends on the degree of saturation, void ratio, moisture content, and dry density of the material. Johansen (1975) developed a couple of empirical equations that give reasonable predictions of unfrozen thermal conductivity using these variables. Thermal conductivity for a road section is estimated and the temperature variation with depth is modeled in Chapter 6.

Figure 3-4 shows a schematic drawing of heat flow through a rectangular body. The heat conduction involves transfer of kinetic energy from molecules in the warm part of the material, to the cooler part. The lower diagram shows graphically how the temperature changes with distance. The temperature change ( $\Delta T$ ) at a small interval ( $\Delta x$ ) at a certain distance from the boundary shows changes of some value. Equation 3-5 expresses that temperature change versus distance mathematically.

### 3.1.4.2. Heat capacity

Heat capacity is the amount of energy (heat) required to increase the temperature of a unit mass of a certain material by 1°C. Soil is, however, composed of four different materials: solids, air, unfrozen water, and ice. Therefore, a ratio of heat capacity versus weight has to be taken for each material as is described in Equation 3-6

$$c_m = \frac{1}{m_{total}} (c_s m_s + c_w m_w + c_{ice} m_{ice} + c_{air} m_{air}) \quad [3-6]$$

Where:

$c_m$  is the mass heat capacity [(J/g)/°C]

$m$  denotes mass of each component [kg]

The subscripts s,w, represent solids and water respectively.

If the heat capacity of air is ignored and volume is introduced into Equation 3-6 ( $c_v$  volumetric heat capacity), it can be rewritten as:

$$c_v = c_m \rho_f = \rho_{df} (c_s + c_w w_u + c_{ice} w_{ice}) \quad [3-7]$$

Where:

$c_v$  is the volumetric heat capacity [MJ/m<sup>3</sup> °C]

$\rho_f$  bulk density of the frozen sample [kg/m<sup>3</sup>]

$\rho_{df}$  dry density of the frozen sample [kg/m<sup>3</sup>]

### 3.1.4.3. Latent heat of fusion

Latent heat of fusion is defined as the energy required to change liquid water to ice at its melting point (0°C for water), without a change in temperature. The temperature remains

constant when a material undergoes a phase change. The latent heat for water is 333.7 kJ/kg, but for any given soil:

$$L_{soil} = \rho_d L_{water} \frac{w - w_u}{100} \quad [3-8]$$

Where:

$\rho_d$  is the dry density [kg/m<sup>3</sup>]

$L_{soil}$  and  $L_{water}$  are latent heat of fusion ( $L_{water} = 333.7$  [kJ/kg])

#### **3.1.4.4. Thermal expansion**

When water freezes it increases its volume by approximately 9%. Water behaves differently than most liquids, which expand when they are heated and contract when cooled. The formation of ice lenses due to expansion of slowly freezing water has been explained in Section 3.1.1.

### **3.2. Freezing and thawing of a road section**

During winter when the road freezes, the bearing capacity is up to tenfold the summer bearing capacity [Janoo and Shoop 2004], mainly due to increase in cohesion associated with ice bonding. In the spring when temperatures rise, the road thaws. As thaw proceeds, the ice melts, releasing excess water resulting in increased pore pressure and a reduction in overall bearing capacity if the pressures do not dissipate rapidly. Due to frozen (impermeable) soil beneath the thawed section, the released water can only drain horizontally or evaporate from the surface.

Material used to construct roads should be non-frost susceptible to prevent frost heave and ice lens formation. Materials that are not frost susceptible usually are stronger than materials that are frost susceptible, (for example coarse gravel versus clay). Therefore, strong materials that will not undergo frost heave are usually specified for use in the construction of a road section. However, the native soil underneath the road can be frost susceptible and undergo frost heave. It is desirable that the road section is thick enough to insulate the native soil, thus preventing it from freezing. If the insulation cannot be ensured, it is possible to allow the road to heave, especially if the native soil is uniform to ensure no differential heave occurs. The road will not be damaged if the native soil undergoes uniform heave and settlement, and is strong enough to support traffic during thaw weakening.

Classical thermodynamics can be applied to a road section. The differential equation for heat flow, Equation 3-5, is solved for a road section in Chapter 6. The heat flow between the air temperature and the road was modeled with reasonable results; however, improvements of the model are possible.

### ***3.2.1. Heat flow in road sections***

Heat flows from the warmer region to the colder region. During the winter, the energy will flow from the road upward to the surface and into the air. During spring the energy flow is reversed, and the warm air contributes to thawing the road section. This heat transfer and flow can be modeled with a few simplifications (see Chapter 6).

The thermal conductivity can be calculated for the layered road. Values of heat capacity and latent heat for the road must be considered in the calculations. The differential equation (Equation 3-5) only predicts the flow of heat. It does not account for phase changes. One of the most important variables in the heat flow equation is the energy input into the system. The energy input (or output) can be obtained by evaluating the air temperature over a specific period. Solar radiation, warming up the darkened road plays an important role in transferring heat to the road surface.

### ***3.2.2. Air temperature***

The air temperature is not a variable that can be applied directly when evaluating the conditions of a road. The air temperature is measured 1.8 m from the ground surface, and is not representative of the temperature at the road surface, or in the top part of the active layer of the soil.

During a warm spring day radiation from the sun warms the black asphalt, causing the temperature in the top part of the road to be considerably warmer than the air temperature. On the other hand, snow or a vegetative cover insulates the ground from the air temperature, causing the air temperature to be cooler than the temperature in the uppermost part of the soil. Wind chill can have significant effects. The air temperature is measured in a sheltered white box (no radiation) whereas the bare ground does not have any shelter. The wind (chill) removes heat quickly so the surface cools rapidly.

Although the air temperature should not be used, it is used as a part of the heating or cooling source for freezing and thawing of road sections, mainly because the actual road surface temperature is rarely available. The air temperature is easy to measure, and is

often useful for other applications. Road temperature is usually warmer than the air temperature but there are a few exceptions.

### **3.2.3. Freezing and thawing indices**

A degree day is a widely used concept in meteorology. It is the duration of one day multiplied by the average temperature over that day. For example if the average temperature is  $-5^{\circ}\text{C}$  that specific day is considered to be -5 degree days. If the average temperature for January is  $-3.4^{\circ}\text{C}$  and there are 31 days in January, the month would consist of  $31 \times -3.4 = -105.4$  degree days.

The freezing and thawing indices are cumulative functions that sum degree days over a chosen period.

Freezing index (FI [degree days]) is calculated according to

$$FI = \sum (0^{\circ}\text{C} - T_{average}) \quad [3-9]$$

Where:

$T_{average}$  is the average air temperature of the day

The road thawing index (TI [degree days]) is slightly more complicated

$$TI = \sum (T_{average} - T_{ref}) \quad [3-10]$$

Where:

$T_{ref}$  is the air temperature at which the road starts to thaw

Freezing index calculated from the air temperature is called FI, and  $FI_{\text{surface}}$  when calculated from surface temperature. The same notation will be used for the thawing index that is  $TI$  and  $TI_{\text{surface}}$ .

As explained in Section 3.2.2, the air temperature is not the same as the temperature at the top of the road or within the upper section of the road. Therefore a reference temperature must be introduced. It is the air temperature at which the road thaws and needs to be calibrated for each location. Typical values for  $T_{\text{ref}}$  are between  $-0.5^{\circ}\text{C}$  to  $-5^{\circ}\text{C}$  [Ovik et al. 2000 and van Deusen et al. 1997]. In Sections 5.2.1.3 and 5.2.1.4,  $T_{\text{ref}}$  for Dyrastadir (2001-2002) and Thingvellir (1998-1999) are calculated.

When the temperature cools during the fall and freezing begins, the freezing index is occasionally calculated for these short periods. These periods are called early freeze. Early thaw must follow, and for that period the thawing index is calculated. Each freezing period must be evaluated and the frost penetration determined, in order to establish if the drainage during the following thaw would be limited and thus capable of limiting downward drainage.

When continuous freezing begins, the negative degree days are summed up to calculate the freezing index. Once the air temperature reaches the value at which the road begins to thaw (the reference temperature,  $T_{\text{ref}}$ ), the summation of the thawing index starts.

It is quite common that the institution that supervises a particular road system evaluates the thermal properties of a typical road section. The differential equation for heat flow and other thermodynamic problems are solved for various temperature conditions. From those calculations, empirical relationships are developed and then used to establish the date to impose and remove the SLR.

Due to changes in the weather-conditions and regional variation in the structure of roads, these empirical relationships often differ with location. The Minnesota Department of Transportation has been pioneering this field of study. The FI for the winters in Minnesota ranges from 200 to 1000 °C days, and the roads are constructed of fine-grained subgrade soils [van Deusen et al. 1998].

### **3.2.4. Insulation**

The road surface temperature is quite different from the air temperature. The ratio between the FI for the air and surface temperature ( $FI_{\text{surface}}/FI_{\text{air}}$ ) is called  $n_f$ , and the ratio for the TI is called the  $n_t$ . The coefficients  $n_f$  and  $n_t$  represent the influence of the air temperature near the surface. The coefficients are very dependant on the surface material. Table 3-1 shows typical values for different materials.

### **3.2.5. Frost penetration**

The modified Berggren Equation is a theoretical formula that uses most of the thermodynamics concepts previously discussed to evaluate frost penetration. Equation 3-11 is the modified Berggren Equation. It is based on the Stefan Equation with an added correction factor,  $\lambda$ . It assumes that the only thermal energy (heat) that must be removed

when freezing a soil is the energy associated with the latent heat. Therefore the formula only determines the depth of the 0°C isotherm.

$$P = \lambda \sqrt{\frac{2k v_s t}{L}} \quad [3-11]$$

Where:

$P$  frost penetration

$L$  latent heat of the soil

$k$  unfrozen thermal conductivity of the soil

$v_s$  the difference between the soil moisture temperature and the melting point of the soil.

$t$  is the duration of the freezing period,

$\lambda$  is a correction coefficient distinguishing modified Berggren and the Stefan equation.

There is a relationship linking the  $v_s$  and  $t$  together:  $v_s = FI_{\text{surface}}/t$ .

The coefficient  $\lambda$  is found in a design chart [Andersland and Ladanyi 2004] where the input parameters are the thermal ratio,  $\alpha$ , and a fusion parameter  $\mu$ . The thermal ratio is defined as the ratio between the FI calculated from the air temperature and the top-road temperature. The fusion parameter  $\mu$ , is a ratio of the volumetric heat capacity compared to the latent heat of fusion of the road structure, multiplied by the absolute value of the negative air temperature at the start of the freezing period.

$$\mu = \frac{c_v}{L} \Delta T_s \quad [3-12]$$

Where:

$\Delta T_s$  is degrees below freezing at the start of the freezing period, the other terms are as defined before.

The Minnesota Department of Transportation [Ovik et al. 2000] use an empirical relationship to evaluate the frost penetration based on the FI

$$P = -0.328 + 0.0578\sqrt{FI} \quad [3-13]$$

Where

$P$  is the frost penetration [m]

$FI$  is the air temperature freezing index.

Equation 3-13 gave good results when compared to measurements in frost tubes in Minnesota. It should be emphasized that these kinds of formulas are highly regional and may not be suitable everywhere. Some characteristic thermodynamics values of the material in the road and the weather pattern during winter determine the constants in the formulas. Similar empirical relationships could be developed for any location if sufficient temperature and frost penetration data were available.

### **3.3. Icelandic weather conditions**

The majority of the people living in the United States and Canada live between 30°N and 45°N latitude, whereas people in Europe live 10 to 15° further north [Calvin 1998]. The reason for this difference can be found through studying oceanography, and it has an important moderating influence on the climate of the northern Europe. The seas north of

Canada freeze during winter and the icecap isolates the cold air coming from the arctic, allowing for development of much colder air temperatures. The sea that surrounds Iceland does not freeze, and is on the contrary rather warm considering its northern location. The ocean around the island warms up the cold air coming from the north and west. Figure 3-5 shows a schematic drawing of the ocean currents around Iceland. The average temperature between January and March in Reykjavík (64°N) is  $-0.8^{\circ}\text{C}^2$  whereas the average temperature for the same months in Edmonton (53°N) is  $-11.0^{\circ}\text{C}^3$ .

The air temperature in Iceland fluctuates considerably, causing numerous freeze and thaw cycles that seriously affect structures such as roads. The weather can be quite variable, especially in the highlands, due to the intense interaction between warm and cold air. The air usually has high humidity and precipitation is rather high. Typical freezing index for an Icelandic winter is quite variable depending on elevation and location. They can be as low as  $50^{\circ}\text{C}$  days and as high as  $1000^{\circ}\text{C}$  days.

### **3.4. Axle load limitations**

During spring when a road thaws, it is in a weakened state due to increased pore water pressure and reduced cohesion. Bjarnason et al. (1999) reports that the stiffness of the road during spring thaw varies from approximately 25-50% of fully drained stiffness. Therefore axle load limitations are generally applied to road sections to prevent damage caused by truck traffic. Damage caused by heavy axle loads is not linearly dependent on load, but for every load increment, there is an increase in damage related to the fourth

---

<sup>2</sup> <http://reykjavik.is/upload/files/RVK-enskur.pdf> (accessed 15<sup>th</sup> October 2005)

<sup>3</sup> <http://www.worldclimate.com/cgi-bin/data.pl?ref=N53W113+1102+71123W> (accessed 17<sup>th</sup> October 2005)

power [Ovik et al. 2000]. Hence, reduced axle load can be justified, and the Icelandic Road Administration reduces the maximum allowable load from 11.5 to 10.0 tons per axle during spring thaw.

The laws that deal with the axle load limitations<sup>4</sup> are quite complicated as they consider factors such as type of tires and air pressure, type of axle, and spacing between axles.

The Icelandic Road Administration is responsible for ensuring that regulations regarding axle load are observed. Specially designed mobile scales are located at various places on the highway system during spring and trucks are tested randomly.

According to Eva Hlin Dereksdóttir, an operations engineer at Samskip, a transportation company with approximately 50% of the market share of road transportation in Iceland, the cost associated with imposition of spring load restrictions is approximately 1,000,000 to 2,000,000 IKr, (\$20,000-40,000 CAD<sup>5</sup>) per day for Samskip.

In a financial report for the year 2004 from the Icelandic Road Administration published in 2005<sup>6</sup>, it is reported that the total cost of repair for the road system was approximately 1,811,000,000 IKr (\$33 million CAD). The repair involved general repair and repaving of asphalt, and reconstructing road sections. In Kestler et al. (1999) the use of a damage model showed that 40% of the damage to the road system occurs during the thaw period,

---

<sup>4</sup>

<http://reglugerd.is/interpro/dkm/WebGuard.nsf/538c26748c8e2a9d00256a07003476bd/001c81acbdd2f0120025704300567a93?OpenDocument> (accessed 13<sup>th</sup> October 2005)

<sup>5</sup> 1\$ CAD is assumed to be equivalent of 55 Ikr

<sup>6</sup>

[http://www.vegagerdin.is/vefur2.nsf/Files/Skyrslasamgonguradherra2004/\\$file/Skyrsla%20radherra%202004.pdf](http://www.vegagerdin.is/vefur2.nsf/Files/Skyrslasamgonguradherra2004/$file/Skyrsla%20radherra%202004.pdf) (accessed the 17th January 2006)

Janoo and Shepherd (2000) reported that up to 90% of the damage to the pavement can occur during thaw-weakening periods. The percentage of damage caused by heavy vehicles has not been studied in Iceland yet, however it is known that the damage caused by personal cars is insignificant compared to the heavy vehicles. If the duration of thaw is assumed to be 6 weeks (42 days) then the expenses due to spring thaw restrictions is around \$2,520,000 CAD ( $30,000 \times 42 \times 2$ ) for transportation companies, however the cost of repair is \$13.2 million CAD ( $0.4 \times 33$  million). Therefore, it can be seen that the cost for transportation companies due to axle load limitations is insignificant compared to the annual cost of maintenance required the road system.

#### ***3.4.1. The onset and removal of spring load restrictions***

There are numerous empirical guidelines regarding when to apply or remove spring highway load restrictions. Most of the guidelines are based on empirical relationships involving the FI and/or TI. Most of the literature that deals with thawing index agrees that load restrictions should be applied when the TI reaches 15°C days, and must be applied when TI is 30°C days. By then approximately 10-15 cm of the top part of the road has thawed [Ovik et al. 2000].

Other reasonable ways to determine the start of load restrictions could be based on the evaluation of frost depth using frost tubes and/or measurements of moisture content/electrical conductivity profiles in the road.

The most common way to estimate the onset of restrictions is via visual inspection and deflection testing on the road surface (falling weight tests). Both of these approaches are

time consuming and require the inspector to travel and inspect the roads. By the time the inspector becomes aware of the critical state of the road, it may already be too late. In addition, it is often required to give three to seven days notice before spring load restrictions can be fully implemented.

Due to a rapid decrease in strength and stiffness of the road base during thaw, it is critical to implement the restrictions as early as possible. One day at the beginning of the restriction period is equivalent to 28 days at the end of the restricted period in terms of damage inflicted to the road structure [Ovik et al. 2000].

In some jurisdictions, load restrictions are applied on fixed calendar dates. Obviously this is not an accurate method, but it might be suitable for areas that have stable weather patterns and where adequate experience concerning road conditions is available.

Norway has an interesting way of dealing with spring load restrictions - they simply do not apply any. The Norwegian road administration have concluded that the cost of the spring load restrictions to the society is greater than the cost of repairing the damage attributed by the heavy axle loading each spring [Ovik et al. 2000].

There are also a few ways to determine the removal of these restrictions. The falling weight deflection test is more reliable for estimating the removal than the onset of the restriction, as the test indicates how the road regains its structural stiffness, thus strength with time. However the tests are expensive and time consuming.

It is quite common to set a fixed duration for the load restrictions, with two weeks being the minimum [Ovik et al. 2000]. The duration varies regionally and depends on the depth of frost penetration and climatic conditions during spring. The Minnesota Department of Transportation sets the restrictions for a fixed duration of 8 weeks, however, the department recommends additional research to be carried out to evaluate the load restriction duration [Ovik et al. 2000].

Duration estimates based on FI are the most widely used since they include the conditions of the previous winter. The Washington State Department of Transportation (WSDOT) recommends the use of the two following equations:

$$D \text{ [days]} = 0.018 \times FI + 25 \quad [3-14]$$

$$TI = 0.3 \times FI \quad [3-15]$$

Equation 3-14 computes the days of load restrictions considering the FI of preceding winter. However it does not take into account weather conditions throughout the thaw period, which is a disadvantage.

Equation 3-15 recommends removing load restrictions when the TI reaches the computed value according to the formula. The FI of the past winter is the only input parameter.

The Minnesota Department of Transportation (MnDOT) came up with Equation 3-16 to predict the duration of recovery based on the frost penetration depth,  $P$ , from Equation 3-13.

$$D \text{ [days]} = 0.15 + 0.010 \times FI + 19.1 \times P - 12090 \times \frac{P}{FI} \quad [3-16]$$

Equation 3-16 has the same setback as Equation 3-14, that is it does not include any evaluation of the weather during the thaw season.

Equation 3-17 (also developed by MnDOT) is similar to Equation 3-15, and is based on the TI which must be reached before restrictions are removed. The FI of previous winter determines the TI value.

$$TI = 4.154 + 0.259 \times FI \quad [3-17]$$

All of these equations are developed to be used under specific regional weather conditions and may not be suitable for other jurisdictions.

In Chapter 5, Equations 3-14 to 3-17 are used on real data from Dyrastodum and Thingvollum. The moisture content is measured at these locations, hence the exact conditions of the road is known when the equations suggest removal of the axle load limitations. In this way the applicability of the equations for Icelandic conditions was estimated.

### **3.5. Back calculated layer moduli**

Deflection testing during spring thaw is a good indicator of the behaviour of the road section. The Falling Weight Deflectometer (FWD) test is a standard, widely used test to evaluate the stiffness of the road section. In the test, a 500 kg load is dropped on the road

and the deflection at fixed distances from the weight is measured. A typical setup is shown in Table 3-2 and Figure 3-6.

Figure 3-6 from Erlingsson (2004), shows a typical deflection basin in a FWD test. If the deflection and location of the deflection sensors as well as the cross-section of the road is inserted in the linear elastic back calculation software, Evercalc<sup>7</sup>, the Young's modulus of the layers can be calculated. There is a considerable difference in the stiffness of the road depending on the time of the year. The stiffness is greatest during the winter when the road is frozen. During spring, when the road has its highest moisture content, it is less stiff than during summer when the road section is fully drained.

Equations 3-18 to 3-20 are deflection-based parameters. The Surface Curvature Index (SCI) uses  $D_0$  and  $D_2$  and is supposed to indicate the state of the upper layers of the roadway. The Base Damage Index (BDI) is an indicator of the state of the base layers within a road section. Typical deflection curves during thaw, as are shown in Figure 3-6, indicate that the base layers deform considerably less than the top layers. The area of the basin is an overall indicator of the state of the road.

If falling weight deflection tests are carried out every year and the results are corrected for temperature, the designer can get a good idea of the integrity of the road. The deflection  $D_0 - D_5$  is usually measured in  $\mu\text{m}$  ( $10^{-6}$  m)

---

<sup>7</sup> Designed by the Washington state Department of Transportation (WsDOT),

Surface curvature index

$$SCI = D_0 - D_2 \quad [3-18]$$

Base damage index

$$BDI = D_2 - D_4 \quad [3-19]$$

Basin area

$$Area = \frac{1}{D_0} \sum_{i=1}^{N-1} [(D_{i-1} + D_i) * (r_i - r_{i-1})] \quad [3-20]$$

It is commonly accepted that the first deflections  $D_0$  and  $D_1$  are representative of the top layers (15 cm), whereas  $D_4$  and  $D_5$  indicate the condition of the base layers.

### 3.6. References

Andersland, O.B., and Ladanyi, B. 2004. Frozen ground Engineering, Second edition, John Wiley & Sons Inc., New Jersey.

Bjarnason, G., Erlingsson, S., Petursson, P., and Thorisson, V. 1999. Constructed Unbound Road Aggregates in Europe (COURAGE) Icelandic Final report. Public Road Administration Iceland.

Benson, H. 1996. University Physics revised edition, John Wiley & Sons Inc., New Jersey.

Calvin, W.H. 1998. The great climate flip-flop. The Atlantic Monthly 281(1):47-64. Available from <http://WilliamCalvin.com/1990s/1998AtlanticClimate.htm> [Accessed January 17, 2006].

Chamberlain, E.J. 1981. Frost susceptibility of soil Review of index tests. CRREL Monograph 81-2, U.S. Army Cold Regions Research and Engineering Laboratory. Hanover, New Hampshire.

Erlingsson, S. 2004. Mælitækni til strýringar á þungatakmörkunum, Áfangaskýrsla 2, Icelandic Road Administration/University of Iceland. [in Icelandic].

Janoo, V., and Shepherd, K. 2000. Seasonal variation of moisture and subsurface layer moduli. U.S. Army Cold Regions Research and Engineering Laboratory Transportation Research Record 1709. pp.98-107.

Janoo, V., and Shoop, S. 2004. Influence of spring thaw on pavement rutting; Taylor and Francis Group, London.

Johansen, Ø. 1975. Thermal conductivity of soils. PhD discussion, Norwegian Technical University Trondheim; Also U.S. Army Cold Regions Research and Engineering Laboratory Translation 637, July 1977.

Johnson, T.C., Berg, R.L., Chamberlain, E.J., and Cole, D.M. 1986. Frost action predictive techniques for road and airfields: A Comprehensive Survey of Research Findings. U.S. Army Cold Regions Research and Engineering Laboratory CRREL Report 86-18.

Kestler, M. A., Hanek, G., Truebe, M., and Bolander, P. 1999. Removing spring thaw load restrictions from low-volume roads: development of a reliable, cost-effective method. Proceedings, 7<sup>th</sup> International Conference on Low-Volume Roads, May 23-26, Baton Rouge, LA. Transportation Research Record, no. 1652, v. 2. Washington, D.C. National Academy Press, pp188-197.

Ovik, J.M., Siekmeier, J. A., and van Deusen D. 2000. Improved load restrictions guidelines using mechanistic analysis. Minnesota Road Research Project (Mn/Road Project)  
Available from: <http://www.lrrb.gen.mn.us/pdf/200018.pdf> [accessed 27<sup>th</sup> March 2006].

Strauss, W.A. 1992. Partial differential equations, an introduction, John Wiley & Sons Inc.

van Deusen, D., Schrader C., Bullock, D., and Worel. B. 1998. Recent research on springtime thaw weakening and load restrictions in the state of Minnesota, Transportation Research Record, National Resource Council, Washington, D.C.,

van Deusen, D., Schrader, C., and Johnson, G. 1997. Evaluation of spring thaw load restriction and deflection interpretation techniques. Proceedings, 8<sup>th</sup> International Conference on Asphalt Pavements, August 10-14, Seattle, WA.

### 3.7. Tables

Surface	Freezing, $n_f$	Thawing, $n_t$
Pavement free of snow and ice	0.9	
Asphalt pavement	0.9-0.95	1.4-2.3
Sand and gravel	0.9	2.0
Turf	0.5	1.0
Concrete pavement	0.7-0.9	1.3-2.1

**Table 3- 1: Example of n-factors after Andersland and Ladanyi (2004).**

<b>FWD sensor configuration</b>						
Sensor No.	0	1	2	3	4	5
Offset from where load is dropped, cm	0	20	30	45	60	90

**Table 3- 2: Typical sensor configuration for FWD**

### 3.8. Figures

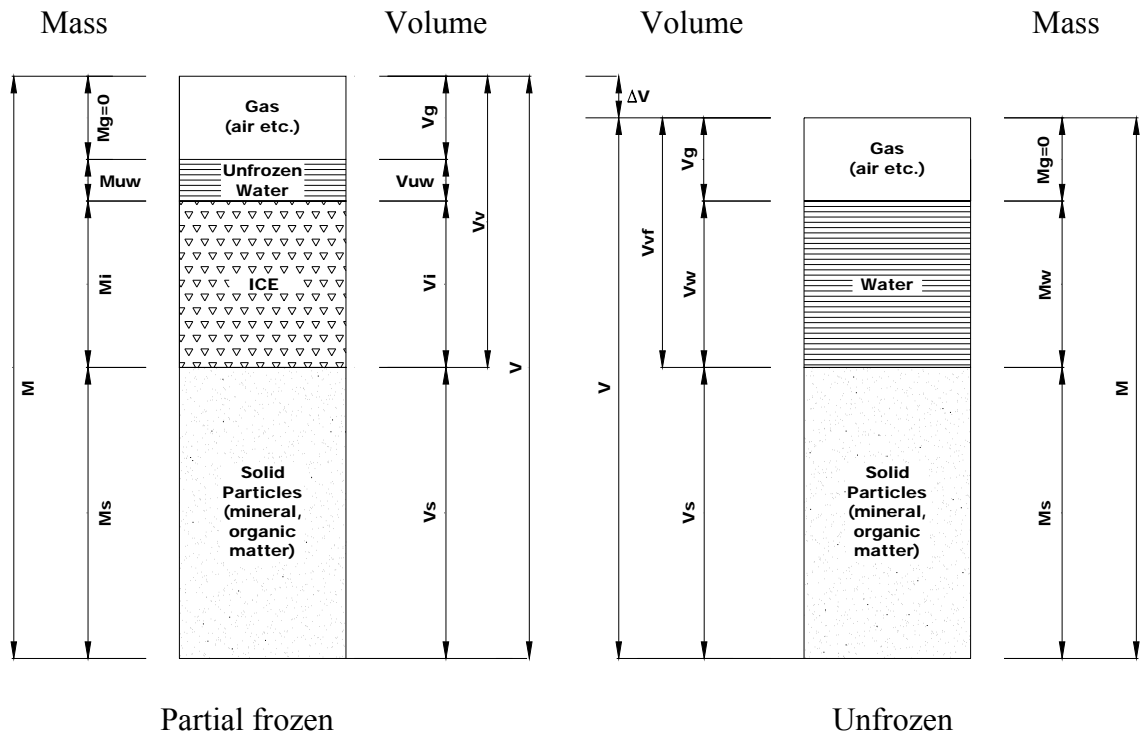


Figure 3-1: Mass/volume relationship for unfrozen and partially frozen soil.

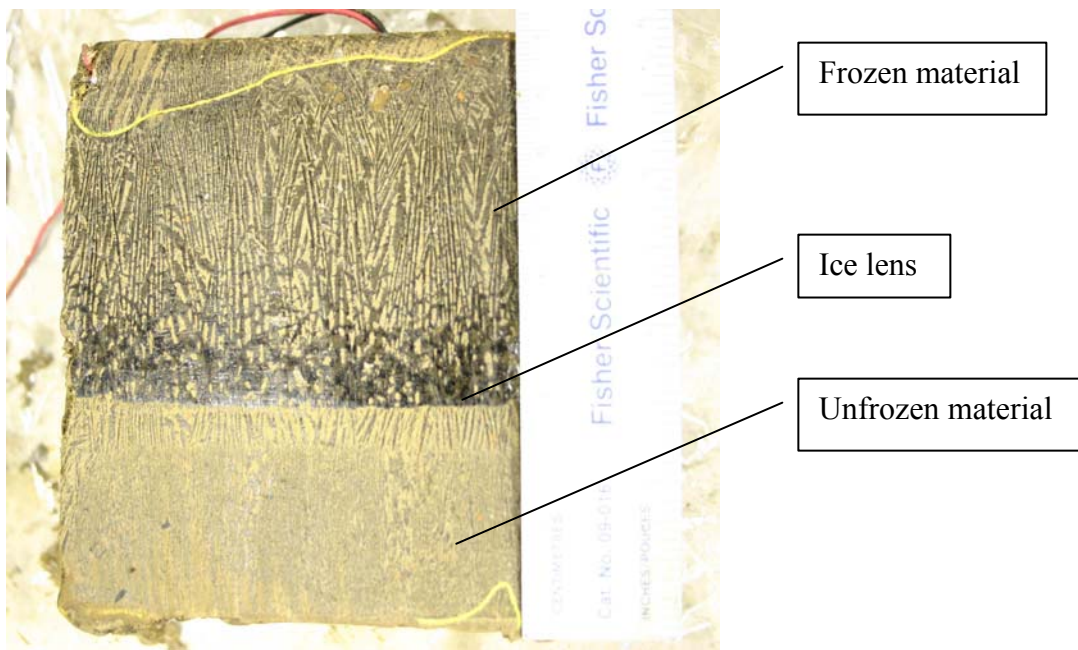


Figure 3-2: Frozen core sample showing ice lens formation, (Photograph taken by Bale, B.)

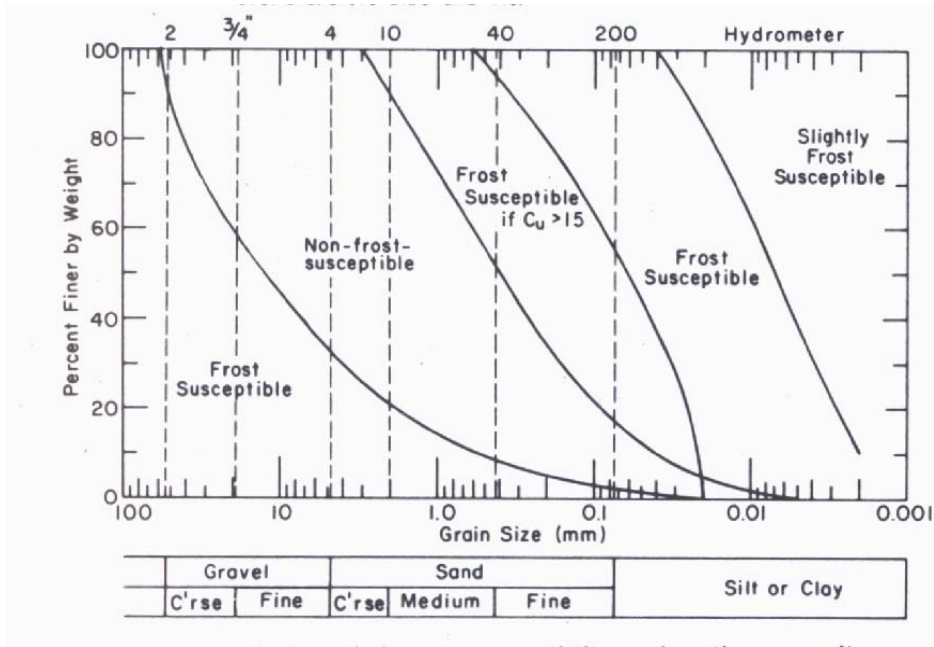


Figure 3-3: Limits of frost susceptibility of soils according to Chamberlain (1981)

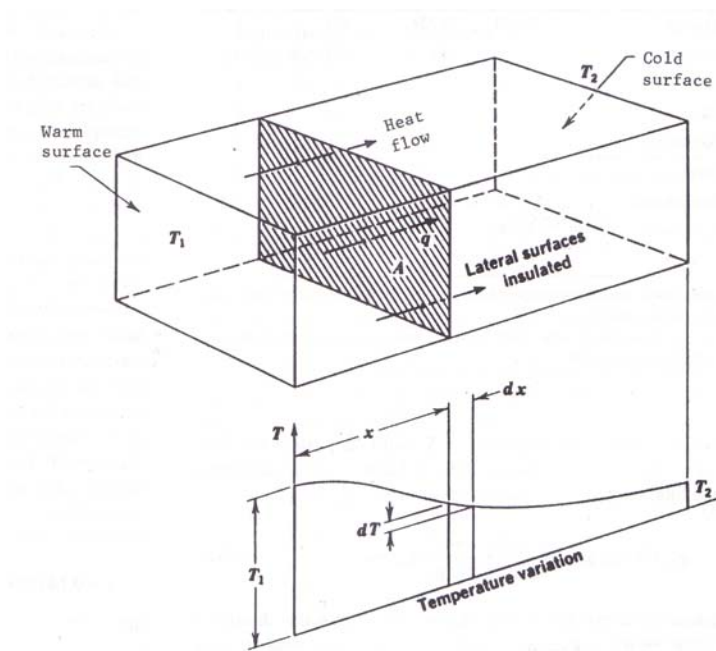


Figure 3-4: Schematic drawing of heat flow after Andersland and Ladanyi (2004).

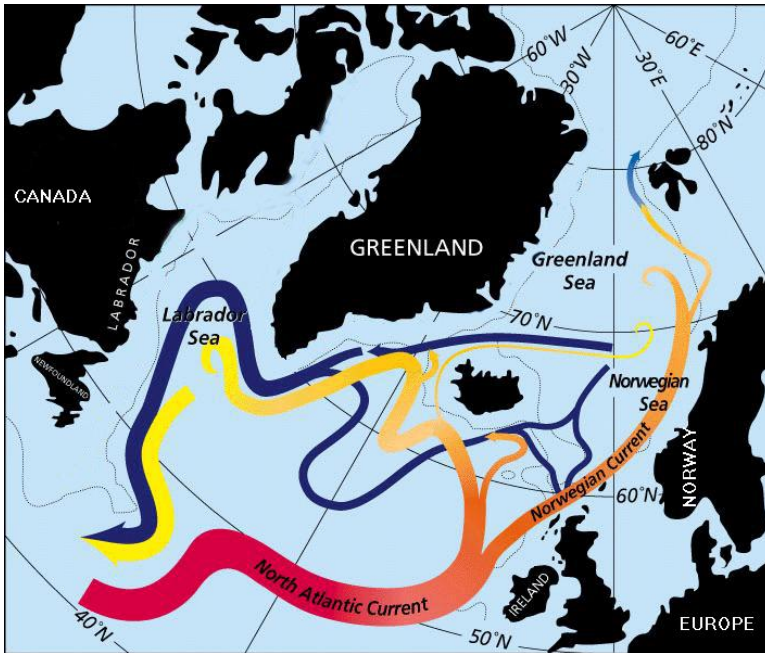


Figure 3-5: Schematic drawing of the ocean currents around Iceland from Calvin (1998)

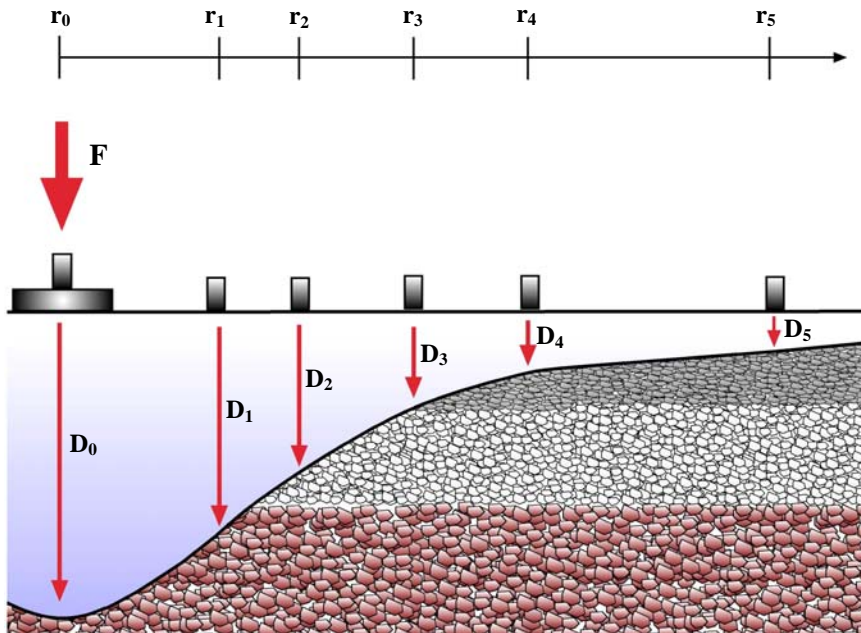


Figure 3-6: Typical deflection basin from Erlingsson (2004)

## **4. DATA COLLECTED**

### **4.1. Monitoring data from Icelandic road sections**

Since 1998, test-sections around Iceland have been monitored by the Icelandic Road Administration (ICERA). Two test sites in the southwest of Iceland were monitored from 1998-2000, measuring moisture content and temperature with depth in the road section, with nearby weather stations used to collect air temperatures. Some Falling Weight Deflectometer tests (FWD) were carried out between 1986 and 1999. The location of the test sites and nearby weather stations are shown in Figure 4-1 [Bjarnason et al. 1999]

In 2001, the instrumentation in southwest Iceland was excavated and re-installed in a road sections in northern Iceland to monitor two new sections. New and specially designed electrical conductivity probes were installed at both new test sites. A test site equipped only with the conductivity probe was installed during the fall of 2002 at Breidaváðsmelur (near Blönduós), and another in 2003 at Saudarkroksbraut. Figure 4-2 illustrates the locations of these sections. The electrical conductivity probe was improved in 2003 and a new version was installed at all four test locations.

Early in 2005, four new test sites were added, at various locations in Iceland. The improved electrical conductivity probes were installed at each site. The sites are at Ogur, Fagradalur, Myvatnsheidi and Hvalnes; their locations are shown in Figure 4-3

Two progress reports have been published about the test section in north Iceland; Erlingsson (2004b) and Erlingsson (2002a). The results from southwest Iceland have been studied and reports written about the project, [Bjarnason et al. 1999].

## **4.2. Monitoring stations and description of test sites**

The test sections are quite variable; the ones in southwest Iceland were constructed to monitor how an extra thin, low-volume road would withstand a typical design load. The test sections in northern Iceland are built according to the national design guidelines. The sites in north Iceland are part of Highway 1, the main land route that connects the less populated, rural areas of Iceland.

Some of the test sections have been evaluated carefully, while some have not been studied at all. At Vatnskard, for example, a pit was dug in the road, various equipment installed, and samples of the base layers and the subgrade were taken for testing. An automatic weather station has operated there for several years, therefore typical winter temperatures are well established. On the other hand, at the road section at Saudarkrokur (Stekkur), only one hole was drilled for the installation of the conductivity probe, and no further information is available.

### ***4.2.1. Sections 1.4.1 and 1.4.2 in southwest Iceland***

The sections are located in southwest Iceland, in Hvalfjorður, and is only at 15 meters above sea level (m.a.s.l). and therefore experiences mild winters. The freezing index for the winter 1998-1999 was 60°C days. The AADT (Average Annual Day Traffic) was

2044 in 1997 but fell to 445 in 1998 when a tunnel under Hvalfjorður was completed [Bjarnason et al. 1999].

In Table 4-1, the thickness of the layers is summarized for both test sections 1.4.1 and 1.4.2. The thickness is not sufficient, according to guidelines used by the ICERA. This particular road is a test project for studying how weak, low-volume roads would withstand environmental impact. The material used to construct the road purposely did not fulfill the requirements recommended by the design codes.

#### ***4.2.2. Section 3.2.3.1 in southwest Iceland***

Section 3.2.3.1 is located at Thingvellir, in southwest Iceland; the average annual daily traffic (AADT) is 370 vehicles and it is located at elevation 173 m.a.s.l. The average freezing index for 1999-2005 was 230°C days. Table 4-2 shows the thickness and classification of the layers. As with sections 1.4.1 and 1.4.2, the layer thickness and material quality do not follow the guidelines for low-volume highways.

All three of the previously mentioned sections were constructed in 1986 with 30mm bituminous surface. Various repairs on the sections have been made since 1986, such as repavement and crack filling. When the tests were carried out, the road surface was in good condition [Bjarnason et al. 1999].

#### ***4.2.3. Dyrastadir in northern Iceland***

Dyrastadir is located in northern Iceland at an elevation of 84 m.a.s.l. During winter 2001-2002, the freezing index (FI) was 316°C days. Information about traffic is not

available. The thicknesses of the layers in the road section are summarized in Table 4-3. The road was built on top of an existing road.

#### ***4.2.4. Vatnsskard in northern Iceland***

The test site at Vatnsskard is at an elevation of 427 m.a.s.l. and the thicknesses of the layers in the road section are shown in Table 4-4. The FI for winter 2001-2002 was 627°C days. Traffic data is not available for the test site. Grain size distribution for both Dyrastadir and Vatnsskard is available and presented in Appendix B

#### ***4.2.5. Blonduos in northern Iceland***

An electrical conductivity probe was installed on the 25<sup>th</sup> of October 2002. There is no data available about the cross-section or the traffic volume. The FI from 1995 to 2005 is on average 257°C days. The test site is at approximate elevation of 15 m.a.s.l.

#### ***4.2.6. Saudarkrokur in northern Iceland***

An electrical conductivity probe was installed on the 16<sup>th</sup> of December 2003. No data is available about the cross-section or the traffic. The test site is at approximate elevation of 20 m.a.s.l. The FI for winter 2004-2005 is 188°C days.

#### ***4.2.7. Recently installed test sections at various locations***

No meteorological data, traffic data, or cross-section information are available from the test sites at Ogur, Fagradalur, Myvatnsheidi or Hvalnes. The elevations of the sites have not yet been measured. These sites were installed at the beginning of 2005 and further investigation and testing of the road sections are planned.

Figure 4-3 shows the location of the test sections that are currently active; the figure is a screen-capture from a program that was developed for the ICERA to monitor the condition of the various test sections located around Iceland.

### **4.3. Data available**

Following is a summary of the data collected from the test sections at various time and locations. Table 4-5 provides an overview of the test sections in southwest Iceland, only monitored by temperature and moisture content sensors, which operated from 1998 to 2000. Table 4-6 summarizes the sections in northern Iceland which were installed in 2001 and are still running; the sections are monitored by temperature and moisture content sensors as well as electrical conductivity probes. Finally, Table 4-7 is a summary of recently installed equipment and the available data from the recently installed sections at the different locations in Iceland.

#### ***4.3.1. Data from test sections in southwest Iceland***

- Section 1.4.1 and 1.4.2. at Hvalfjordur (installed in 1998, operated until 2000).
  - 3 TDR moisture content probes at each section, 2 temperature sensors at section 1.4.1.
- Section 3.2.3.1 at Thingvellir (installed in 1998, operated until 2000).
  - 3 TDR moisture content probes, 2 temperature sensors.

#### ***4.3.2. Data from test sections in northern Iceland***

- Vatnsskard; installed on the 17<sup>th</sup> of October 2001

- 6 temperature sensors, 9 moisture content sensors (Imko and Campell), 1 air temperature sensor, 1 electrical conductivity probe with 16 temperature sensors and 16 conductivity sensors.
- Dyrastadir Nordurardal; installed on the 23<sup>rd</sup> of October 2001.
  - 6 temperature sensors, 9 moisture content sensors (Imko and Campell), 1 air temperature sensor, 1 electrical conductivity probe with 16 temperature sensors and 16 conductivity sensors.
- Breidavadsmelur (Blonduos); installed on the 25<sup>th</sup> of October 2002.
  - 1 electrical conductivity probe with 16 temperature sensors and 16 conductivity sensors.
- Stekkur (Saudarkrokur) installed on the 16<sup>th</sup> of December 2003.
  - 1 electrical conductivity probe with 16 temperature sensors and 16 conductivity sensors.

No test pit was dug during installation at Breidavadsmelur and Stekkur, therefore, no samples of the material were taken, but data from the nearby quarries are available.

By comparing the results from the electrical conductivity probe with the moisture content and temperature measurements at both Vatnskard and Dyrastadir, an estimation of the accuracy and reliability of the single conductivity probes at Breidavadsmelur and Stekkur can be made.

### ***4.3.3. Data from new test sections at various locations in Iceland***

Four sections were installed at various locations in Iceland; they are all equipped with the most recent edition of the electrical conductivity probe (16 temperature sensors and 16 conductivity sensors)

- Hvalnes; installed on the 1<sup>st</sup> of February, 2005.
- Myvatnsheidi; installed on the 31<sup>st</sup> of January, 2005.
- Ogur; installed on the 3<sup>rd</sup> of March, 2005.
- Fagridalur; installed on the 28<sup>th</sup> of January, 2005.

### ***4.3.4. Falling weight deflection***

Falling Weight Deflectometer tests were carried out in southwest Iceland, but they were randomly dated and the available data are not continuous. The tests began in 1986 and were carried out until 1999. During 1998 and 1999, the tests were more organized and the rates of measurements were increased during spring thaw.

In northern Iceland, FWD tests were carried out at Dyrastadir and Vatnsskard, with data available from 2001 and to present. This data is more useful than the data from the test sites in southwest Iceland, because the tests were more consistent and frequent, especially during spring thaw. However, the tests were seldom carried out long enough into the summer to measure how the road section regained its strength following spring thaw.

### ***4.3.5. Frost tubes***

Until a few years ago, decisions about axle load limitations in Iceland were primarily based on data from 90 frost tubes installed at various locations around the island. Approximately 15 measurements have been taken from each tube each winter, with data

available from 1999–2004. Each measurement estimates depth to the frost lens from the surface and thickness of the lens [Ingólfsson and Bjarnason 1985]. This information could be useful when comparing the moisture content and electrical conductivity of frozen and unfrozen soil. The external situation is known (air temperature) and the temperature profile in the frozen soil, is known as well. Therefore, the material properties of the soil can be determined.

#### **4.4. Description of testing equipment**

At the test sites there is a data logger (from Imko Micromodultechnik GmbH, Germany) and a transmitting device. The data logger records the data from the instruments hourly and sends it to be processed each week during winter and spring and approximately biweekly during summer and fall. The typical equipment setup is shown in Figure 4-4, with the data logger and the transmitting device at the side of the road.

##### ***4.4.1. TDR moisture content probes***

The moisture content varies significantly depending on seasonal conditions (freeze or thaw) but, not so much on precipitation [Bjarnason et al. 1999]. The moisture content is measured with a TDR equipment, (Time Domain Reflectometer), that measures the unfrozen volumetric moisture content based on electromagnetic technology. An electrical pulse is transmitted into the soil and the time it takes to travel the known distance is calibrated against the moisture content of the soil, assuming certain fixed soil density [Bjarnason et al. 1999]. The calculation of the dielectric constant is based on the time it takes to travel the known distance. The dielectric constant can be converted to the unfrozen volumetric moisture content by using Topp's equation [Topp et al. 1980]. The

TDR determines the unfrozen volumetric moisture content; since when the water freezes, the ice becomes a solid material with a different dielectric constant. The moisture content probes are from the manufacturer IMKO and the brand name is Trime EZ. The probes are cylindrical, with two rods pointing out; Figure 4-5 shows both Imko and Campell TDR equipment.

The sensors are mounted in predrilled holes in the undisturbed road section, because the probes are sensitive to air gaps in the soil. The undisturbed road section is very dense and it is important to keep it as intact as possible.

The moisture content probe measures the unfrozen volumetric moisture content, or the ratio between the volume of unfrozen water in the sample and the total volume of the sample, as in Equation 4-1. However, the gravimetric moisture content, using the weight of the water versus the total weight of the sample, (Equation 4-2) is more widely used in geotechnical engineering.

$$W_{\text{vol}} = \frac{V_{\text{water}}}{V_{\text{tot}}} \quad [4-1]$$

$$W_{\text{grav}} = \frac{m_{\text{water}}}{m_{\text{dry}}} \quad [4-2]$$

The dry density of the soil surrounding the probes is assumed to be  $1400 \text{ kg/m}^3$ , and if not the correction has to be made using:

$$w_{vol}^{corr} = w_{vol} - \left( 12.12 \cdot \frac{\rho_{dry}}{\rho_w} - 17.05 \right) \quad [4-3]$$

Where:

$\rho_{dry}$  = dry density of the soil

$\rho_w$  = density of water

$w_{vol}$  is the measured volumetric moisture content

$w_{vol}^{corr}$  is the corrected volumetric moisture content

If gravimetric moisture is to be calculated, Equation 4-4 can be used to convert volumetric moisture content to gravimetric moisture content.

$$w_{grav} = \frac{\rho_w}{\rho_{dry}} \cdot w_{vol}^{corr} \quad [4-4]$$

The sensors from the manufacturer Imko have proved to be reliable; the accuracy of the probes is approximately  $\pm 0.1\%$  [Bjarnason et al. 1999].

#### **4.4.2. Campell scientific moisture content probes**

Moisture content probes from Campell scientific have been used at previous test sections, however, they can not be synchronized with the Imko data logger and are not capable of transmitting data automatically. Therefore maintenance personnel have to travel to the locations of the test sections and manually download the information. The fact that the information cannot be accessed as easily as with the Imko equipment, has made the Campell equipment less desirable. When something breaks down in the Imko equipment it is usually noticed immediately and fixed as soon as possible. However, when the

Campell equipment breaks down there is no notification, therefore there tends to be long periods without the data; overall, the Campell equipment is less reliable than the Imko ones.

At the beginning of the project, the Campell equipment was used for comparison and confirmation of the Imko equipment. Currently, the Campell equipment is mostly ignored.

#### ***4.4.3. Electrical conductivity probe***

The design of the electrical conductivity probe is funded by the Icelandic Road Administration. It is still being developed and the probes installed at the most recent test sites are designed to be economic in production. The first version was installed in 2001 (in northern Iceland) and the second version in 2003. Currently, to the author's knowledge, there are 9 installed probes which are hourly gathering measurements of the conditions in the road section.

The electrical conductivity probe is a cylinder 112 cm in height and 5 cm in diameter; 16 temperature sensors and 16 electrical conductivity sensors are attached on probe (Figure 4-6). The sensors are located at the following depths (cm) from the surface: 10, 15, 20, 25, 30, 35, 40, 50, 60, 70, 80, 90, 100 and 110.

Moisture content and electrical conductivity change quickly and dramatically during the phase change of water (thaws or freezes) but the temperature changes more gradually.

Therefore, relative conductivity or moisture contents are more accurate than temperature in determining the actual state of the road section.

One critical problem with the previous versions of the probes occurred. The material surrounding the probes was coarse and did not hold the moisture sufficiently, causing unreasonable fluctuations in the measurements. If the top layer of the road thawed, then water could flow along the coarse material surrounding the probe, causing the conductivity to increase unreasonably at more depth.

The installation technique was altered slightly. Now the probe is installed by drilling a hole (10 cm diameter) in the road and sliding the rod into it, and then a silty soil [grain size distribution is shown in Appendix B, Figure B-3] is compacted around the probe. When using material that has fine grain size distribution, the conductivity changes more gradually and reasonably. The flow of water along the rod is limited and the silty material holds the moisture close to the probe.

Electrical conductivity is, by definition, the capability of a material to transport electrical charges. The material in the road is gravel, water (frozen or liquid) and air. The conductivity of the air and gravel can be considered constant with temperature because the change in conductivity caused by the phase change of the water is much more significant. The salinity and other chemicals in the water, greatly affect the conductivity and the freezing point, but it can be assumed that the amount of those chemicals do not

change with time. The conductivity of purified water is three orders of magnitude less than surface water in the mountains with its dissolved minerals.<sup>1</sup>

When water is in liquid form, the ions in the liquid are more capable of transferring the electrical charges than if they are in a solid, more rigid and crystallized state of ice. Therefore a decrease in conductivity can be expected when the water goes through the phase change (liquid to solid). Using the same arguments, the conductivity should be maximized during spring when the road is thawing and the soil is saturated. A decrease should be noticed when the road drains again, since the air in the voids of the soil is normally a poor conductor.

As explained above, conductivity is the ability of a material to transport particles with electrical charges. The inverse of conductivity is resistivity, the ability to hold particles with electrical charges. For some reason, the literature has focused considerably more on the resistivity of soil rather than the conductivity. In Table 4-8, these concepts and units are explained.

Figure 4-7 [Hoekstra and McNeill 1973] describes the resistivity for three types of soils and one rock type. The resistivity for saturated sand and gravel is of particular importance to this thesis. The resistivity drops as the gravel reaches 0°C, while the conductivity does exactly the opposite (since it is the inverse of resistivity). Therefore, it can be expected that the conductivity is lower for frozen soil than it is for thawed (saturated) soil.

---

<sup>1</sup> <http://www.phoenixelectrode.com/conductivityguide.php> (18 November 2005)

Archie's law, Equation 4-5, gives the ratio between the electrical resistivity of a rock mass and pore fluid given information about the porosity of the rock mass. The most practical application for Archie's law is to measure the electrical resistivity of a rock-mass and its pore fluid directly and this gives an estimate of the porosity. The relationship was designed for solid rock-mass but can be used on coarse material. As shown in Figure 4-7 the resistivity of Biatite Granite (0.1% moisture content) and sand and gravel (saturated) is quite similar. Archie's law can not be used if the sample contains clay, because the resistivity of the clay dominates the evaluation.

$$E_{\text{rock}} = E_{\text{fluid}} \times a \times n^{-m} \quad [4-5]$$

Where:

$E_{\text{rock}}$  is the electrical resistivity of the rock

$E_{\text{fluid}}$  is the electrical resistivity of the pore fluid

$a$ , and  $m$  are constants depending on the geometry of the pores, typical values for  $a$  and  $m$  are 1 and 2 respectively

$n$  is the porosity of the rock.

Figure 4-8 shows relative (see section 4.4.4) conductivity measurements at 45 cm depth during the 2003-2004 season at Vatnskard. The relative conductivity in the section is around 40%, and slowly increases to approximately 60% in the fall, mostly because of increased precipitation and reduced evaporation. By the 1<sup>st</sup> of December, the road section is frozen to 45 cm depth (indicated by the low conductivity) and the section stays frozen until the middle of March. During spring thaw, the conductivity suddenly increases

because of excessive water (the section is oversaturated). As soon as the road drains, the conductivity decreases again, to a summer value of around 40%.

In Figure 4-9, the conductivity measurements in the test section at Dyrastadir is examined for the period of spring 2002 to spring 2006. The data are rather discontinuous, but a certain trend, concerning the cyclic pattern during spring and winter, thawing and freezing, is clear. The relative conductivity drops during winter and suddenly spikes during spring thaw. Frozen sections have electrical conductivity approximately around 15-30%, whereas when the road is oversaturated and/or thawing, measurements of the conductivity are often near 100%.

Figure 4-10 presents the data from Vatnsskard (spring 2002 to spring 2006) which is more consistent than at Dyrastadir (Figure 4-9). The same behaviour as before can be observed: low conductivity during winter and then during spring, the conductivity peaks because of excessive water during thaw. The measurements from 2002 are from the first version of the probe; the rather high values observed during summer are not present in the measurements from the second version of the probe. It is interesting to look at the data for summer 2005 and see how the conductivity represents the drainage of the road section, as the conductivity slowly decreases as the water drains.

The characteristics of the electrical conductivity measurements are therefore similar to what could have been expected from previously published literature.

The measured drop in the moisture content (as described in Section 5.3 and Figure 5.8) during winter is because the TDR only measures the unfrozen moisture content (gravimetric or volumetric); as soon as the water freezes, it is not included in the moisture content. The TDR sends out an electromagnetic pulse and measures the time it takes for it to travel a known distance, and from that information it calculates how much water (liquid) there is on average in the sample. However, the drop in electrical conductivity is because of the difference in material properties of liquid water and the solid state of ice. The liquid water conducts much better than the ice. The reason why the electrical conductivity of the soil decreases in the winter is therefore not quite the same as the reason why the moisture content measured by the TDR decreases. However it is worth looking into if there is any mathematical relationship between the two decreases.

#### ***4.4.4. Calibration of the electrical conductivity probe***

The probe was calibrated so that a completely dry (or frozen) sample should show 0% “relative conductivity”, while a completely saturated sample should show 100%.

A probe was fitted in a plastic bottle, the silty material compacted around the probe, and the material was then frozen and thawed for different moisture contents. By repeating this process, calibration for the probe was achieved. This calibration has proved to be quite accurate; most of the values lie within the 0-100% range and in the cases when the values are higher than 100%, the sample is most likely oversaturated.

#### ***4.4.5. Falling weight deflectometer test***

As explained in section 3.5, a 500 kg load was dropped on the center of the lane and deformations were measured at fixed locations, 0 to 90 cm from where the load is dropped. The trailer with the FWD equipment is driven around the highways, stopping at predefined locations, which are repeatedly tested. From the measured deformations of the road section, the stiffness modulus and other parameters indicating the conditions of the test section can be derived.

#### ***4.4.6. Frost tubes***

The frost tubes are made of two pipes; an approximately 4 cm diameter transparent pipe is put in an approximately 5 cm diameter pipe. The inner pipe is sealed off and filled with liquid that is blue when it is unfrozen but white when it freezes. The colouring material does not change the freezing point of the water. The pipes are installed in the center of the road by drilling a hole and then attaching the larger diameter pipe to the asphalt. The inner pipe can slide up and out of the bigger diameter pipe, allowing monitoring personnel to lift the inner tube and measure the frost depth. The pipes were approximately 1.5 m long and the thermal properties of the pipes do not affect the heat flow with the material that surrounds the tube [Ingólfsson and Bjarnason 1985]. Over 90 tubes have been installed in the Icelandic road system by the ICERA and for many years the Icelandic Road Administration mainly used information from those frost tubes to decide when to apply load restrictions.

## 4.5. The road cross-section

Iceland is a sparsely populated country; Highway 1 goes around the island, connecting villages. The road is almost always just one lane in each direction, and would probably be considered a typical low-volume highway (maybe even secondary highway) in Canada. However, Highway 1 is very important since most commercial goods for the villages are transported by trucks. Ships used to sail around the island but the delivery time and quality of service have been improved by using trucks.

The Icelandic Road Administration has its own quality control regulations, which are mostly based on Norwegian standards. When designing roads, the Norwegian standards are used<sup>2</sup>, a few regional design rules have been created, and are followed because of previous experience of local conditions.

Typically, there is a 2.5 cm asphalt cover (surface dressing), underlain by 5-15 cm of base material. The subgrade varies in thickness but a layer thickness of about 50 cm is not uncommon. Base and subgrade layers are often divided up in two layers, for example, upper and lower subgrade. Figure 4-11 shows two options for road sections, according to Icelandic guidelines [Erlingsson 2002b].

There is seldom a shortage of gravel in Iceland. If a grain size distribution curve for a material shows that less than 3% is smaller than 20  $\mu\text{m}$ , then the material is considered frost-free. If 3-12% of the total mass of the material is less than 20  $\mu\text{m}$ , it is classified as

---

<sup>2</sup> <http://www.vegvesen.no/vegnormaler/> accessed the 13<sup>th</sup> of October

being a little frost sensitive material; there are two other classifications: average and very frost sensitive. Gravel or sand is almost always frost free or little frost sensitive. Frost susceptibility is discussed in more detail in Chapter 3.

The road must isolate the native soil, especially if the soil is frost sensitive such as peat. If the frost penetration depth is more than the thickness of the road section, the road will probably frost heave. Frost heaving may not cause damage to the road, if the entire road lifts equally and slowly settles again, but it can put extra strain on the road, especially on the asphalt. At the sides of the road, where the cross-section is thinner, the road cannot isolate the native soil. Therefore, deformations often occur at the sides of the road section, but if the road is designed adequately, the deformations will not affect its use.

Drainage is vital to the integrity of the road. If there is no water in the road section, a lot of problems can be avoided, but that is seldom the case. Rain enters the road-structure through cracks in the asphalt, although roads are usually designed with a slight slope that causes the water to run off to the shoulders of the road. The coarse material in the road usually drains quickly, but if there is an impermeable layer, such as an ice lens or frozen soil, the water is trapped. The ground water table is usually not in the road structure itself, but if the road is, for example, built into a slope where water is present, some preventive measures must be taken. Drains or geotextile could for example be installed.

The design of a road depends on the type of road (freeway, highway, secondary highway, or country road), the traffic and the forecasted development, and the percentage of the

traffic that is heavy vehicles. Allowable axle load, available material, the material properties and the native soil on which the road is going to be built must be considered [Erlingsson 2004a]

The roads in Iceland are designed for a 10-ton axle load (11.5 on the driving axle), however, there are all kinds of exceptions-restrictions to the law, depending on the type of tires, trailers, the number of axles and spacing between them, and so on. Studies [Kestler et al. 1997] have shown that trucks with reduced tire pressures cause less damage therefore they are subjected to less restrictions. Heavy trucks with multiple axles tend to create high cyclic pore pressures that cause considerable damage to the road section, and therefore are subjected to more strict regulations. The regulations can be accessed online<sup>3</sup>.

## **4.6. Summary**

This chapter summarizes the development in equipment used to evaluate spring load restrictions in Iceland over the last two decades. Starting with simple frost tubes, later moisture content and temperature sensors were installed, and most recently development of an electrical conductivity probe. Summary of available data is given in this chapter as well as description of the equipment and testing methods used to acquire the data. The ongoing projects to improve decisions regarding SLR at the ICERA are described and future plans introduced.

---

3

<http://reglugerd.is/interpro/dkm/WebGuard.nsf/538c26748c8e2a9d00256a07003476bd/001c81acbddd2f0120025704300567a93?OpenDocument>

## 4.7. References

- Bjarnason, G., Erlingsson, S., Petursson, P., and Thorisson, V. 1999. Constructed Unbound Road Aggregates in Europe (COURAGE) Icelandic Final report. Public Road Administration Iceland.
- Erlingsson, S. 2004a Mechanistic Pavement Design Methods – A Road to Better Understanding of Pavement Performance, Nordisk Vejteknisk Forbund -Via Nordica 2004, Copenhagen, June 7-9th, 8 pages
- Erlingsson, S. 2004b. Mælitækni til strýringar á þungatakmörkunum, Áfangaskýrsla 2, Icelandic Road Administration/University of Iceland. [in Icelandic].
- Erlingsson, S. 2002a. Mælitækni til strýringar á þungatakmörkunum, Áfangaskýrsla 1, Icelandic Road Administration/University of Iceland [in Icelandic]
- Erlingsson, S. 2002b. 3-D finite element analyses of test road structures – Comparison with measurements, Proceedings 6<sup>th</sup> International conference on the bearing capacity of roads, railways and airfields BCRA 2002, Lisbon, Portugal, pp. 145-157.
- Hoekstra, P., and McNeill, D. 1973. Electromagnetic probing of permafrost. In North Am. Contrib., 2<sup>nd</sup> International Conference on Permafrost, Yakutsk, U.S.S.R. Washington, D.C. National Academy of Sciences, pp 517-26.

Ingólfsson, G. and Bjarnason, G. 1985 (3). KUAB 50 Sænska falllóðið, Ný aðferð við mælingar á burðarþoli vega. Vegamál fréttabréf (Icelandic Road Administration) 8. árg. – 3.TBL, 12-16, [In Icelandic].

Kestler, M. A., Berg and R. L. and Moore T. L. 1997. Reducing damage to low-volume roads by using trucks with reduced tire pressures. Transportation Research Record, 1589: 9-18.

Topp, G.C., Davis, J.L., and Annan, A.P. 1980. Electromagnetic determination of soil water content: Measurements in coaxial transmission lines. Water Resources Research, 16, 574-582.

## 4.8. Tables

Section	Layer	Thickness [cm]	USCS
1.4.1	Base course	15	GW-GM
	Subbase 1	25	GW-GM
	Subbase 2	45	SW-SM
1.4.2	Base course	13	GW-GM
	Subbase 1	25	SM
	Subbase 2	56	SW-SM

Table 4- 1: Thickness and classification of layers in sections 1.4.1. and 1.4.2. [Bjarnason et al. 1999]

Section	Layer	Thickness [cm]	USCS
3.2.3.1.	Base course	15	SP
	Subbase 1	29	SP
	Subbase 2	50	SP-SM

Table 4- 2: Thickness and classification of layers in section 3.2.3.1 [Bjarnason et al. 1999]

Section	Layer	Thickness	USCS
Dyrastadir	Bituminous surface dressing	7	
	Base course 1	9	GW
	Base course 2	16	GW
	Subbase	12	GP-GM
	Subbase	20	GW
	Subgrade	-	GP

Table 4- 3: Thickness and classification of layers in the section at Dyrastadir [Erlingsson 2002a]

Section	Layer	Thickness	USCS
Vatnskard	Bituminous surface dressing	3	
	Base course	17	GP-GM
	Subbase	40	GW-GM
	Subgrade	-	-NA- (sand)

**Table 4- 4: Thickness and classification of layers in the section at Vatnskard [Erlingsson 2002a]**

Sections	Elevation [m a.s.l.]	Temperature Sensors	Moisture content. probes	FWD	Air temperature
1.4.1.	14	2	3	YES	NO*
1.4.2.	15	-	3	YES	NO*
3.2.3.1.	173	2	3	YES	NO*

\*Nearby weather-stations used for approximate readings

**Table 4- 5: Overview of available data from test sections in southwest Iceland.**

Section	Elevation [m.a.s.l.]	Air temperature	Temp. sensors	Moisture content		FWD	Electrical Conduct. probe	Grain size distribution
				Campell	Imko.			
Vatnsskard	427	Yes	6 (16)*	6	3	Yes	Yes <sup>‡</sup>	Yes
Dýrastaðir	83.6	Yes	6 (16)*	6	3	Yes	Yes <sup>‡</sup>	Yes
Blonduos	~15	Yes	Yes (16)*	No	No	No	Yes <sup>†</sup>	No <sup>+</sup>
Stekkur	~20	Yes	Yes (16)*	No	No	No	Yes <sup>§</sup>	No <sup>+</sup>

\*There are 16 temperature sensors on each probe.

<sup>‡</sup> Installed March 2002; 16 conductivity sensors, were replaced in January 2003 at Dyrastadir and in March 2003 at Vatnsskard; 16 temperature- and 16 conductivity-sensors.

<sup>†</sup> Installed October 2002 but replaced in March 2003; 16 temp.- and 16 conductivity-sensors.

<sup>§</sup> Installed December 2003 16 temperature- and 16 conductivity-sensors.

**Table 4- 6: Overview of available data from test sections in northern Iceland.**

	Air temperature	Temperature Sensors	Electrical Conductivity probe
Hvalnes	Yes	16 in the probe	Yes
Myvatnsheidi	Yes	16 in the probe	Yes
Ogur	Yes	16 in the probe	Yes
Fagridalur	Yes	16 in the probe	Yes

**Table 4- 7: Overview of available data from recently installed sections at various locations in Iceland.**

Measurement	Application	Units
Resistance	Electrical circuit	Ohm ( $\Omega$ )
Conductance	Electrical circuit	ohm-1 ( $\Omega^{-1}$ ) = siemens (S)
Resistivity	High purity water	Ohm·cm ( $\Omega\cdot\text{cm}$ )
Conductivity	Most water samples	siemens/cm (S/cm)

**Table 4- 8: Resistivity/conductivity and appropriate units<sup>4</sup>**

<sup>4</sup> [http://www.wileywater.com/Contributor/Sample\\_2.htm](http://www.wileywater.com/Contributor/Sample_2.htm) (accessed 18 November 2005)

## 4.9. Figures



Figure 4- 1: Map of test sections in southwest Iceland and nearby weather stations [Bjarnason et al. 1999]



Figure 4- 2: Map of test locations in northern Iceland [Erlingsson 2004b]

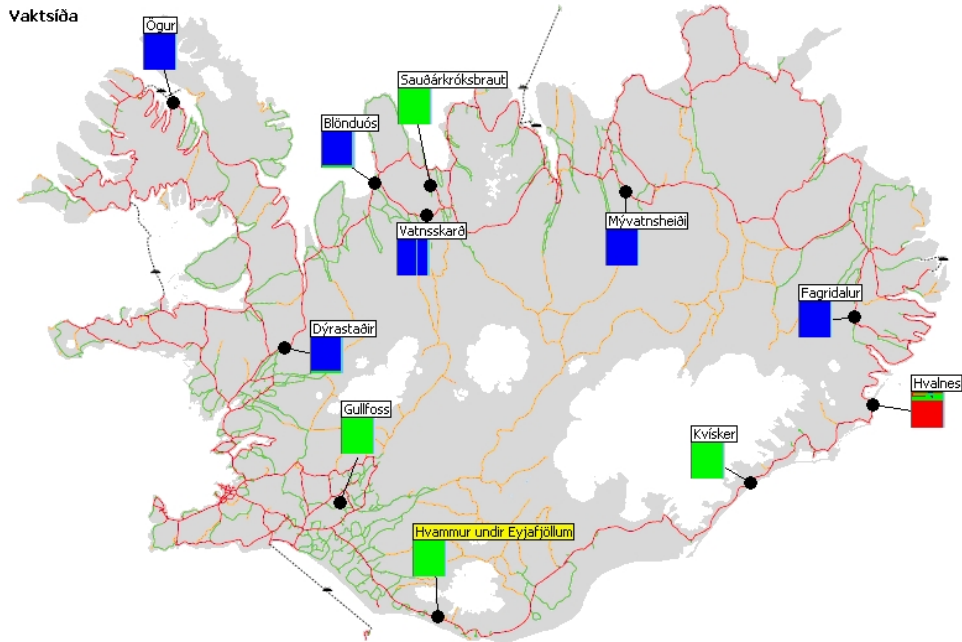


Figure 4- 3: Screen-capture from a monitoring program for the Icelandic test sections shows the approximate location.



Figure 4- 4: Data logger and transmitting device [Erlingsson 2002a].

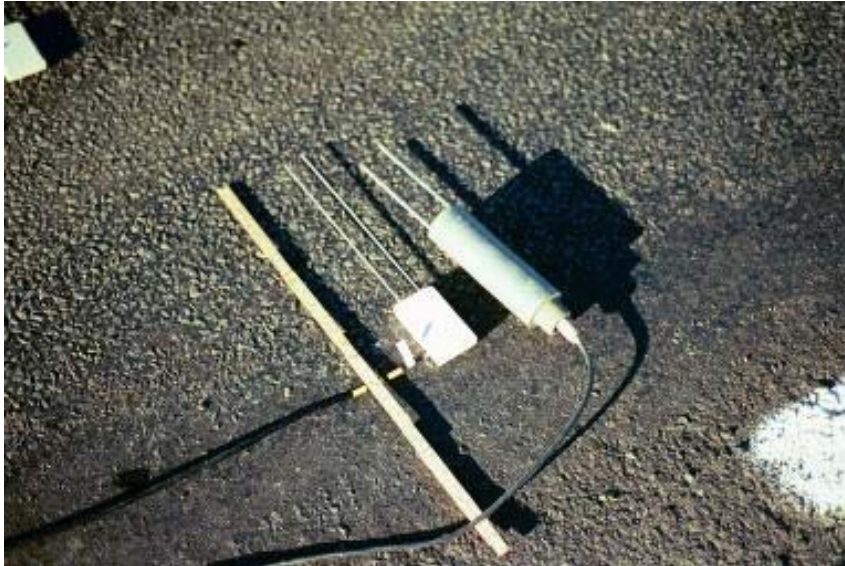


Figure 4- 5: IMKO (right) and CAMPPELL (left) moisture content probes [Erlingsson 2002a]



a)



b)



c)

Figure 4- 6: Pictures taken from the installation of one of the conductivity probes. [Erlingsson 2004b]

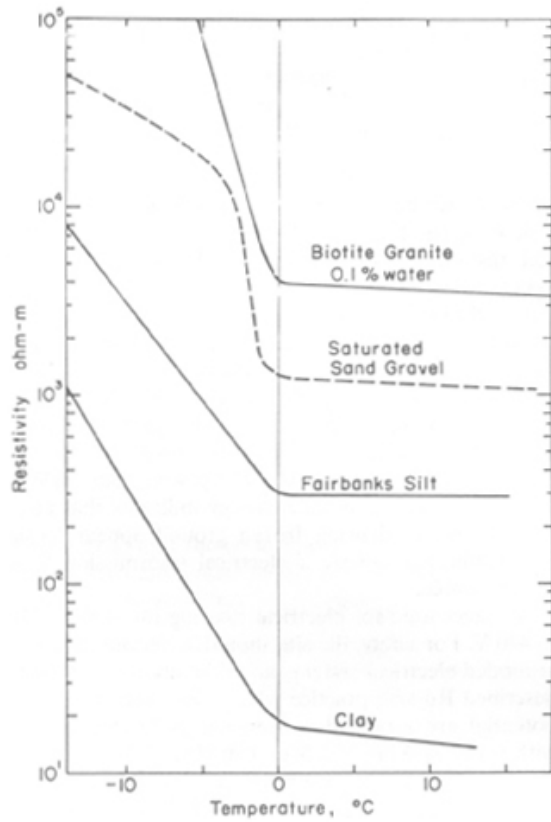


Figure 4- 7: Resistivity of various materials changing with temperature [Hoekstra and McNeill 1973]

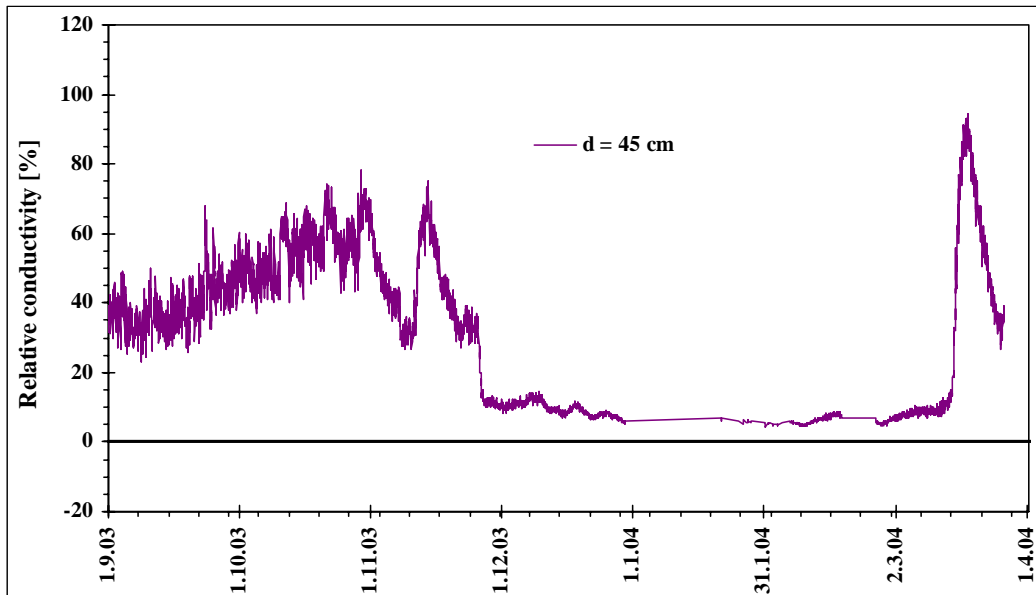


Figure 4- 8: Conductivity measurements from Vatnsskard winter/spring 2003-2004, at 45 cm depth in the road section

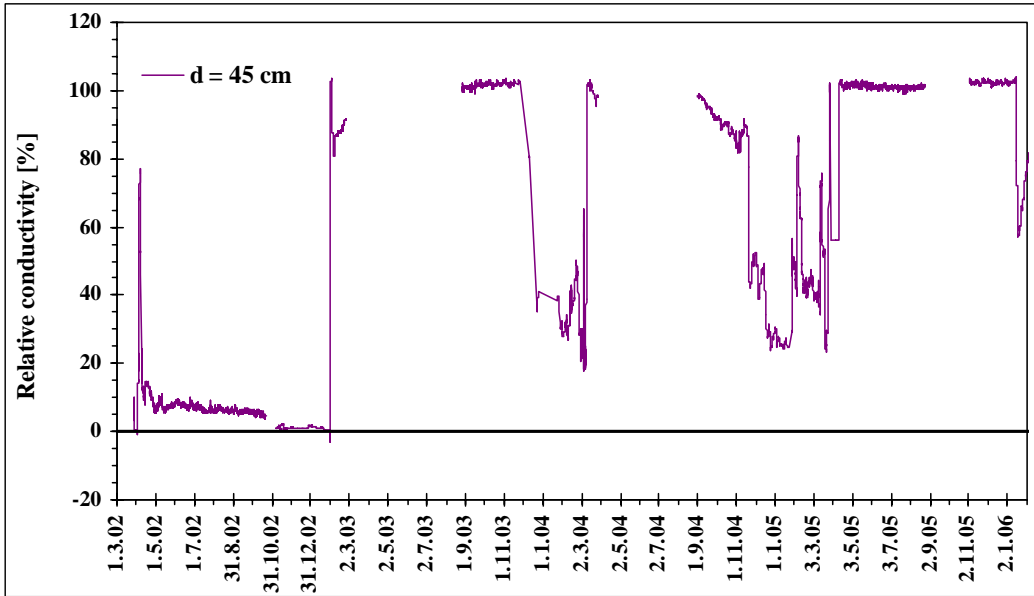


Figure 4- 9: Conductivity measurements from Dyrastadir 2003-2005, at 37cm depth in the road section.

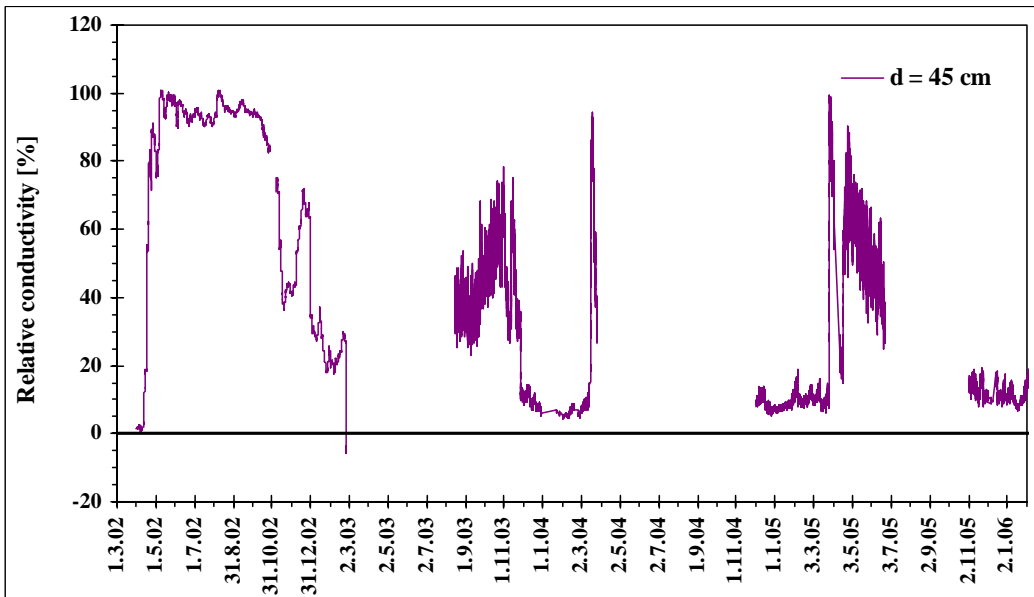
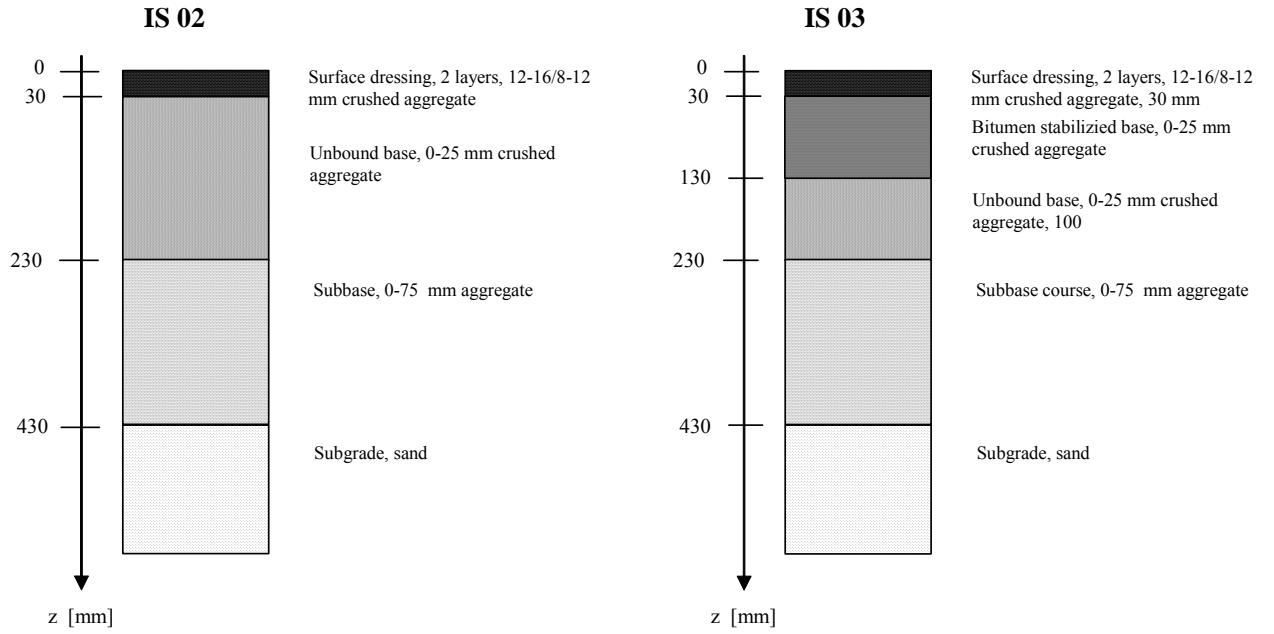


Figure 4- 10: Conductivity measurements from Vatnsskard 2002-2005, at 45cm depth in the road.



**Figure 4- 11: Two options for a road sections according to Icelandic design guidelines. [Erlingsson 2002b]**

## **5. IMPORTANT PARAMETERS**

### **5.1. Introduction**

In this chapter, data collected by the Icelandic Road Administration (ICERA) over the last several years is analyzed and presented. The project started by gathering data from road sections in the south west of Iceland. Soil temperature and moisture content with depth, as well as air-temperature were collected at three sections at two different locations. Later, a more advanced monitoring system was used at numerous locations in northern Iceland. The advanced stage of monitoring of the road at a number of locations is still ongoing. An electrical conductivity probe was specially designed by the ICERA to measure the conductivity and temperature with depth within the road cross-section. At each location, air temperature is measured independently. For the first two locations established in north Iceland, moisture content and temperature with depth were also monitored for comparison and calibration of the newly designed electrical conductivity probe. Currently, more probes are being installed at new locations thus adding to the available data on the freezing and thawing conditions in various road cross-sections.

In this chapter the objective is to analyze the data and try to evaluate which parameters are of importance in determining the bearing capacity of the roads during thawing periods. The relationship between electrical conductivity, moisture content, and temperature will be explored.

## 5.2. Air temperature

At most locations, the air temperature is monitored. From the air temperature two useful parameters can be derived; namely the freezing and thawing indices (FI and TI). It is relatively simple to monitor the air temperature; therefore, many empirical formulas using FI and TI have been derived and are reported in the literature.

Road administration agencies in Minnesota, Washington, Finland, and others have calibrated FI and TI for their local conditions [Ovik et al. 2000] to road performance. As a result, the agencies responsible for roads at these locations can predict thawing of a road cross-section with reasonable accuracy solely based on the local air temperature.

Equations 5-1 and 5-2 for FI and TI respectively are widely used in evaluation of freeze and thaw within soils and road cross-section.

To successfully carry out the calibration, simultaneous measurements of the moisture content and air temperature have to be available. This data is available for several of road cross-sections in Iceland.

$$FI = \sum (0^{\circ}\text{C} - T_{mean}) \quad [5- 1]$$

$$TI = \sum (T_{mean} - T_{ref}) \quad [5- 2]$$

Where:

$FI$  is the freezing index [degree days]

$TI$  is the thawing index [degree days]

$T_{mean}$  is a daily average temperature in  $^{\circ}\text{C}$

$T_{ref}$  is the reference freezing temperature which varies as pavement thaws, in  $^{\circ}\text{C}$ .

The reference temperature is a variable depending on the local conditions. It is determined by evaluating when thaw begins using the moisture content, electrical conductivity or similar measurements that estimate the conditions within the road cross-section. The average air temperature at the beginning of thaw (around 3-4 days) is taken as  $T_{ref}$ . The thawing of the road does not start when the air temperature is at  $0^{\circ}\text{C}$ . Typical values ranges from -1.5 to -5  $^{\circ}\text{C}$  according to Ovik et al. (2000) and van Deusen et al. (1997). The reason that  $T_{ref}$  is usually lower than  $0^{\circ}\text{C}$  is due to solar radiation, salinity of the water, traffic loading, or other factors that contribute to a reduction of the phase change temperature. The thawing index calculated from the air temperature records does not account for the solar radiation affects on the road, thus thaw occurs prior to when air temperature data would predict through use of temperature boundary conditions alone.

In Ovik et al. (2000), the  $T_{ref}$  starts at  $-0.9^{\circ}\text{C}$  in January,  $-2.3^{\circ}\text{C}$  in February and  $-4.3^{\circ}\text{C}$  in March to account for increasing number of solar hours per month, this results in warming

of the dark pavement surface. Saarelainen (in press), discusses the importance of distinguishing between the air temperature and ground temperature at a given location.

The  $T_{ref}$  in the thawing index determination varies throughout the year due to variation in the solar radiation received at different locations. During winter (November –February), little effect is observed, since thawing usually does not occur. However, during March-May, a significant increase in solar radiation is observed and should be included in thaw evaluations. The article from Saarelainen (in press) contains theoretical evaluations of this thawing mechanism.

An example of how  $T_{ref}$  is determined is shown in Figures 5-1 and 5-2 based on data measured in the 2001-2002 season at the Dyrastadir test location. It is assumed that thawing starts on the 26<sup>th</sup> of March and the average temperature for the 26<sup>th</sup> to the 28<sup>th</sup> of March is approximately -1.5°C (see also in Appendix C) therefore  $T_{ref}$  is set to that value. Similar results were achieved using the data from Thingvellir (1998-1999). Thawing was again assumed to take place on the 17<sup>th</sup> of April, resulting in an average value of -1.8°C for  $T_{ref}$ , (see Appendix D).

These calculations of  $T_{ref}$  could be redone for a few seasons at the same location to establish more reliable values of  $T_{ref}$  and be used to assist with establishing the onset/removal of spring traffic load restrictions on the highway system.

Two cases were examined in terms of FI and TI: Dyrastadir 2001-2002, and Thingvellir 1998-1999. Various formulas evaluating the onset and removal of the load restrictions

were used and compared to the actual condition, measured in the road cross-section, to establish how reliable these predictions are when applied in the field, see Section 5.2.1.1.

### **5.2.1. Onset of spring load restrictions.**

Thaw depends greatly on local conditions; however some general guidelines have been presented. After each freezing period, when thaw begins, the TI is calculated. If the freezing has penetrated deep enough in the road section, load restrictions should be imposed. This requires engineering judgment and knowledge of local conditions.

There is usually one significant freezing period during the winter. The knowledge of when thaw begins can be found by examining weather data from previous winters. After the main freezing period spring load restrictions (SLR) are applied, Yesiller et al. (1996), Ovik et al. (2000) and other references agree that the SLR should be applied when TI reaches 15, however the SLR must be applied no later than when TI equals 30.

#### **5.2.1.1. Duration of Spring Load Restrictions**

There are various empirical formulas that try to predict the duration of the spring load limitations. Below is a summary of formulas reported in the literature.

It is useful to calculate the frost penetration depth during the freezing portion of the winter according to Ovik et al. (2000):

$$P = -0.328 + 0.0578\sqrt{FI} \quad [5- 3]$$

Where

P is the frost penetration depth [m]

Equation 5-3 cannot be used to determine the frost depth during thaw because different conditions apply to the thawing of the road compared to freezing. Equation 5-4 is presented by van Deusen (1998), and it states that the SLR duration in days is dependent on the FI of the previous freezing period and the total frost depth.

$$D \text{ [days]} = 0.15 + 0.010 \times FI + 19.1 \times P - 12090 \times \frac{P}{FI} \quad [5-4]$$

Equation 5-3 calculates the frost depth (where the only variable is FI). Equations 5-3 and 5-4 can therefore be combined with only one variable, which is the FI. Linear regression for data used to develop Equation 5-4 gave  $R^2=0.5$ , which is not very compelling. The standard deviation of error is 8 days (see Figure 5-3).

It should be noted that the weather conditions during the thaw are not used at all for the formulas outlined above. For example; if the air temperature is 10°C for the next ten days or only 0.5°C, this is not taken into account. This is the reason for the poor reliability of using Equation 5-4 and similar equations that ignore the weather condition during thaw in predicting the beginning and the duration of SLR.

Ovik et al. (2000) recommends that the minimum duration for spring load restriction is two weeks. They also report that due to the complexity of the problem, many road administration agencies simply assume that the axle load restrictions will be applied for 8 weeks from the onset date.

The Washington State Department of Transportation (WSDOT) [Ovik et al. 2000], uses Equation 5-5 to predict the duration of the limitations.

$$D \text{ [days]} = 0.018 \times FI + 25 \quad [5-5]$$

As in Equation 5-4, the weather conditions during thaw are not accounted for. The only variable is the FI from the previous freezing period.

Equation 5-6 was developed by the Federal Highway Association (FHWA). It gives a value of the thawing index and when the TI reaches that value the limitations may be removed.

$$TI = 0.3 \times FI \quad [5- 6]$$

Equation 5-7 can be found in Yesiller et al. (1996). It is slightly modified from Equation 5-6. Equation 5-7 gives lower values for TI than Equation 5-6 for FI greater than 100, and higher TI-value for FI less than 100.

$$TI = 4.154 + 0.259 \times FI \quad [5- 7]$$

None of these equations include any material properties of the road cross-section, which makes them regionally dependent and empirical.

To gain some time in the decision making process it is recommended that a long term weather forecast is used to evaluate the air temperature.

#### **5.2.1.2. Applicability of formulas**

The methods described in Chapter 5.2.1.1., were used and designed for local road conditions, where FI is between 200-1100 °C days, and the mean annual air temperature is between 4.4°C and 10°C [Yesiller et al. 1996]

#### **5.2.1.3. Dyrastadir (2001-2002)**

Yesiller et al. (1996) provides a clear approach on how to evaluate axle load limitations while using FI and TI of the immediately past and present freezing and thawing conditions. This section follows guidelines given in that article.

In Figure 5-4 the moisture content in the cross-section of the road is plotted versus time. Each line represents a different depth within the section. The slightly longer and thicker vertical lines on Figure 5-4 denotes when the Icelandic Road Administration applied and removed the spring load restrictions.

Thawing started the 26<sup>th</sup> of March and the average temperature for the 26<sup>th</sup> to the 28<sup>th</sup> of March is approximately -1.5°C (see Appendix C) therefore  $T_{ref}$  is set to that value.

A few early freeze and thaw periods occurred during the 2001-2002 season, but the frost was not able to penetrate deep enough during those periods. The frost period between the 20<sup>th</sup> of November and the 5<sup>th</sup> of December resulting in a frost penetration of 14 cm is marginal when it comes to applying SLR to the road system.

The main freezing period starts the 22<sup>nd</sup> of January and lasts until the 21<sup>st</sup> of March, then thawing begins. It is logical to apply the spring load restrictions on the 21<sup>st</sup> of March, however, the difficult part is to decide when to remove the restrictions.

Numerous options to determine when to remove the restrictions are available based on the formulas described previously. The maximum FI for the described freezing period was 315°C days. It is often an input in the equations used to evaluate the duration of the SLR. Durations of the axle load limitation are calculated and summarized using the various relationships described in Section 5.2.1.1. (See Table 5.1).

The Icelandic Road Administration (ICERA) removed the SLR the 7<sup>th</sup> of April. Figure 5-4 shows the suggested removal dates calculated in Table 5.1. It is obvious that the road had not fully thawed when the ICERA removed the SLR, since the peak value for moisture content at 30 and 36cm depth has just occurred and the peak at 55cm had not yet occurred. Equation 5.4 and the use of 14 days for the duration yield similar results when compared to the removal date used by the ICERA. Both these durations were too short based on physical measurement within the road. The fixed 8-week restriction ensures that the road would have completely drained. However, it is possible to allow heavy traffic on to the road sooner; therefore use of the 8-week duration is too cautious.

Equations 5.5, 5.6 and 5.7 all predict similar durations (31, 27, and 26 days respectively) and are probably fairly reliable when used to predict the duration of the SLR. The sensors located at 90 cm and 120 cm depth show peak values just after the suggested removal date, and sensors at 12, 30, 36 and 50 cm depths all show that the road had decreased in moisture content and thus can carry the heavier traffic loads at the Dyrastadir location.

#### **5.2.1.4. Thingvellir (1998-1999)**

Calculations of  $T_{ref}$  were done by using air temperature measurements from the 17<sup>th</sup> of April resulting in a value of  $-1.8^{\circ}\text{C}$  for  $T_{ref}$  (see Appendix D).

Figure 5-5 shows that a short freeze-period starts the 14<sup>th</sup> of October and ends the 7<sup>th</sup> of November, the FI only reached about  $46^{\circ}\text{C}$  days. The frost penetration is less than 10 cm according to Equation 5-3 therefore, the period is not critical. Frost depth of 15 cm is

often used as a benchmark for SLR. The main freezing period starts the 13<sup>th</sup> of December and thaw begins the 3<sup>rd</sup> of April. The freezing index for that season was 280°C days.

The 1998-1999 season at Thingvellir is a good example of why it is not possible to use formulas that specify a fixed number of days from the beginning of thaw for removal of SLR. Thaw begins the 3<sup>rd</sup> of April. However, there is a short frost period from the 12<sup>th</sup> to the 18<sup>th</sup> of April. The road is not going to thaw during that time, rather it is going to freeze again. The most reasonable method would be to add those 7 days to the estimated days needed for the thawing of the road.

The short freezing period (12<sup>th</sup> to the 18<sup>th</sup> of April) during the beginning of thaw causes most of the predictions of the duration to fail. The evaluation can never be completely automated. Some kind of engineering judgment should always be applied.

Equation 5.4 and the fixed 14-day duration as shown in Table 5-2 are greatly inaccurate and, in general, not suitable for determining the duration of thaw. Equations 5.5, 5.6, and 5.7, are somewhat more accurate, resulting in removal of the limitation when moisture content at 15 and 29 cm has peaked and is decreasing. However, the measurement at the depth of 50 cm has not yet reached its peak value. In this case the fixed 8-week limitation is the most reasonable.

No information is available about when the Icelandic Road Administration applied the axle load limitations on that particular road section for that year. Figure 5-5 shows the

volumetric moisture content versus the time at Thingvellir for the examined period. It is quite obvious when the thawing starts as there is a sudden increase in moisture content measured at all the sensors. The various dates for removal, calculated according to the guidelines presented in Section 5.2.1.1, are plotted on Figure 5-5.

### **5.2.2. Air - and road temperature**

It is interesting to compare the temperature in the upper reach of the road and the air temperature. Figure 5-6 shows the comparison between the air temperature and the temperature measured at 7 cm depth in the road. The measurements are from the site at Vatnskard for the winter 2003-2004. The thickness of the surface dressing is approximately 3 cm, the thermostat is located directly underneath the asphalt within the base course.

Measurements during the summer are not stored as they have no importance related to the axle load limitations; therefore measurements from the 15<sup>th</sup> of August 2003 to the 27<sup>th</sup> of March 2004 are available. It is interesting to see that during the early fall and late spring the road temperature is typically warmer than the air temperature, because of the radiation warming of the sun [Saarelainen, in press]. However, during the dark winter the air temperature is usually warmer than the road temperature. This behaviour was also observed at other locations, for example at Dyrastadir for the 2003-2004 winter. Iceland's latitude is around 65°N, and the sun does not shine for long each day during winter. Another contribution is that the top part of the road section isolates the sensor at 7 cm depth and causes the temperature in the road to be different from both the air temperature and the actual road surface temperature.

There are numerous reports that discuss the relationship between the temperature in the top part of the asphalt and the air temperature. The air temperature is predominately colder than the temperature in the asphalt. Those studies should not be confused with comparison of air temperature and temperatures deeper (7 cm in this case) in the road section.

### ***5.2.3. Heat distribution with depth***

Since the temperature is measured at various depths, it is possible to plot the temperature profile for the road. Measurements are taken every hour; therefore, it is possible to plot how the temperature profile for the road section warms during the spring thaw.

Figure 5-7 shows how the temperature changed in the road section at Dyrastodum during the spring of 2004. In the figure there are two sets of data. One is from six independent temperature sensors, and the other one from temperature sensors positioned along the electrical conductivity probe installed in the road.

It is interesting to see how the road thaws mostly from the top downwards. The top and the bottom of the road thaw while the center of the road remains frozen. The center then slowly thaws. By plotting similar data, it is possible to see exactly where the 0°C isotherm is located within the road section. This gives individuals monitoring the road valuable information about the location of the frozen zones in the road.

This relationship between air temperature and the subsurface temperature profile in the road section is modeled in Chapter 6. The predicted temperature profiles are compared to the measured temperature in the road and they agree quite well.

### **5.3. Moisture content**

Moisture content of the materials in the road section significantly influences the bearing capacity and the thermal properties of the material. In fact, the stiffness of the road is directly related to the moisture content [Janoo and Shepherd 2000]. During spring, thawing of the top layers of the road occurs, but the water released cannot drain because the soil beneath remains frozen, thus allowing the road to deform under heavy wheel loads. It is simple to indicate the start of the thawing from the available moisture content profiles, as a very sudden spike is usually observed at a particular depth. In Figure 5-8 the gravimetric moisture content obtained from the TDR sensor at 45 cm depth at the test site at Kjos during the 1998-1999 season is plotted. It can clearly be seen that during the winter the moisture content decreases and then increases sharply over approximately one day during spring thaw. The subsequent drainage is relatively fast compared to sensors closer to the surface.

The moisture content usually measured in this project is volumetric moisture content; which is the ratio between the volume of water and volume of soil in the sample. Gravimetric moisture content, however, is more widely used in geotechnical engineering. Janoo and Shepherd (2000) emphasize the importance of using moisture content instead of temperature within the roads when deciding the onset and duration of axle load limitations. In their case study from the Minnesota Department of Transportation

(MnDOT), the peak moisture content in the road was observed when the temperature was still at -2.4°C. The same layer only warmed to 0°C 23 days later. Not surprisingly, Janoo and Shepherd concluded that the amount of fines in the layers greatly affects the duration of recovery.

Because the material used in the roads in Iceland is coarse grained and the surface dressing is relatively impermeable, precipitation does not generally increase the moisture content in the subgrade by a significant amount [Bjarnason et al. 1999]. The stiffness should also be less dependent on the moisture content because of the lack of fines found in the typical road building material throughout Iceland (Appendix B).

### ***5.3.1. Moisture content compared to electrical conductivity***

In 1998 the Icelandic Road Administration started to experiment with the possibility of using electrical conductivity to measure moisture content within the road. The benefits of replacing the TDR equipment with the conductivity probe would include simpler installation, ease of repair, and lower capital cost<sup>1</sup>. In 2001 the first electrical conductivity probes were installed as well as ordinary volumetric moisture content equipment (TDR sensors) to allow for calibration and comparison between these pieces of instrumentation. Over the next few years the electrical conductivity probe was improved, the installation technique modified, and more reliable measurements obtained.

The measured drop in the moisture content during winter is reported by the TDR only as it measures the unfrozen moisture content (gravimetric or volumetric). As soon as the

---

<sup>1</sup> Erlingsson, S. (personal communication 2006)

water freezes the TDR does not consider it to be part of the moisture content in the soil. The TDR sends out an electric pulse and measures the time it takes for it to travel a known distance. From this information it calculates how much water (in liquid state) on average is in the sample. However, the drop in electrical conductivity is caused by the difference in material properties of liquid and frozen water. The liquid water conducts electricity much better than the ice does.

The electrical conductivity of the soil decreases as the ions become more concentrated while the TDR measures the unfrozen volumetric moisture content. This fundamental difference in the measurements could be one of the reasons for the difficulty in deriving a direct empirical relationship between the moisture content (TDR) and electrical conductivity for this project.

Figures 5-9 to 5-12 from Dýrastaðir for 2003-2004 winter, show the moisture content compared to the electrical conductivity. It is obvious that the moisture content and electrical conductivity show similar behaviour, and as discussed in Section 4.4.3 they respond in similar manner. The electrical conductivity apparently is more responsive than the moisture content measuring equipment, and therefore indicates more clearly the fluctuations of moisture content in the road section with depth. Measurements of electrical conductivity could successfully replace conventional measurements of moisture content for the purpose of determining SLR based on the graphical information.

The water in the soil is the dominant conductor. The electrical conductivity of the soil particles and the air in the voids can be assumed constant and very low. It can therefore be concluded that variations in conductivity are due to variations in overall moisture content. Figures 5-9 to 5-12 show a comparison between the moisture content and electrical conductivity at different depths in the road.

The Icelandic Road Administration is rather confident in the reliability of these probes. Confident enough that when new sites are instrumented with the electrical conductivity probes, the sites are not equipped with the conventional moisture content measurement equipment such as TDR. Attempts to empirically correlate the electrical conductivity to the moisture content have not yet been successful. The exact value of the moisture content is not of particular interest, only the time of the sudden increase.

With depth, the moisture content shows less dramatic fluctuations, due to the slow rate of temperature change. The scale used in the electrical conductivity measurements is highly sensitive, it appears to capture the increased moisture content better than the TDR measurements. For example, in Figure 5-12 which shows moisture content at 90 cm depth and conductivity from 82 and 92 cm depths, the moisture content is nearly constant, whereas the conductivity measurements show more fluctuations during spring thaw. On the other hand, the moisture content sensors close to the surface show practically the same fluctuations as the conductivity measurement.

Figures 5-9 and 5-10, which show the moisture content at 12 and 30 cm depths as well as nearby electrical conductivity, clearly indicate that measurements of moisture content and electrical conductivity show similar trends

Figure 5-9 is the only graph that shows the moisture content reaching a peak value and remaining at this level for several days. Meanwhile, the conductivity measurement shows the road draining slightly during this period. This is the largest inconsistency in the comparison of these two measuring systems. The most likely explanation is that the road is in fact slightly draining and the sensitive conductivity measurements show that whereas the TDR measurements do not.

Another difference is the sudden increase in the electrical conductivity at 82 and 92 cm depths when moisture content at 90 cm does not record any change (see Figure 5-12).

Apart from these two cases, the moisture content and the electrical conductivity data show the same behaviour, especially for the time of the increased water content at a particular depth. The two measurement techniques generally show changes in measurements occurring at the same time. This is the main objective of the study: to know the time when the moisture content changes occur.

If Figures 5-9 to 5-12 are compared, it can be seen how the moisture content and electrical conductivity show a more delayed reaction as the depth increases. There is relatively little change between Figures 5-9 and 5-10, which show moisture content and

electrical conductivity at 12 and 30 cm depth respectively. However, Figure 5-11 shows one peak compared to two at Figures 5-9 and 5-10. This indicates that the first thaw did not penetrate to 55 cm depth. It is also interesting how quickly the melt water drains in Figure 5-11 compared to Figures 5-9 and 5-10. The drainage in the road must be quite good by the time the road section thaws half a meter.

### ***5.3.2. Moisture content compared to temperature***

Air temperature and moisture content for the spring of 2002 are shown on Figures 5-1 and 5-2. When the air temperature rises above zero, a sudden spike is observed in the moisture content. Two short thaw periods occur in the beginning of February and another in the middle of March. Those two periods mainly affect the sensor at 12 cm depth and only slightly the one at 30cm depth. The main thaw period then starts around the 25<sup>th</sup> of March with a very distinct and sudden increase in moisture content; first at 12 cm and then followed by all the sensors in the order of their embedment depth.

Figures 5-13 to 5-15 show the temperature and moisture content versus time for different depths. As expected, when the temperature is below 0°C the unfrozen moisture content is at its minimum value and when the temperature approaches the melting point of the water from below, a sudden increase in moisture content is noticed as the water changes phase.

As mentioned earlier, Janoo and Shepherd (2000) noticed that the maximum moisture content occurred when the temperature in the road was -2.4°C. Similar behaviour is observed in the data from spring 2004 at Dýrastaðir. Although most of the peaks in

moisture content occur approximately at 0°C, the road starts to thaw at a negative temperature, with -3°C as a common value indicating when moisture contents change.

Figure 5-14 illustrates the moisture content and temperature at 30 cm depth, moisture content starts to increase when the temperature is around -3°C. As the road approaches 0°C the moisture content peaks. For the graph showing temperature and moisture at 12cm depth (Figure 5-13), the fluctuations are significantly more than those measured by the sensors located deeper in the road section (Figures 5-14 and 5-15). Warm air temperatures for a relatively short time significantly affect the measurements of temperature and moisture content near the surface. The radiation from the sun during the day and freezing temperatures during the night affect this upper layer of the road. Sensors located deeper in the section at 55 cm, Figure 5-15 for example, show more dampened moisture content variations. The temperature varies more slowly at depth; therefore, moisture content does as well. Again, the peak moisture content appears to occur around 0°C.

It is obvious that the road temperature and moisture content respond in a similar manner, especially for temperatures around 0°C. The correlation is not as good as for moisture content and electrical conductivity, but there is surely a relationship between road temperature and moisture content.

Examples of road agencies using temperature in a road section to determine the onset of axle load limitations can be found in the literature. Kestler et al. (1999) describe how the

U.S. Department of Agriculture and Forest Service (USFS) determine the onset of axle load limitations. For the last 10-15 years the USFS have measured subsurface temperatures in the road and have applied the load limitations when the temperature reaches 0°C. This method has proven to be an excellent method of determining when to start the spring load restrictions.

The method used by USFS would probably function well in Iceland because the maximum moisture content appears to occur at 0°C. However, it would be better to limit the axle loading just before the road starts to thaw. According to Ovik et al. (2000) the damage done each day at the beginning of thaw is equivalent to 28 days at the end of the thaw. When the temperature in the road is -3°C, the moisture content is significantly reduced. This would be a better reference temperature than the 0°C used by USFS. Looking at Figures 5-13 and 5-14, which show temperature and moisture content at 12 and 30 cm depths, the -3°C suggestion is reasonable. However at greater depth, as is shown in Figure 5-15 at 55 cm depth, the temperature was around -1°C on the 25<sup>th</sup> of February and yet the moisture content did not increase. The moisture content at 55cm depth is shown in Figure 5-15 peaks when the temperature reaches 0°C.

Therefore, the focus for the onset of SLR should be on the temperature near the top of the road cross-section. Increasing temperatures around -3°C in the top part of the road section and favourable air temperature forecast for continued thaw are a strong indication of increased moisture content, typically occurring within the next couple of days. Temperature in the road section can therefore be used as an indicator for onset of SLR.

When clean, coarse material freezes, the value for unfrozen gravimetric moisture content should be close to zero [Hivon and Segó 1995]. If the volumetric moisture content from Figures 5-13 to 5-15 is corrected for density and converted to gravimetric moisture content (Chapter 4.4.1), the values are in the range of 3-8%. This variation from the expected behaviour could be explained by the amount of fines in the gravel, error in the TDR measurements, or a poor assumption of the dry density of the gravel.

#### **5.4. Falling weight deflection tests.**

As discussed in Chapters 3 and 4, the FWD test is carried out by dropping a 500 kg load at the center line of the road, from 10 to 15 cm height. The deflections are then measured at fixed locations, 20 to 90 cm from where the load was dropped. From the deflection measurements it is possible to infer the Young's modulus for the layers in the road section.

One of the practical implications of the FWD test data collected at the test sections is that the moisture content of the road is known. The moisture content affects the stiffness of the road section. It is of special interest to see how the stiffness of the section changes during spring thaw, as the frozen water contributes greatly to the cementation of the soil. Ovik et al. (2000) reports that the increase in the base layer stiffness modulus at the end of thaw, relative to the value at mid thaw, ranges from 15 to over 100%. Bjarnason et al. (1999) noticed that stiffness of the road during spring thaw varied from approximately 25-50% of fully drained stiffness. However, during winter when the road is completely frozen, the bearing capacity can be up to tenfold the normal summer bearing capacity

[Janoo and Shoop 2004], mainly due to increased cohesion. For coarse grained material like used in the sections at Vatnskard and Dyrastodum a different behaviour can be expected. Reduction in stiffness during spring thaw will not affect coarse material nearly as much as fine grained material.

From the FWD test data it is possible to calculate the Young's modulus of the different layers in the road section. The results from the tests can be used with the program EVERCALC (developed by WsDOT) to calculate the Young's modulus for up to 5 layers in the section. Young's modulus is useful for deciding upon the allowable axle load based on the theory of elasticity, or as an input parameter in formulas that estimate rutting.

Figures 5-16 a and b and 5-17 a and b show the average deflection at the second drop (measured at the place where the load is dropped,  $D_0$ ) compared to the moisture content profile in the road.

Figures 5-16 a and b shows the FWD measurements and the moisture content measurements for the 2001-2002 season at Dýrastöðum. The change in stiffness can not be solely attributed to the change in moisture content. It is mostly caused by the cementation of the frozen water binding the soil particles together. The stiffness during winter is much greater than the stiffness of the fully thawed and drained section. During spring the transition between those two stages occurs. The layers in the road become nearly oversaturated during spring, and although the stiffness of the road section is still relatively high, the disintegration of those partly thawed layers is considerable. At the end

of the spring when the road is fully drained the stiffness recovers slightly. Figure 5-17 a and b from the 2001-2002 season at Vatnskard show a similar tendency in the stiffness of the section. During winter the road is stiff, and during spring it loses its stiffness as the bonding between the soil particles in the road thaws. During summer when the road is drained, the stiffness is constant. No recovery due to drainage of nearly oversaturated layers in the section is noticed in Figure 5-17a and b. In the beginning of May there is a short freezing period and the stiffness of the road increases accordingly, due to the regained cementation between the soil particles.

The road sections at Vatnskard and Dyrastodum are constructed of a coarse material. The bearing capacity of gravel is less sensitive to moisture content than finer grained material. Although the stiffness and bearing capacity of the road are higher during spring than during summer, the breakdown of the road occurs mainly during spring. Layers of the road become oversaturated because frost presence deeper in the section prevents downward drainage. The FWD-test does not account for cyclic pore pressure build-up similar to that which occurs when heavy vehicles with multiple axles passes, many light cars could even have similar effects. Cyclic pore pressures build-up under these cyclic conditions result in the road deforming (by rutting for example), and/or the material in the road section softens.

The extra stiffness of the section during the frozen period is also observed in other similar studies. The Minnesota Department of Transportation adds 10% to their maximum allowed axle load during these frozen periods. That is quite dangerous, if the road is not

monitored extensively, the damage caused by this additional weight during spring thaw would be severe [Ovik et al. 2000].

Figure 5-18 shows the moisture content profile for the spring thaw at Dýrastaðir. The two vertical lines around the beginning of April are the onset and removal of the axle load limitations, determined by the ICERA. Figure 5-19 shows the measured deflection at the second drop. Figures 5-18 and 5-19 are based on the same data as Figure 5-17 a and b but the focus is on the spring thaw.

The deflection of the second drop is an indicator of the combined stiffness of the whole section. Surface curvature index (SCI), Equation 5-8, is representative for the upper layers in the road section. The base damage index (BDI), given in Equation 5-9, is supposed to indicate the condition of layers deeper in the section.

Surface curvature index

$$SCI = D_0 - D_2 \quad [5- 8]$$

Base damage index

$$BDI = D_2 - D_4 \quad [5- 9]$$

Where:

$D_0$ ,  $D_2$  and  $D_4$  are deflections at a 0, 30 and 60 cm respectively from the location where the 500 kg load is dropped.

The surface curvature index and base damage index for the spring thaw at Dýrastöðum 2002 are shown on Figures 5-20 and 5-21 respectively. Logically, the top part of the road

thaws first and it can be seen that the SCI shows reduced stiffness before it can be noticed in the BDI. The SCI has reached its minimum value when the axle load limitations are removed. The BDI, on the other hand, shows no sign of reduction when the axle load limitations were applied. When the SLR are removed, the BDI has still not reached its minimum value, indicating that they were removed too soon. The use of SCI and BDI could greatly assist with decisions about the application of SLR, especially the removal of the restriction. The FWD is not suitable for determining the onset of SLR because it is very time consuming and expensive to frequently monitor the road system. Also, by the time the FWD indicates that the road is losing its stiffness, it already has and most likely has been at a weakened state for a period of time

Comparing Figures 5-18, 5-20 and 5-21 indicate that the moisture content at 12 cm depth has peaked and somewhat drained (most likely horizontally) to a certain extent. The fact that the moisture content has peaked explains the sudden increase in the SCI, and why it has reached its maximum value. However, when the axle load limitations are removed, the sensors at 30 and 36 cm depth show that the moisture content has recently peaked but has not drained yet. The sensor at 55 cm indicates that the moisture content has not peaked at that depth. These facts about the moisture content in the base layers can explain why the BDI has not yet reached its minimum value when the SLR are removed.

The same behaviour is observed between the moisture content and the stiffness of the section as would be observed between the electrical conductivity and the stiffness if they were to be compared.

## 5.5. Summary

In this chapter various parameters affecting spring load restrictions were discussed. Examples of the influence of the parameters and how they affect decisions on application of axle load limitations are given.

- Two examples demonstrating the use of air temperature to evaluate conditions in a road section were discussed.
- Temperature measurements with depth in road sections were introduced and examples of the application of the measurements given.
- Data from moisture content and electrical conductivity measurements were presented and compared. Fairly good correlation was observed between these variables, for the application of determining SLR these variables are interchangeable.
- Temperature and moisture content were compared, and guidelines for onset of axle load limitations were introduced. When temperature in the top part of a road section is  $-3^{\circ}\text{C}$  and predicted conditions for thaws are favourable, axle load limitations should be applied.
- Measurements from Falling Weight Deflectometer were compared to moisture content. The measurements from the FWD do not show significant loss of stiffness during spring thaw.

## 5.6. References

- Bjarnason, G., Erlingsson, S., Petursson, P., and Thorisson, V. 1999. Constructed Unbound Road Aggregates in Europe (COURAGE) Icelandic Final report. Public Road Administration Iceland.
- Hivon, E.G., and Segoo, D.C. 1995. Strength of frozen saline soils. *Canadian Geotechnical Journal*. **32**(1): 336-354.
- Janoo, V., and Shepherd, K. 2000. Seasonal Variation of Moisture and Subsurface Layer Moduli. U.S. Army Cold Regions Research and Engineering Laboratory Transportation Research Record 1709: 98-107.
- Janoo, V., and Shoop, S. 2004. Influence of spring thaw on pavement rutting; Taylor and Francis Group, London.
- Kestler, M. A., Hanek, G., Truebe, M., and Bolander, P. 1999. Removing spring thaw load restrictions from low-volume roads: development of a reliable, cost-effective method. In Proceedings, 7th International Conference on Low-Volume Roads, May 23-26, 1999, Baton Rouge, LA. In: Transportation Research Record, no. 1652, v. 2. Washington, D.C.: National Academy Press, 188-197.

Ovik, J.M., Siekmeier, J. A., and van Deusen D. 2000. Improved load restrictions guidelines using mechanistic analysis. Minnesota Road Research Project (Mn/Road Project) Available from: <http://www.lrrb.gen.mn.us/pdf/200018.pdf> [accessed 27<sup>th</sup> March 2006].

Saarelainen, S. Thaw penetration, thaw weakening and permanent deformation on pavements. In Proceedings of the Frost committee text for ISSMGE Osaka Conference. Osaka, Japan, 11 – 15 September 2005. International Society of Soil Mechanics and Geotechnical Engineering. 5 pages [in press].

van Deusen, D., Schrader C., Bullock, D., and Worel. B. 1998. Recent Research on Springtime Thaw Weakening and Load Restrictions in the State of Minnesota, Transportation Research Record no 1615, National Resource Council, Washington, D.C.

van Deusen, D., Schrader, C., and Johnson, G. 1997. Evaluation of Spring Thaw Load Restriction and Deflection Interpretation Techniques, Proceedings, Eighth International Conference on Asphalt Pavements, Seattle, WA.

Yesiller, N., Benson, C. H., and Bosscher, P. J. 1996. Comparison of Load restriction timings determined using FHWA guidelines and frost tubes, Journal of Cold Regions Engineering 10 (1) March 1996.

## 5.7. Tables

<b>Relationship</b>	<b>Outcome</b>	<b>When to remove SLR</b>
Equation 5.4	16 days	5 <sup>th</sup> of April 2002
Minimum 2 weeks	14 days	3 <sup>rd</sup> of April 2002
Fixed 8 weeks	56 days	15 <sup>th</sup> of May 2002
Equation 5.5	31 days	20 <sup>th</sup> of April 2002
Equation 5.6	TI= 95	17 <sup>th</sup> of April 2002
Equation 5.7	TI=86	16 <sup>th</sup> of April 2002
Axle load limitations removed by the ICERA		7 <sup>th</sup> of April 2002

**Table 5- 1: Duration of SLR for Dyrastadir determined using various relationships reported in the literature**

<b>Relationship</b>	<b>Outcome</b>	<b>When to remove SLR</b>
Equation 5.4	7 days	9 <sup>th</sup> of April 1999
Minimum 2 weeks	14 days	16 <sup>th</sup> of April 1999
Fixed 8 weeks	56 days	26 <sup>th</sup> of April 1999
Equation 5.5	30 days	2 <sup>nd</sup> of May 1999
Equation 5.6	TI= 84	27 <sup>th</sup> of April 1999
Equation 5.7	TI=77	27 <sup>th</sup> of April 1999

**Table 5- 2: Durations of SLR for Thingvellir determined using various relationships reported in the literature**

## 5.8. Figures

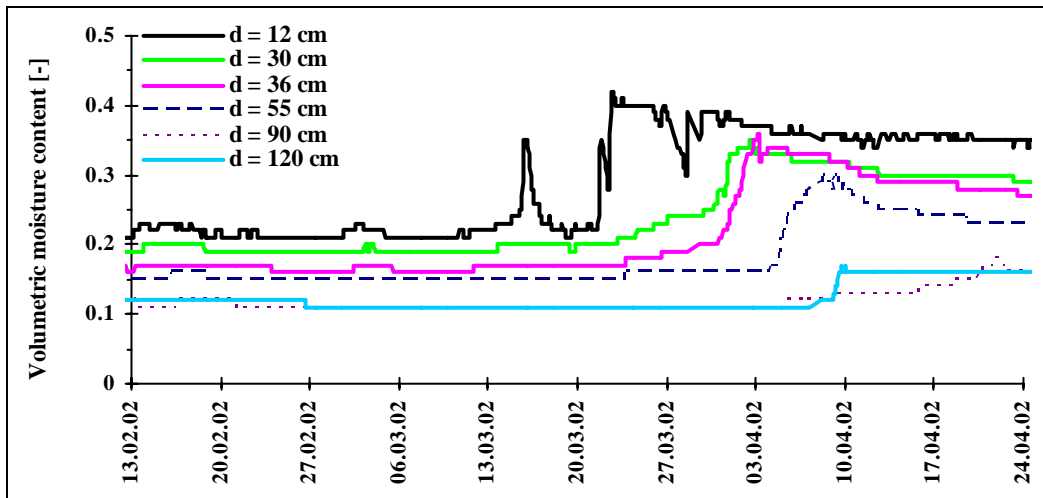


Figure 5- 1: Moisture content measurements from TDR during spring 2002, Dyrastadir.

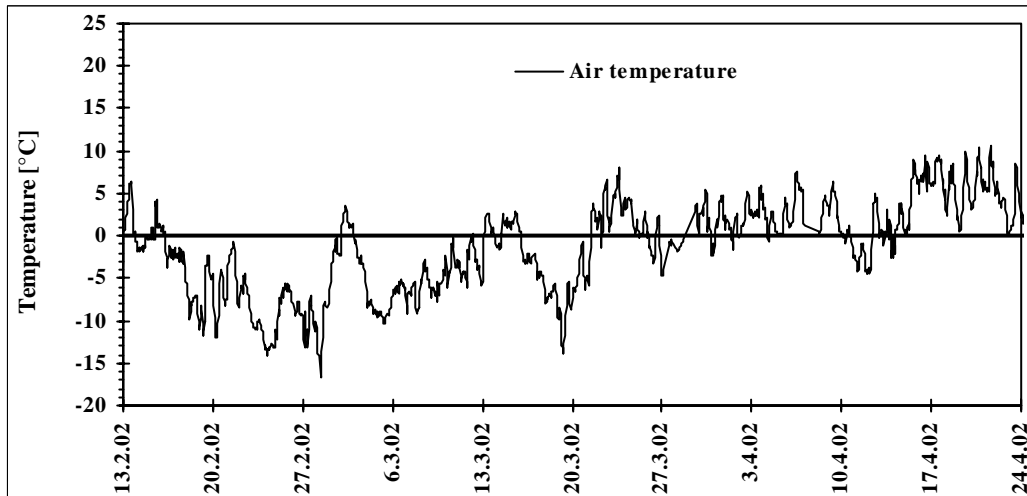


Figure 5- 2: Air temperature measurements during spring 2002 Dyrastadir.

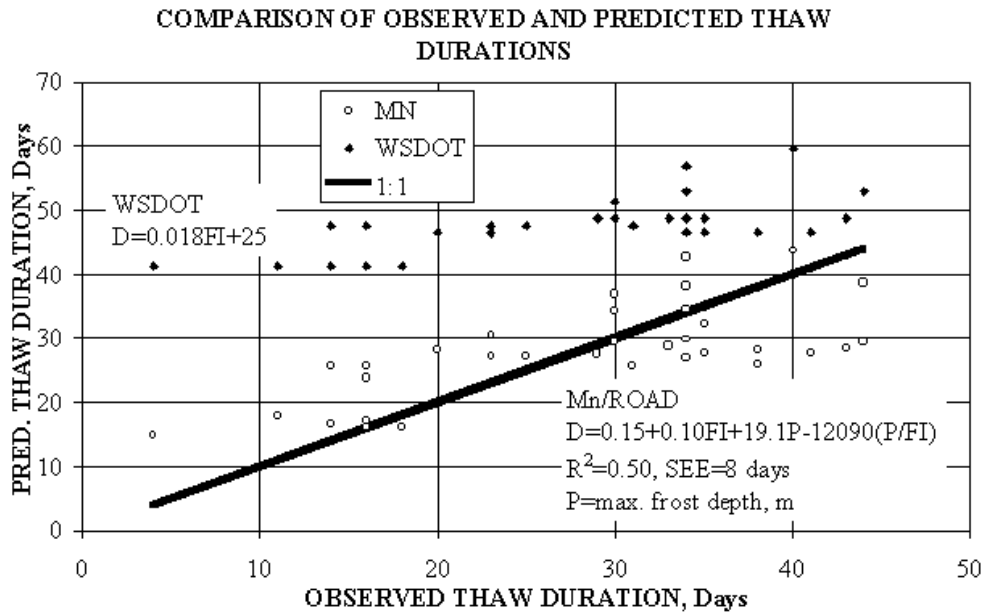


Figure 5- 3: Comparison of observed and predicted thaw durations from WSDOT and Mn/Road, modified from van Deusen et al. (1998)

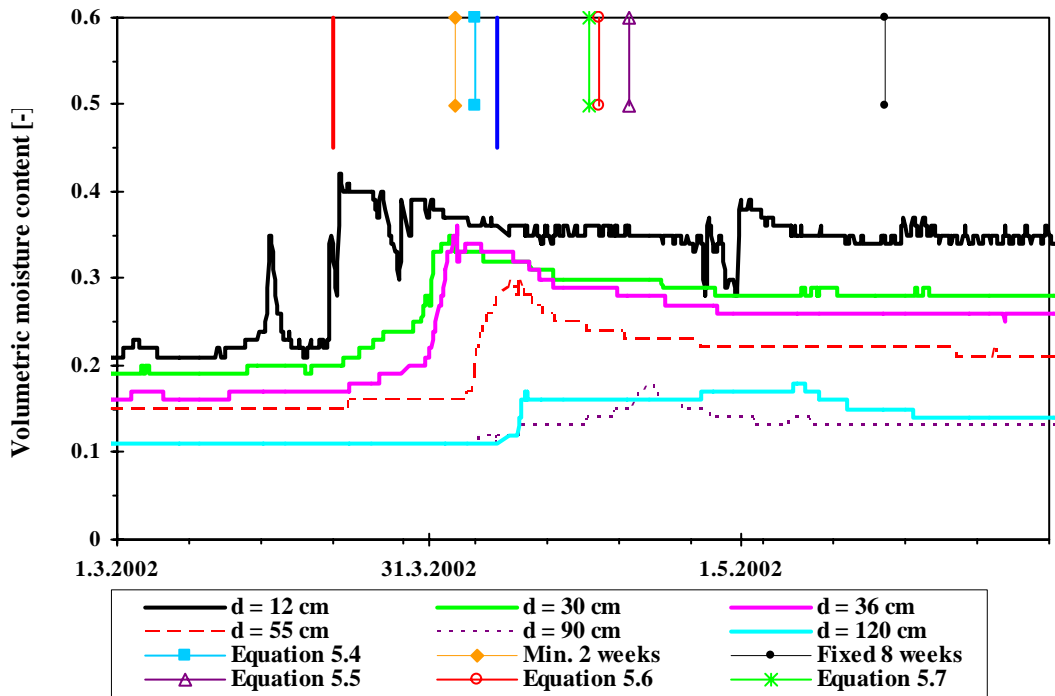


Figure 5- 4: Measured volumetric moisture content vs. time, and evaluation of various methods determining onset and removal of axle load limitations, Dyrastadir spring 2002.

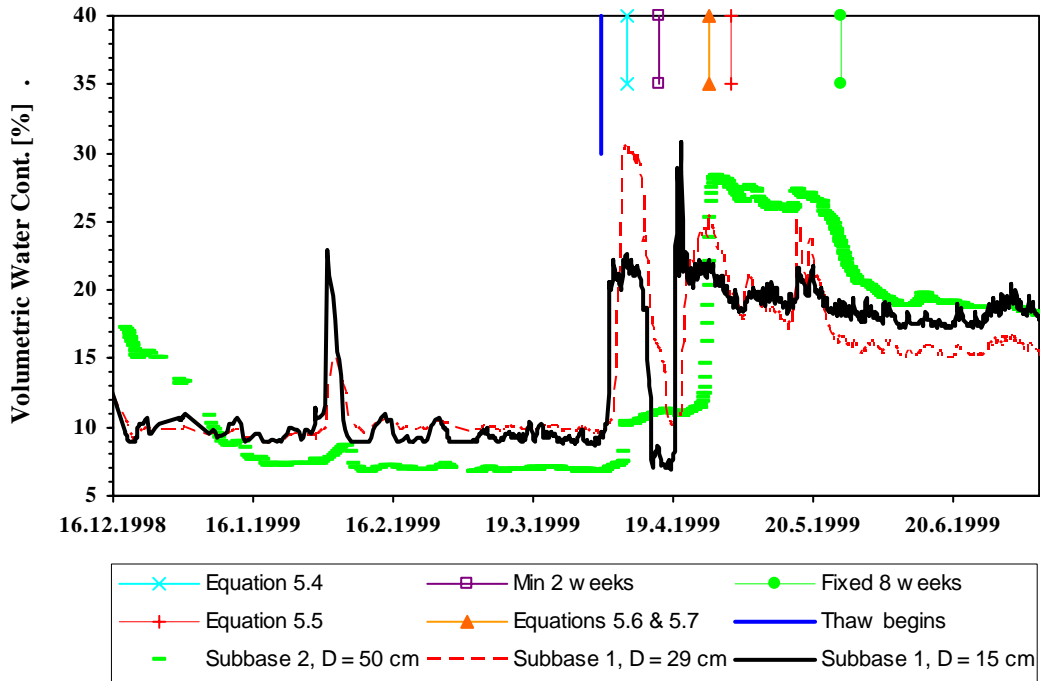


Figure 5- 5: Evaluation of various methods determining onset and removal of axle load limitations, Thingvellir spring 1999.

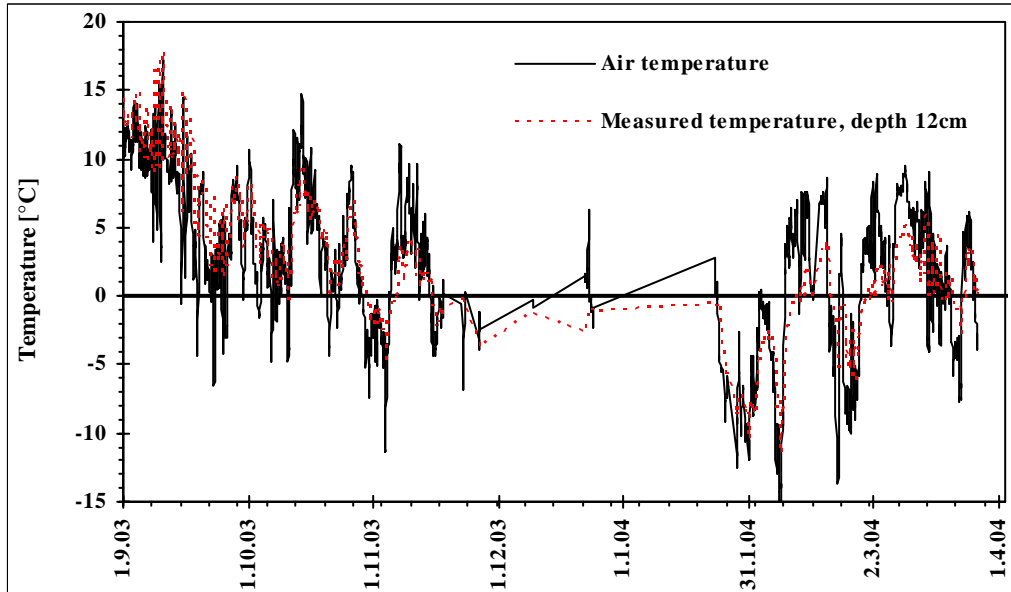


Figure 5- 6: Comparison between air temperature and temperature at 7cm depth in the road section at Vatnskaard 2003-2004.

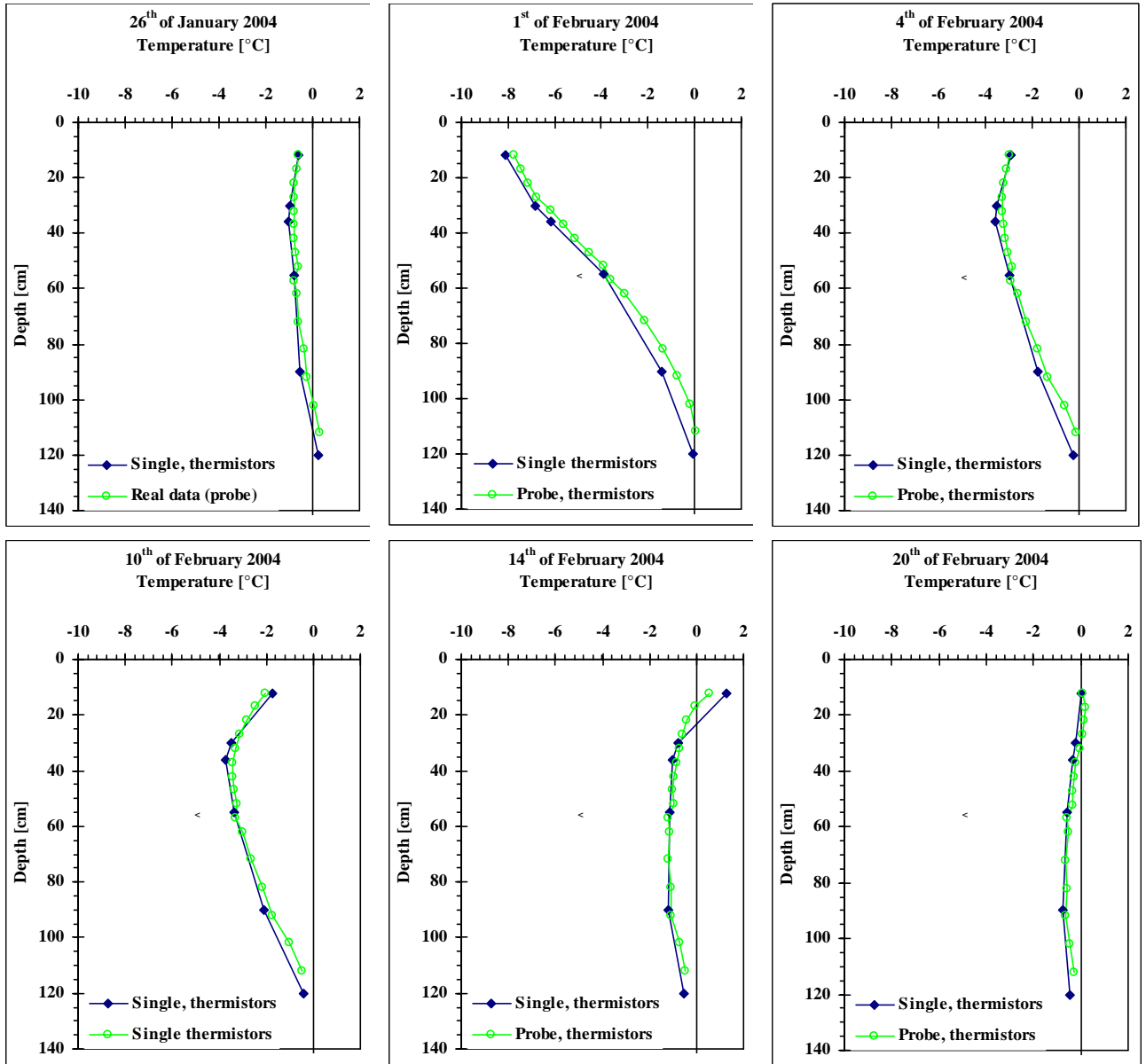


Figure 5- 7: Heat distribution in the road during spring thaw at Dyrastadir January and February 2004

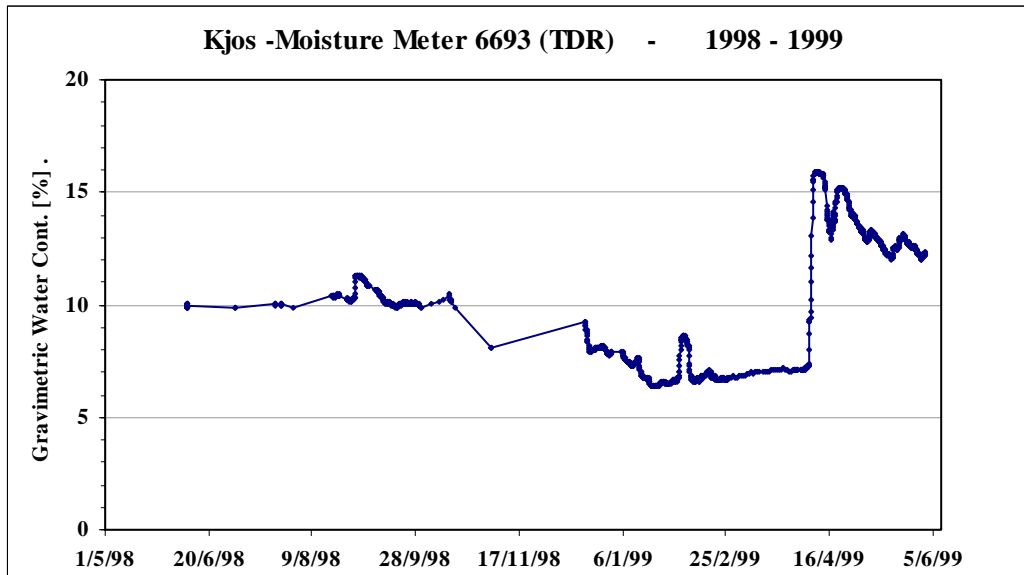


Figure 5- 8: Measurements of moisture content at Kjos during 1998-1999 (modified from Bjarnason et al. 1999)

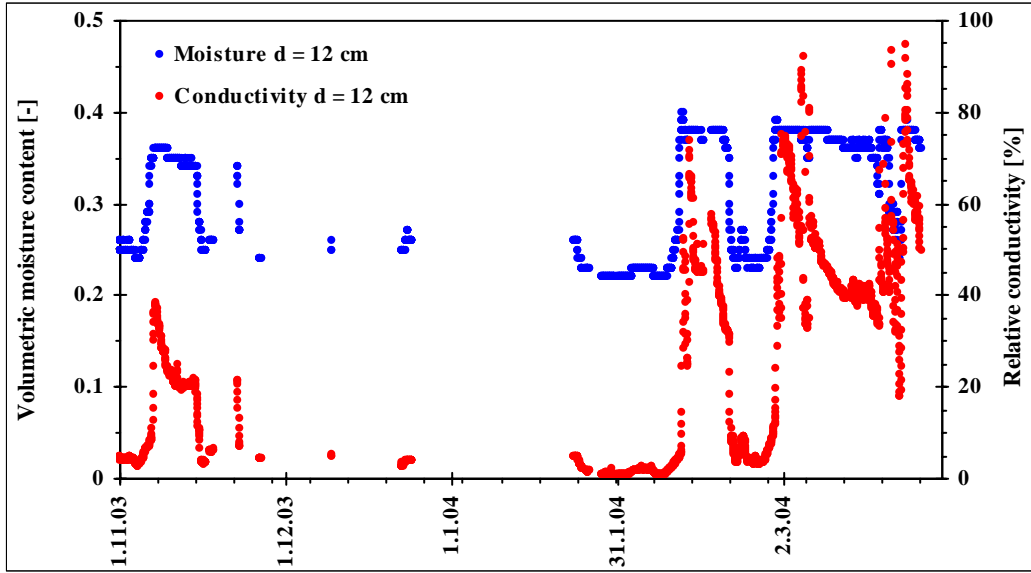


Figure 5- 9: Comparison of relative conductivity and volumetric moisture content at Dyrastadir 2003-2004, 12 cm depth

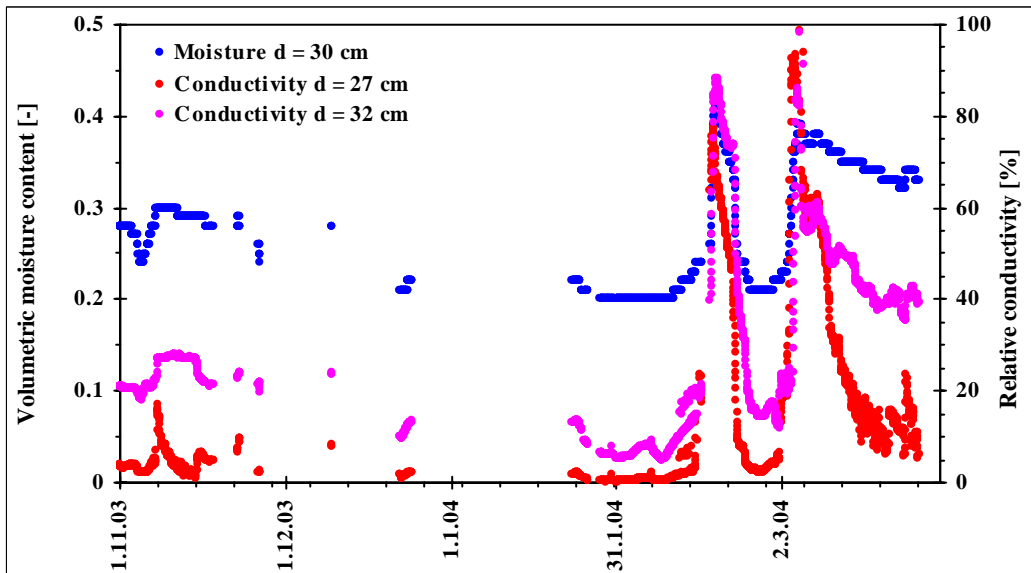


Figure 5- 10: Comparison of relative conductivity and volumetric moisture content at Dyrastadir 2003-2004, approximately at 30 cm depth

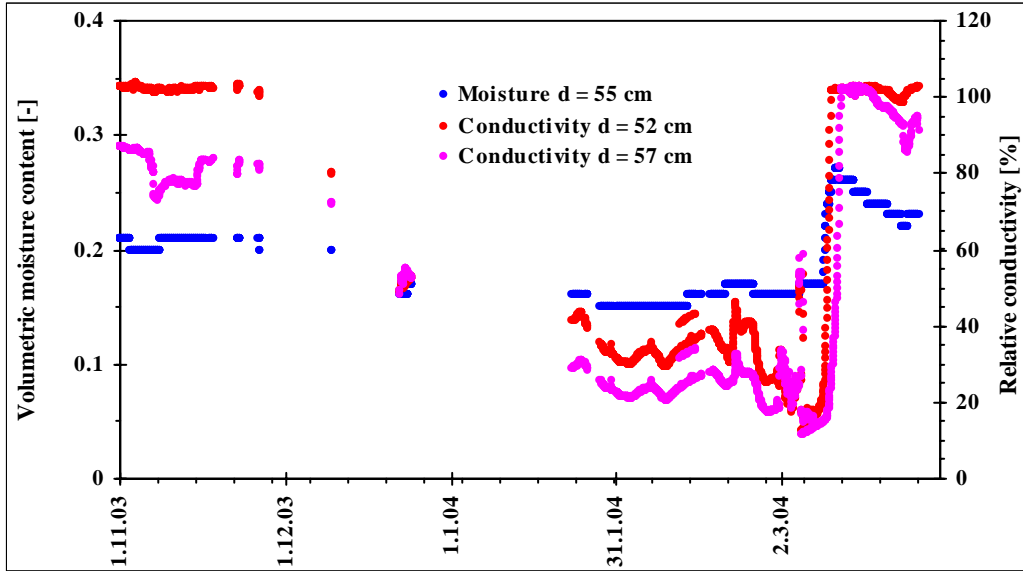


Figure 5- 11: Comparison of relative conductivity and volumetric moisture content at Dyrastadir 2003-2004, approximately at 55 cm depth

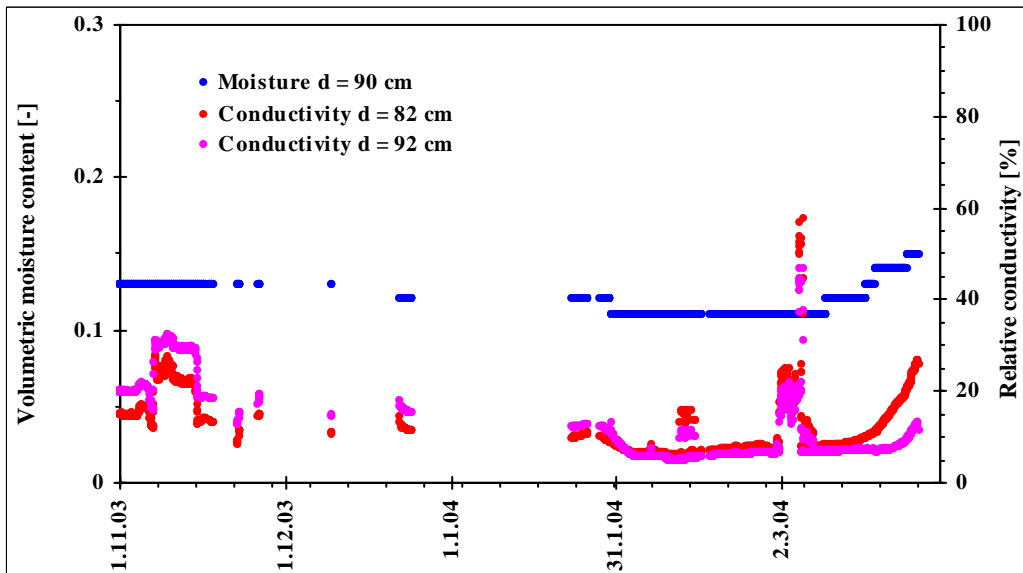


Figure 5- 12: Comparison of relative conductivity and volumetric moisture content at Dyrastadir 2003-2004, approximately at 90 cm depth

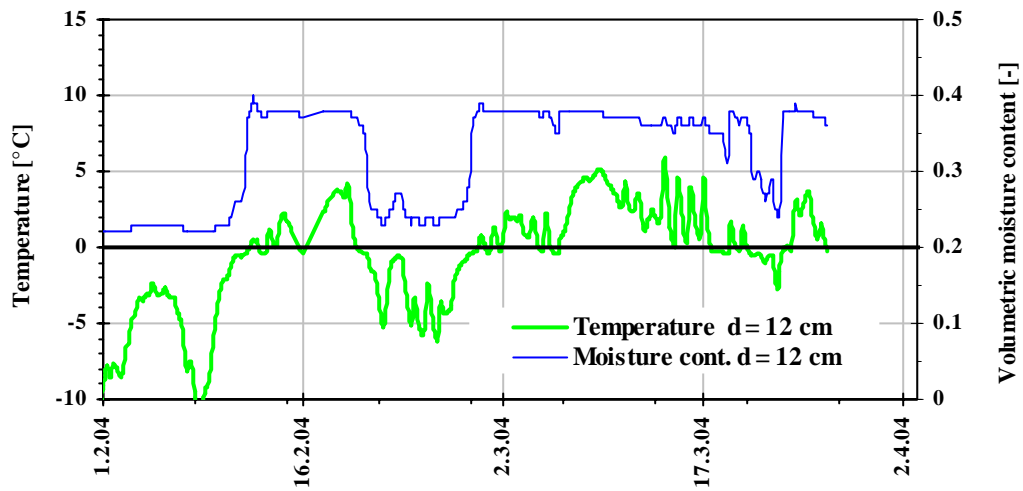


Figure 5- 13: Moisture content and temperature at 12 cm depth during thaw at Dyrastodum 2003-2004

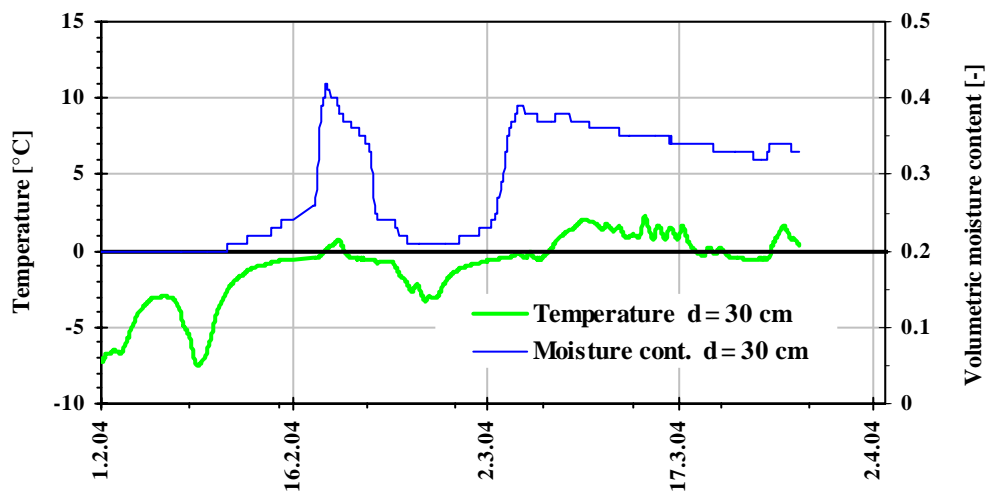


Figure 5- 14: Moisture content and temperature at 30 cm depth during thaw at Dyrastodum 2003-2004

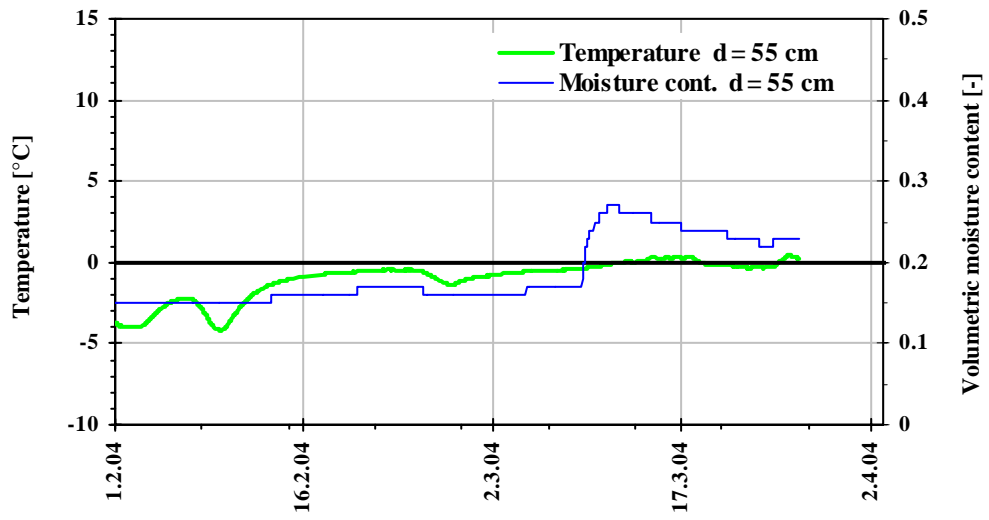
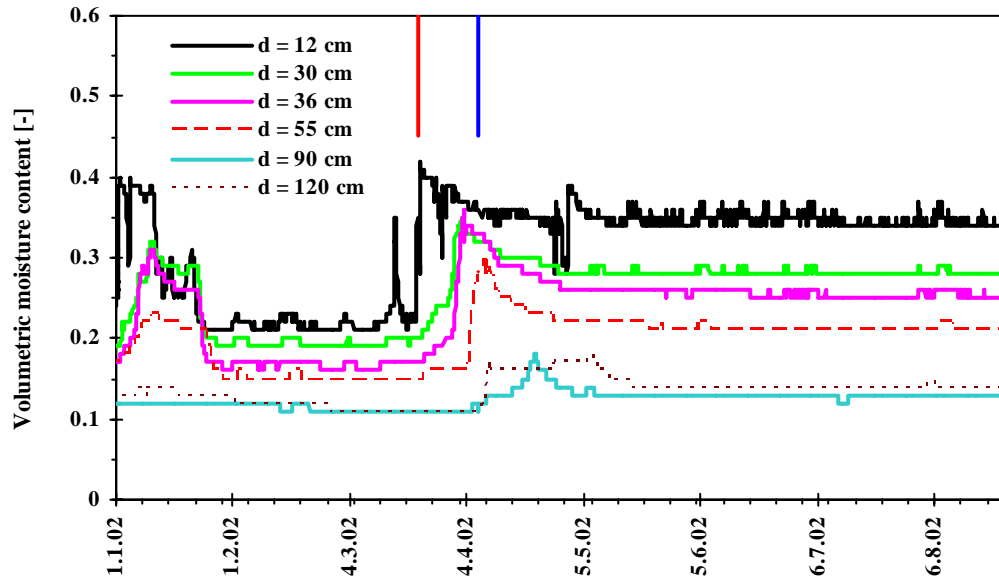
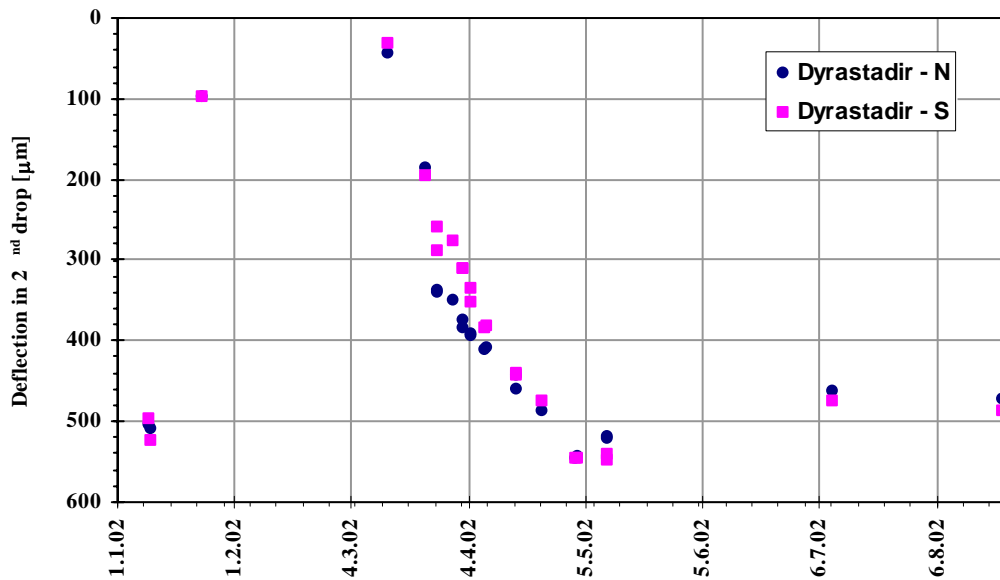


Figure 5- 15: Moisture content and temperature at 55 cm depth during thaw at Dyrastodum 2003-2004

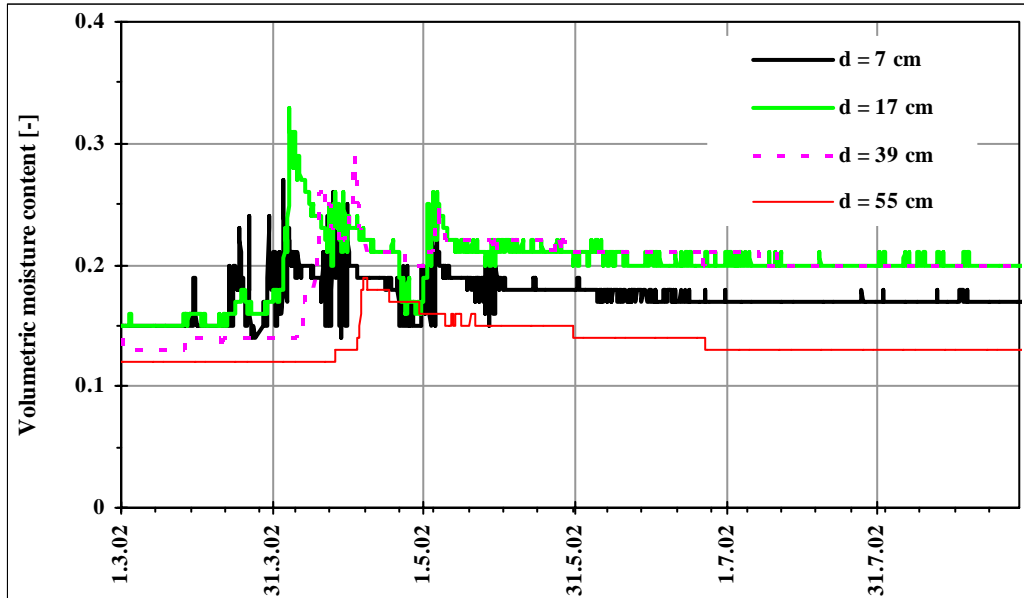


a)

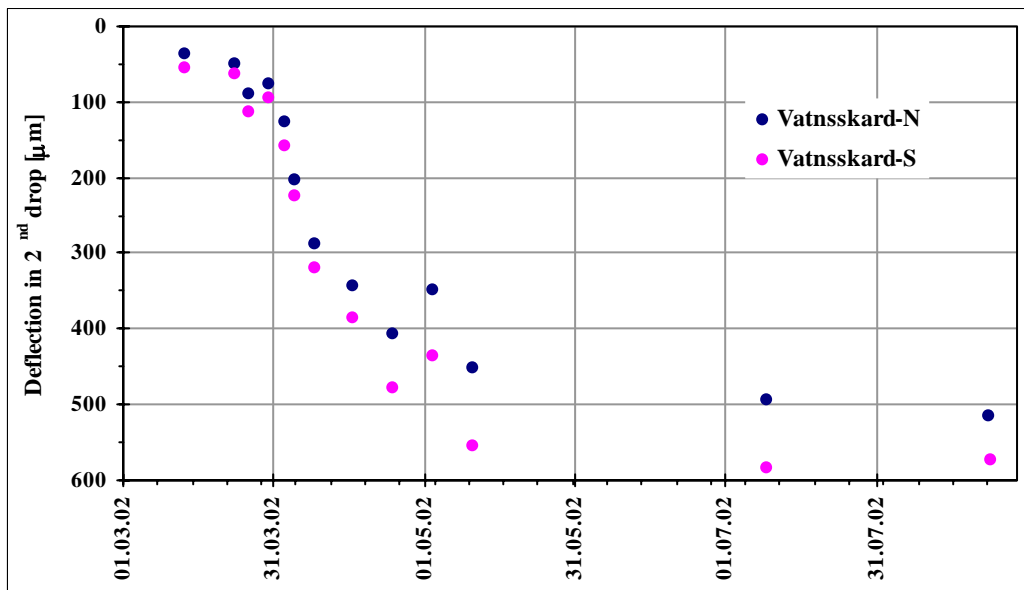


b)

Figure 5- 16: Moisture content profile compared to deflection data during the 2001-2002 season at Dýrastöðum, a) Moisture content profile and onset/removal of SLR, b) Data from FWD-tests



a)



b)

Figure 5- 17: Moisture content profile compared to deflection data during the 2001-2002 season at Vatnskarði a) Moisture content profile, b) Data from FWD-tests

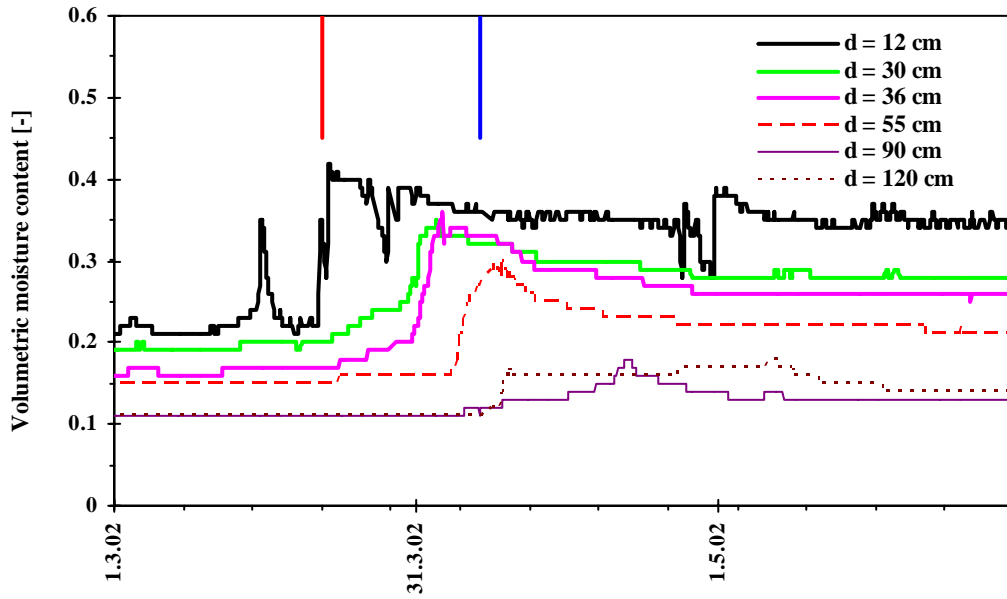


Figure 5- 18: Moisture content profile and onset/removal of SLR for the spring thaw 2002 at Dýrastöðum

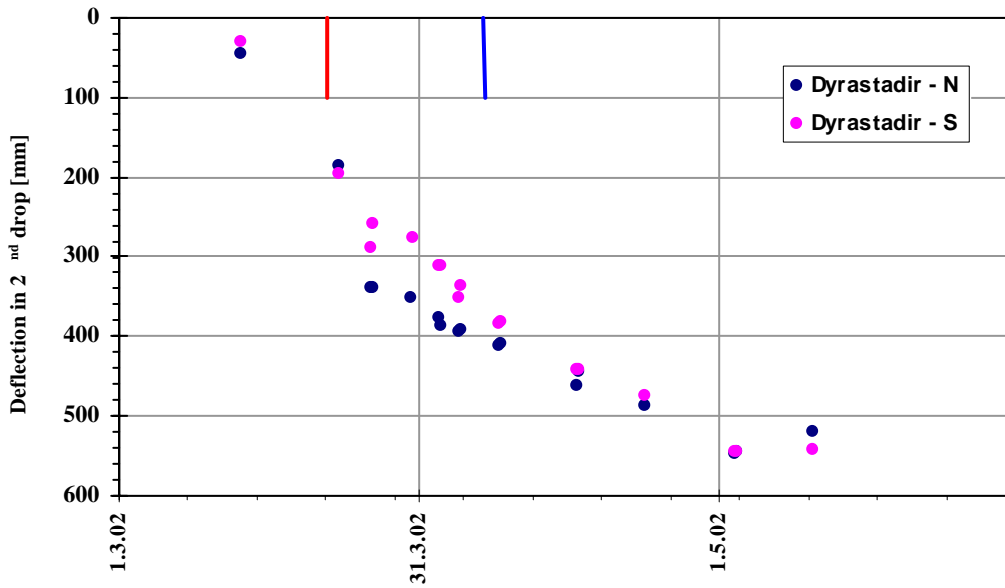


Figure 5- 19: Measurements of deflection of the road section during spring thaw 2002 at Dýrastöðum

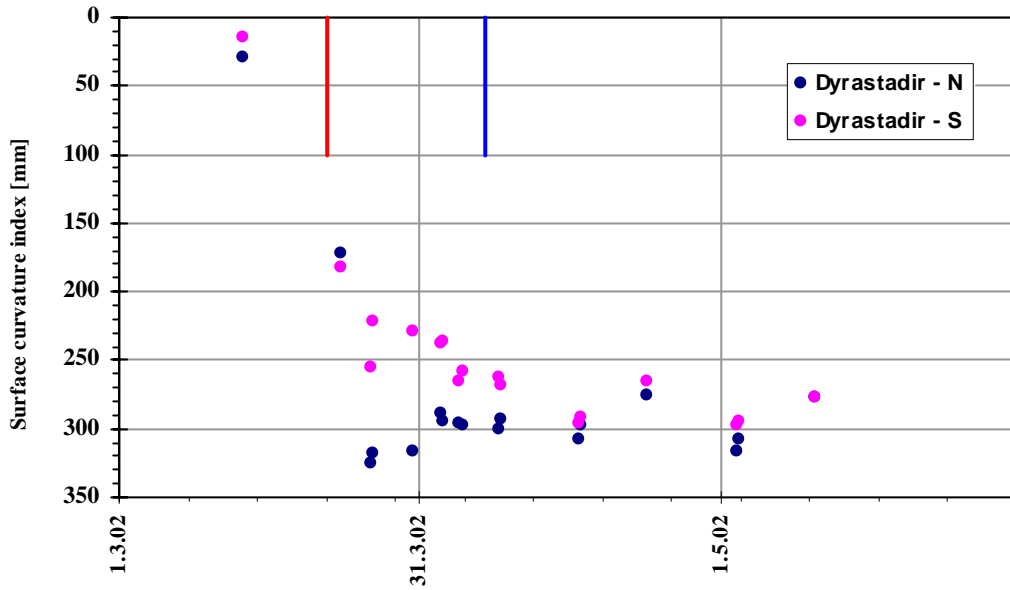


Figure 5- 20: Measurements of the surface curvature index during spring thaw 2002 at Dyrastodum

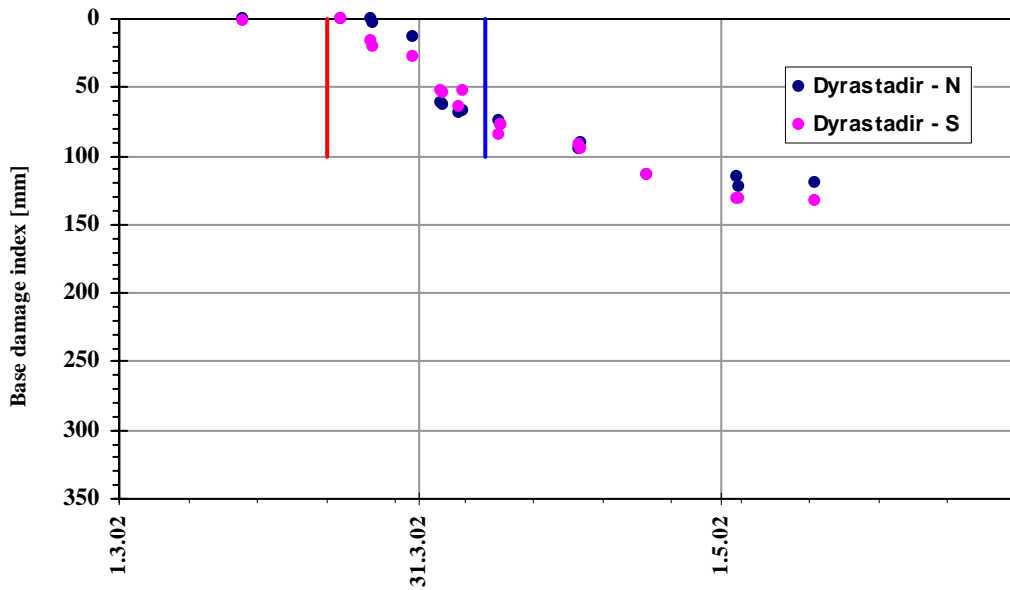


Figure 5- 21: Measurements of the base damage index during spring thaw 2002 at Dyrastodum

## **6. Modeling of heat flow in a road section**

### **6.1. Introduction**

This chapter compares measured temperature profiles with predicted temperature profiles to determine the thermal properties of a road section. The software TEMP/W from GEOSLOPE, which allows evaluation of thermal changes in the ground due to changes in air temperature, was used to formulate these predicted temperature profiles.

The level of sophistication is not significantly improved by using a two-dimensional analysis, and therefore the predictions relied on a one-dimensional analysis. The predictions also assume that the different layers in the road have similar material properties. The measured temperature profiles used in this analysis were collected by the ICERA (Icelandic Road Administration).

The ICERA has been collecting data at hourly intervals to evaluate road conditions at Dýrastöðum and Vatnskarð since 2001. The ICERA established temperature profiles beneath the centerlines of roads and determined air temperature using a nearby (>100 m) weather station. Temperatures were measured at different depths using two kinds of equipment. An electrical conductivity probe measured one set of profiles using twelve sensors located at either 5 or 10 cm intervals to a depth of 120 cm. The other measurements came from six independent temperature sensors located at depths of 12, 30, 36, 55, 90, and 120 cm. These sensors are manufactured by Campbell scientific, model-number TP100. These ICERA measurements are part of an ongoing project to

improve techniques for determination of axle-load limitations during spring thaw in Iceland.

The ICERA study forms a critical component of the following analysis by first providing the air temperatures; these temperatures are the most significant input parameters in predicting the temperature profile. Although the ICERA measured the air temperature hourly, an average daily value was sufficient for assessing the thermal properties of the road. In addition to these measurements, the ICERA road temperature profiles form a second critical component of this study by providing the benchmark for comparing the predicted values with the measured values. However, in spite of the sophistication of the temperature profiles taken by the ICERA, the two sets of measurements revealed discrepancies, suggesting that the measurements themselves may contain some errors.

The TEMP/W software calculates temperature profiles based on soil thermal properties based on air temperatures as input. The air temperatures and initial temperature profile for this study derive from the ICERA measurements, and when combined with determinations of thermal properties of the road section, TEMP/W calculates the temperature profiles for the remainder of the modeling period. These predicted temperature profiles are then compared to the actual measured profiles for this interval.

Soil thermal properties are important because they control heat flow and therefore can alter the temperature profiles. Some of these properties are relatively well understood, such as the latent heat of water. Other factors, such as the thermal conductivities of

materials in a road, the changing phases of water, and the properties of frozen soil, are much more variable. To limit the number of unknown variables, the first case involved a road section in an unfrozen state. Estimates for initial thermal properties (case 1) relied on assessments found in published sources. Determining the optimum values for the thermal properties began with a trial-and-error approach, with incremental changes to the properties being introduced to limit the error between the measured and projected profiles.

Case 2 involved frozen temperatures, requiring adjustments to the thermal properties based on the addition of frozen values. This case assessed fluctuations in air temperature around 0°C observed during a mid-winter thaw, making temperatures difficult to predict because of the combined complexity of the material properties of thawed, frozen, and partially thawed/frozen soil. Applying the same trial-and-error process slightly improved the estimated values for the thermal properties.

Once the difference between the calculated and measured values approximated the variation observed in the two measured data sets from the Dyrastadir site, the analysis began on the third case at Vatnskard. Although the two sites have inherently different characteristics and structures, these differences were overlooked based on the prior assumption of consistency in material properties of the roads. By repeating the procedure applied to cases 1 and 2, case 3 offered an additional analytical comparison and added another degree of sophistication to the assessment of thermal properties. A second round of analyses using the improved parameters calculated from the third case further refined

the evaluation of the thermal properties. After a few iterations, the thermal properties in this study matched published values, and the predicted temperature profiles fell within reasonable proximity to the measured profiles. Given the number of permutations that represent the thermal properties, there are numerous adaptations that could improve the solution; however, the attained values were sufficient for the aims of this study.

## **6.2. Description of cases**

The modeling included three cases: cases 1 and 2 at Dyrastadir and case 3 at Vatnskard; following is a description of each case.

### **6.2.1. Case 1**

The section for case 1 is located at Dyrastadir. The duration modeled was from the 24<sup>th</sup> of November until the 24<sup>th</sup> of December, 2002. This period was chosen because the air temperature is relatively uniform and consistent; see Figure 6-1. The air temperature was above but near zero, allowing for a temperature profile prediction that did not have to account for freezing of the road and therefore reduced the unknown parameters.

### **6.2.2. Case 2**

The section for case 2 was again located at Dýrastaðir. The time period modeled was from the 23<sup>rd</sup> of January until the 21<sup>st</sup> of February, 2003. This period was during a thawing period in the winter, when the ICERA applied axle load limitations. For the first half of this period, the road section remained frozen, but in the second half, thaw occurred; see Figure 6-2. The fluctuations in air temperature made it difficult to model the temperature profiles. The differences between the two measured datasets (one from the electrical conductivity probe and the other from the set of six independent

temperature sensors) were on average  $0.25^{\circ}\text{C}$  (difference in measurement varies from  $0.01$  to  $0.61^{\circ}\text{C}$ ).

### **6.2.3. Case 3**

The section for case 3 is located at Vatnskarð; see Figure 6-4. The time period examined was from the 28<sup>th</sup> of November until the 28<sup>th</sup> of December, 2003. The temperature in this case fluctuated throughout the period (see Figure 6-3) and was therefore difficult to model. The differences between the two measured datasets are on average  $0.37^{\circ}\text{C}$  (difference in measurements varies from  $0.09$  to  $0.68^{\circ}\text{C}$ ). Case 3 uses the material properties calculated in cases 1 and 2 to predict the temperature profiles at a separate location. Case 3 acts as a test case for validating the material properties determined in the previous two cases. Additionally, case 3 confirms the methodological approach used in this chapter.

## **6.3. Variables**

Determining the material properties could involve numerous variables; however, in an effort to keep the modeling as simple and accurate as possible, this chapter focuses on the main variables, as described below. Conventional values found in the literature provided the basis for the assumptions made for the less significant variables, also listed below. These variables and assumptions are used as input in the differential equation for heat flow.

The software TEMP/W from GEOSLOPE solves the differential equation for heat flow:

$$Q = -k A \frac{\delta T}{\delta x} \quad [6-1]$$

Where:

$Q$  is heat flow [J s] often used with area then  $Q/A$  [J s/m<sup>2</sup>]

$A$  is area [m<sup>2</sup>]

$k$  is thermal conductivity [J/s m °C]

$\delta T/\delta x$  is the thermal gradient [°C/m]

Equation 6-1 does not account for certain variables, such as the phase change of water as it approaches 0°C. However, the software program has this capability.

To solve a differential equation such as Equation 6-1, boundary- and initial conditions have to be defined. The boundary conditions were: the temperature at six meters depth was fixed at 5°C and an averaged daily air temperature was applied to the top section of the road. The initial temperature profile (the 1<sup>st</sup> day of the 30 day modeled period) of the road section was given to the program as an initial condition.

### **6.3.1. Assumptions used during model runs**

- At a depth of six meters, the temperature is constant at 5°C (one of the boundary conditions used by TEMP/W).
- The water is assumed to be non-saline and therefore freezes and thaws at 0°C.

- The temperature used in the model was calculated hourly, allowing for two possible air temperature calculations. One option involved taking an average of all the measurements throughout the 24 hour period. The other option involved taking the average of the maximum and minimum temperature during the period. This second option was initially tried, and the difference between these two methods was negligible so to maintain consistency the first option was used throughout the model.
- Latent heat of fusion for water is  $333.7 \text{ kJ/m}^3$ .
- External factors such as precipitation and wind were ignored.

### ***6.3.2. Thermal conductivity***

The thermal conductivity is a function of the saturation, moisture content, and unit weight of the gravel. Two of the input parameters in TEMP/W are values for unfrozen and frozen thermal conductivity. The frozen and unfrozen thermal conductivity for gravel is discussed in Andersland and Ladanayi (2004) and Côté and Konrad (2005). The TEMP/W program generates a graph depicting how temperature affects conductivity, similar to that shown in Figure 6-5. The determination of this variable is important because it has significant effects on the results.

### ***6.3.3. Function of unfrozen water content versus temperature***

Figure 6-6 demonstrates the influence that temperature has on the percentage of unfrozen water content in the soil. The figure illustrates two functions, one that represents rock and the other coarse material. The heavily compacted road section is somewhere in between these categories. This function accounts for variations in thermal properties due to

changes in moisture content. This function greatly affects other variables that depend on unfrozen moisture content used by Temp/W.

#### ***6.3.4. Volumetric heat capacity***

Volumetric heat capacity is a measurement of how much energy is required to raise a certain amount of material (kg or m<sup>3</sup>) by one degree Celsius. The volumetric heat capacity calculations ignore the heat capacity of the air in the soil, but include the heat capacity of soil particles as well as that of unfrozen and frozen water. A distinction must therefore be made between frozen and unfrozen volumetric heat capacity.

#### ***6.3.5. Volumetric water content***

Temp/W uses unfrozen volumetric water content, as opposed to the more widely used gravimetric moisture content. The ICERA took actual measurements of the unfrozen volumetric moisture content from the road sections measured with the TDR equipment.

The ICERA measurements indicated a volumetric moisture content of 5% under normal conditions in the road section. However, the volumetric moisture content varied considerably depending on the freeze-thaw cycle. The model relied on a volumetric moisture content of 5% as an input variable. When a road section (coarse material) is frozen, the unfrozen moisture content should be close to 0% [Hivon and Segó, 1995].

During thaw, the moisture content undergoes extreme changes in a short time, therefore making it difficult to select one typical value for moisture content.

As a result of experimentation with different input values for unfrozen volumetric moisture content, it became clear that a single variable is insufficient for determining the moisture content during freeze and thaw conditions. In particular, during thaw, the

unfrozen moisture content varies extensively, thus contributing to the error in the predictions that were based on a single input parameter for unfrozen moisture content.

### ***6.3.6. The thermal modifier function***

The thermal modifier function is similar to but not the same as the widely used n-factor. The n-factor is the ratio between the freezing/thawing index calculated from air temperature and the temperature at the material surface. Different n-factors are calculated for freezing and thawing conditions, and  $n_f$  is based on the freezing index.  $n_t$  based on the thawing index. However, the thermal modifier function used in this analysis is the ratio between the air temperature and the temperature at a depth of 12 cm below the road surface. This upper layer of the road isolates the temperature sensor at a depth of 12 cm, for example, mitigating the effects of the sun's radiation on the darker road surface. Figure 6-7 provides a schematic drawing of the road section and the discussed temperatures. The n-factors use the ratio of freezing and thawing indices based on the asphalt and air temperatures, whereas the thermal modifier function uses the ratio between the ground and air temperatures directly. It is important to emphasize that TEMP/W requires the thermal modifier function, not the n-factors.

Figure 6-8 shows how the thermal modifier function changes with temperature. The air temperature for each day is scaled to account for differences between air and ground temperatures. This scaled temperature is then used by TEMP/W as the boundary condition for the surface of the road. This variable dominated the predictions of the model.

## **6.4. Results**

The results from the predictions were compared to the measured values from the six Campell temperature sensors. Measurements were available for all three road sections, whereas measurements from the conductivity probe were available for only two cases. The stand-alone temperature equipment has also proven to be reliable in previous projects carried out in Iceland [Bjarnason et al. 1999].

### ***6.4.1. Estimation of error***

The error of the prediction was estimated from a table, as shown in Appendix E. Three days were selected over the 30 day period, (11<sup>th</sup>, 20<sup>th</sup> and 28<sup>th</sup>) for each case. The measured temperature profile for each of these three days was compared to the predicted profile at that time, and an average absolute error for that day was calculated. The average error for that particular case was then calculated from the average absolute error from these three days.

The predicted values were compared to the dataset originating from the six independent temperature sensors as opposed to using the dataset from the thermistors in the electrical conductivity probe. Measurements of temperature profiles in the road section from the electrical conductivity probe were not available for case 1, therefore in order to keep the estimation of error consistent, the dataset from the six independent temperature sensors was used throughout the evaluation.

The biggest difference between the measured and the predicted values occurred predominately in the top part of the road. The reason was mainly that the top of the road

was greatly affected by the external forces of nature, such as the sun heating up the darkened surface. The error in the top part of the road was often dominant in terms of the average error.

The parameters used in the model were compared to calculated parameters. Most of the thermal properties can be derived from basic geotechnical variables using empirical formulas. The dry density of the gravel was assumed to be  $2100 \text{ kg/m}^3$  and the specific gravity ( $G_s$ ) to be 2.75. If these assumptions are used with Equation F-1, the void ratio can be calculated, and the porosity can be derived from the void ratio by using Equation F-2. The water content ( $w$ ) in the gravel was assumed to be 4%, and degree of saturation ( $S_r$ ) was 37% from Equation F-3.

#### **6.4.2. Thermal modifier function**

Figure 6-8 shows the values used for the thermal modifier function. This function is rarely used in the literature and therefore there are no published values that can be used for comparison. However, values for the n-factors are well established. For temperatures above zero degrees Celsius ( $n_t$ ), the temperature is multiplied by 1.4 to 2.3 and for temperatures below zero ( $n_f$ ) factors varying from 0.3 to 1 are frequently used [Andersland and Ladanayi 2004]; see also Table 3-1. As can be seen from Figure 6-8, the modifying factor for negative temperatures was assumed to be 1.1 (this value gave slightly better results than 1.0), which is similar to published values for the n-factor based on the freezing index.

For above freezing temperatures, a modifying factor less than one was used (0.45) to simulate the isolating effect of the top of the road. The n-factors based on the thawing index were frequently higher than 1 for asphalt, mainly to account for radiation from the sun. However because of the northerly latitude (around 65°N), the test sections were less exposed to sunlight than is normally observed.

When air temperatures during winter rise above zero, the temperature at a 12 cm depth is typically less than the air temperature. Analysis of data from the test sections showed that during December, January and February if the air temperature was positive, the temperature at a 12 cm depth was often approximately half of the air temperature. Those scaled values were used as input parameters for energy in Equation 6-1 solved by TEMP/W.

### ***6.4.3. Thermal conductivity***

Figure 6-5 shows the thermal conductivity versus temperature that was used in the analysis. The frozen conductivity was set as 220 kJ/day/m/°C and the unfrozen conductivity as 180 kJ/day/m/°C. A comparison of values published in Andersland and Ladanayi (2004) shows that the values used in the analysis are high for sand and gravel: they are more representative of rock. It is quite reasonable that the very densely compacted gravel and sand used to construct the road have thermal conductivities closer to published values for solid rock than loosely compacted sand or gravel.

Andersland and Ladanayi (2004) present equations to calculate frozen and unfrozen thermal conductivity depending on the porosity ( $n$ ), degree of saturation ( $S_r$ ), dry density ( $\rho_d$ ), moisture content ( $w$ ), and unfrozen moisture content ( $w_u$ )

The general equation for thermal conductivity is:

$$k = (k_{sat} - k_{dry}) \cdot K_e + k_{dry} \quad [6- 2]$$

where

$k_{sat}$  is the saturated thermal conductivity. There are different formulas for unfrozen and frozen soil.

$k_{dry}$  is the dry thermal conductivity, and

$K_e$  is the Kersten number.

There are two different formulas for  $k_{sat}$  depending on whether unfrozen or frozen conductivity is to be calculated. Equation 6-3 is for unfrozen conductivity and Equation 6-4 is for frozen.

$$k_{sat-unfrozen} = 0.57^n k_s^{1-n} \quad [6- 3]$$

where

$n$  is the porosity of the soil.

$k_s$  is the thermal conductivity of solid particles.

In Côté and Konrad (2005), the thermal conductivity of basalt particles is assumed to be 1.7 W/m °C.

$$k_{sat-frozen} = 2.2^n \cdot k_s^{1-n} \cdot 0.269^{w_u} \quad [6- 4]$$

where

$w_u$  is the unfrozen moisture content.

For frozen soil, the Kersten number, ( $K_e$ ), is assumed to be equal to the degree of saturation of the soil. However for unfrozen coarse material, Equation 6-5 is used.

$$K_{e-\text{unfrozen-Coarse}} = 0.7 \cdot \log(S_r) + 1 \quad [6-5]$$

where

$S_r$  is the degree of saturation for the soil

Equations for dry thermal conductivity ( $k_{dry}$ ) depend on whether the material is crushed or formed naturally. The gravel in the road is not crushed, but it might be blasted or ripped in a quarry as well as heavily compacted when the road was constructed. Therefore, the formula simulating crushed material was used:

$$k_{dry} = 0.039 \cdot n^{-2.2} \quad [6-6]$$

The frozen and unfrozen thermal conductivity is then calculated with Equations 6-2 to 6-6 with the following parameters: porosity, ( $n$ ), as 23%, unfrozen water content, ( $w_u$ ), as 2%; and degree of saturation, ( $S_r$ ), as 37%. According to the calculations, the unfrozen thermal conductivity was 105 kJ/day m °C and the frozen conductivity was 110kJ/day m°C. The values that gave the best results in the modeling iteration were quite far from the calculated ones. When the calculated values for thermal conductivity were used in the model, the average error for the three cases increased by about 30%. Because of the iteration process and the number of variables, it is possible to achieve reasonable accuracy by using the calculated values and varying the other variables. The solution that is presented here is the most logical combination of variables and assumptions; however, the solution is not unique.

The thermal conductivity is very dependant on the porosity; small variations in porosity, ( $n$ ), cause significant changes in the thermal conductivity. Figure 6-9 shows the relationship between the porosity and the thermal conductivity. The thermal conductivity that gave the best results in the model (220 and 180 kJ/day m °C for frozen and unfrozen respectively) can be obtained by using Equations 6-2 to 6-6 if the porosity is set to 0.14. However, a porosity of around 0.15 is in the lower range for typical values for gravel. The dry density would have to be 23.2 kN/m<sup>3</sup> (assuming  $G_s=2.75$ ) using Equations F-1 to F-3.

#### ***6.4.4. Function of unfrozen water content versus temperature***

A slightly changed default function from Temp/W for rock was used for case 1 and 2 at Dyrastadir; however, a different curve gave better results for case 3 at Dyrastadir. The curves are shown in Figure 6-6.

The modeling of the road should respond better to the correlation to coarse material than rock, as the phase change is closer to 0°C. Theoretically [Hivon and Segó 1995], all the water in the gravel should freeze soon after the temperature drops below 0°C. However, the gravel is quite porous, and some unfrozen water might exist in the pores even though the temperature in the gravel is beneath 0°C [Erlingsson et al. 2002].

#### ***6.4.5. Volumetric heat capacity***

In Andersland and Ladanayi (2004), the heat capacity for sand and gravel is given as 0.89 kJ/kg °C; but the program requires the heat capacity in the units of kJ/m<sup>3</sup> °C. The density

is assumed to be 2100 kg/m<sup>3</sup>, and hence the volumetric heat capacity is 1870 kJ/m<sup>3</sup> °C (does not distinguish between frozen or unfrozen).

Andersland and Ladanayi (2004) also present formulas to calculate the frozen and unfrozen volumetric heat capacity for any given material, depending on moisture content and dry density.

Frozen and unfrozen volumetric heat capacity can be calculated by using Equations 6-7 and 6-8 respectively:

$$c_{v-frozen} = \frac{\rho_d}{\rho_w} \left[ \left( 0.17 + \frac{w}{100} \right) + 0.5 \left( \frac{w - w_u}{100} \right) \right] c_{vw} \quad [6-7]$$

$$c_{v-unfrozen} = \frac{\rho_d}{\rho_w} \left( 0.17 + \frac{w}{100} \right) c_{vw} \quad [6-8]$$

where

$\rho_d$  is the dry density of the soil (2100 kg/m<sup>3</sup>)

$\rho_w$  is the density of water (1000 kg/m<sup>3</sup>)

$w$  is the moisture content

$w_u$  is the unfrozen moisture content

$c_{vw}$  is the heat capacity of water (4.187 kJ/m<sup>3</sup> °C)

By assuming that the moisture content is 5% and the unfrozen moisture content is 2%, then the unfrozen and frozen volumetric heat capacity can be calculated as 1950 and 2050 kJ/m<sup>3</sup> °C respectively.

In the model, 2050 [kJ/m<sup>3</sup> °C] was used for frozen volumetric heat capacity and 1950 [kJ/m<sup>3</sup> °C] for unfrozen volumetric heat capacity.

#### **6.4.6. Volumetric moisture content**

As well as temperature, moisture content is measured with depth of the road section. TEMP/W requires average volumetric moisture content as an input parameter. However, the moisture content in the road profile changes significantly during spring thaw, and therefore different moisture content could be chosen for each day of the simulation. As moisture content varies considerably with depth as well, and therefore it is not possible to choose a single value that represents all parameters. A moisture content of 5% was found to minimize the differences between measured and predicted values. This value was also not far from the average one measured by the TDR equipment in situ. Reducing the period of the prediction and splitting the road in more layers, would improve the prediction because of the increased accuracy for the moisture content. In Table 6-1, the material properties used in the analysis are summarized.

### **6.5. Comparison of measured and predicted values**

The tables in Appendix E compare the results from the prediction with the measured values. The period that was examined in all the cases was 30 days long, with three days being looked at in particular, (the 11<sup>th</sup>, 20<sup>th</sup> and 28<sup>th</sup>).

Tables E-1, E-2, and E-3 in Appendix E show the difference between measured and predicted temperature profile for cases 1, 2, and 3 respectively. The mean average error for cases 1, 2, and 3 is 0.4°C, 0.55°C and 0.55°C respectively. These results from the predictions are quite good keeping in mind that the difference between the two measured datasets was 0.25°C for case 2 and 0.37°C for case 3. The measurements from the conductivity probe were not available for case 1. The comparison for case 1 shows that

the predicted temperatures are predominantly higher than measured ones (approximately 20%). The temperature in case 1 was always above zero, therefore indicating that the unfrozen material parameters could be adjusted to lower the predicted values. The same comparison for case 2 shows that the predicted temperatures are usually higher (~20%) than the measured ones for the upper 36 cm in the road section. However, at greater depth predicted temperatures were lower (~15%) than measured. The road is predicted to thaw faster than measured at depth; improvements to the frozen heat capacity could therefore be possible. Finally in case 3 the measured temperatures generally tend to be warmer (~40%) than the predicted ones, although depending on what day is being examined. For example, measured temperature profile for day 20 in case 3 is on average 0.54°C higher than the predicted one (all predicted values being lower than the measured ones). The material parameters used in the analysis are the parameters that gave the best average results (minimize the difference between the predicted and measured values) for all three cases combined. Different material parameters could have been chosen for each case to minimize the error for that particular case.

Figures 6-10, 6-11, and 6-12 show measured and predicted temperature profiles for cases 1, 2, and 3 respectively. Measured temperature profiles from the six independent temperature sensors and the electrical conductivity probe are compared to predicted profile (measurements from the probe are not available for case 1). Days 1, 11, 20, and 28 were chosen for the comparison, day 1 shows the initial measured temperature profile given to TEMP/W as an initial condition to solve Equation 6-1. Although predicted temperature profiles varies slightly from the measured profiles the shape of the predicted

and measured profiles are always similar. In case 2 (Figure 6-11), the road is initially uniformly frozen with a temperature profile around  $-0.5^{\circ}\text{C}$ , by day 11 the air temperature is  $-5^{\circ}\text{C}$  causing the temperature in the road to decrease. By day 20 and 28 the air temperature has increased up to  $5^{\circ}\text{C}$ , causing the road to thaw.

For agencies responsible for imposing or removing axle load limitations the depth to the  $0^{\circ}\text{C}$  isotherm is of particular interest. Table 6-2 shows a summary of the measured and predicted depth to the  $0^{\circ}\text{C}$  isotherm for case 2 and 3 (case 1 never froze). The results for case 2 are quite convincing, the difference between the two measured distances and the predicted one is on average around 20%, and the predicted depth is predominately deeper than the measured depth. Figure 6-11 presents the results for the prediction for case 2, the plot for the predicted temperature profile never varies extensively from the measured profile,  $\pm 0.5^{\circ}\text{C}$  if the uppermost 15cm are ignored. Hence the results for the depth of the  $0^{\circ}\text{C}$  isotherm are similar. For case 3 the results are not as convincing; the predicted depth to the  $0^{\circ}\text{C}$  isotherm is consistently deeper than the actual measurements. In case 3, as the road section freezes, the depth to the  $0^{\circ}\text{C}$  isotherm is increasing for all measurement shown in Table 6-2, however, the predicted values give a frost penetration in the road to be deeper ( $\sim 40\%$ ) than measured. That indicates that the predicted temperature profile is losing heat more rapidly than is actually the case. Variables that affect the rate at which the heat is removed from the section are: thermal conductivity, volumetric heat capacity, and latent heat of fusion. The temperature distribution of the section in case 3 is very uniform. The lines showing the temperature profile with depth are almost parallel to the

y-axis in Figure 6-12, which causes slight changes in temperature to significantly alter the depth to the 0°C isotherm.

Quite often, one or two values greatly increase the average absolute error, often the measurements nearest to the surface. For example in case 2 at Dyrastodum, both in day 11 and 28, the difference between prediction and measurements in the top part dominates the average absolute error. The temperature in the top part of the road can change quickly, and therefore is difficult to model. Other factors such as the sun's heating of the darkened surface and snow isolating the road can significantly increase the error in these predictions. One of the main reasons for the increase in the error in cases 2 and 3 (~0.15°C increase in mean average error from case 1) is the movement of water. The road was partially frozen and the water melting in the top layers could not drain downward.

## **6.6. Possible improvement**

If the section had been modeled in two dimensions, including the sides of the road, the analysis may have been slightly more accurate. Splitting the road in layers would improve the prediction. The layers have similar but slightly different material properties; if the asphalt had been included the prediction would have been improved. However splitting the road section up into layers would only improve the prediction if studies had been carried out on measuring the material properties. It is possible to physically measure some of them, for example, the thermal conductivity. A detailed study of the material properties should improve the predictions.

The mesh of the model could be improved, the mesh used in the analysis was defined as structured quad in TEMP/W. Horizontal lines divide the section in layers, the heat-flow was assumed to be perpendicular to the surface. The mesh can be seen in Figure 6-13, the section modeled was 1.5 m wide and the height was 6 m. The top sections of the mesh are 5 cm thick, the thickness of the sections increases with depth, at the bottom the sections are 30 cm thick.

The flow of water influences the temperature in the road significantly. During spring when the road is close to saturation and water is draining as in case 2, the flow of water dramatically affects the heat flow in the road. The program Seep/W from Geoslope works with Temp/W and would in some cases improve the prediction. However, it would be quite difficult to model the impeded drainage of the ice lenses and then the transition to fully functional drainage.

The actual measurements are not free of error; improvements on the new electrical conductivity probe would probably make it more reliable than the six temperature sensors. In cases 2 and 3, the average differences between the two measured datasets were 0.25°C and 0.37°C respectively. Variations between single measurements were from 0.01 to 0.61°C for case 2 and from 0.09 to 0.68°C for case 3. One can never be absolutely certain when measuring the “correct” heat distribution in the road section.

## **6.7. Practical implications**

Agencies responsible for determining axle load limitations on roads all over the world face similar problems. The more advanced agencies have spent considerable money and

effort in developing useful and reliable methods to determine appropriate times to apply axle load limitations.

For the case when the temperature distribution of a road section is known, programs like Temp/W become useful tools. Weather forecasts are constantly improving, becoming more accurate and capable of making reliable long-term predictions. Such forecasts could be used as input parameters in programs similar to Temp/W, predicting the temperature profile during the duration of the forecast.

To make the predictions reliable, careful testing of the thermal properties of the materials in roads would have to be conducted. Through the careful establishment of all the unknown parameters, a reasonably accurate prediction of the temperature profile should be achieved. That temperature profile would then greatly aid in making decisions concerning the onset and removal of spring load limitations.

In Chapter 5 the use of temperature profiles in the road section to determine onset of SLR was discussed. The conclusion was to apply SLR when the temperature in the layers closest to the surface was at  $-3^{\circ}\text{C}$  and conditions for continued thaw were favourable. Models presented in this chapter can improve the reliability of guidelines like those by predicting the temperature in the section given the air temperature forecast. Hence removing the uncertainty of how favourable the forecasted air temperatures might be.

## 6.8. Reference

- Andersland, O.B. and Ladanyi, B. 2004. Frozen ground Engineering, Second edition, John Wiley & Sons Inc, New Jersey.
- Bjarnason, G., Erlingsson, S., Petursson, P., and Thorisson, V. 1999. Constructed Unbound Road Aggregates in Europe (COURAGE) Icelandic Final report. Public Road Administration Iceland.
- Côté J. and Konrad J.M. 2005. Thermal conductivity of base-course materials. Canadian Geotechnical Journal. 42(1): pages: 61-78 Available from: [http://pubs.nrc-cnrc.gc.ca/cgi-bin/ps/rp2\\_abst\\_f?cgi\\_t04-081\\_42\\_ns\\_nf\\_cgi1-05](http://pubs.nrc-cnrc.gc.ca/cgi-bin/ps/rp2_abst_f?cgi_t04-081_42_ns_nf_cgi1-05) [accessed the 18<sup>th</sup> March 2006].
- Erlingsson, S. Bjarnason, G., and Thorisson, V. 2002. Seasonal variation of moisture and bearing capacity in roads with a thin surface dressing wearing course, Proceedings 9<sup>th</sup> International Conference on Asphalt Pavements. Copenhagen Denmark.
- Hivon, E.G., and Segoo, D.C. 1995. Strength of frozen saline soils. Canadian Geotechnical Journal. 32(1): 336-354.

## 6.9. Tables

Variables/assumptions	Symbol	Values
Temperature at 6m depth		5°C
Phase change of water		0°C
Temperature calculation (Average/mean)		Average
Thermal conductivity (kJ/day m °C)	$k_{\text{frozen}}$	Frozen = 220
	$k_{\text{unfrozen}}$	Unfrozen = 180
Unfrozen water versus temperature		Default function for rock given in TEMP/W
		Function that simulates behaviour of coarse material
Latent heat of fusion for water (KJ/m <sup>3</sup> )		333.7
Unfrozen water content		5%
Volumetric heat capacity kJ/m <sup>3</sup> °C.	$c_{v\text{-frozen}}$	Frozen = 2150
	$c_{v\text{-unfrozen}}$	Unfrozen = 2000
Thermal modifier function		Above 0°C = 0.45
		Below 0°C = 1.1

**Table 6- 1: Summary of the material properties used for the prediction in Temp/W**

		Depth to the 0°C isotherm [cm]		
		Day 11	Day 20	Day 28
Case 2	<b>Predicted</b>	152	11	39
	<b>Electrical conductivity probe</b>	112	Less than 12	34
	<b>Temperature sensors</b>	More than 120	Less than 12	34
Case 3	<b>Predicted</b>	116	131	148
	<b>Electrical conductivity probe</b>	82	96	112
	<b>Temperature sensors</b>	75	80	99

**Table 6- 2: Depth to 0°C isotherm in the sections modeled in case 2 and 3**

## 6.10. Figures

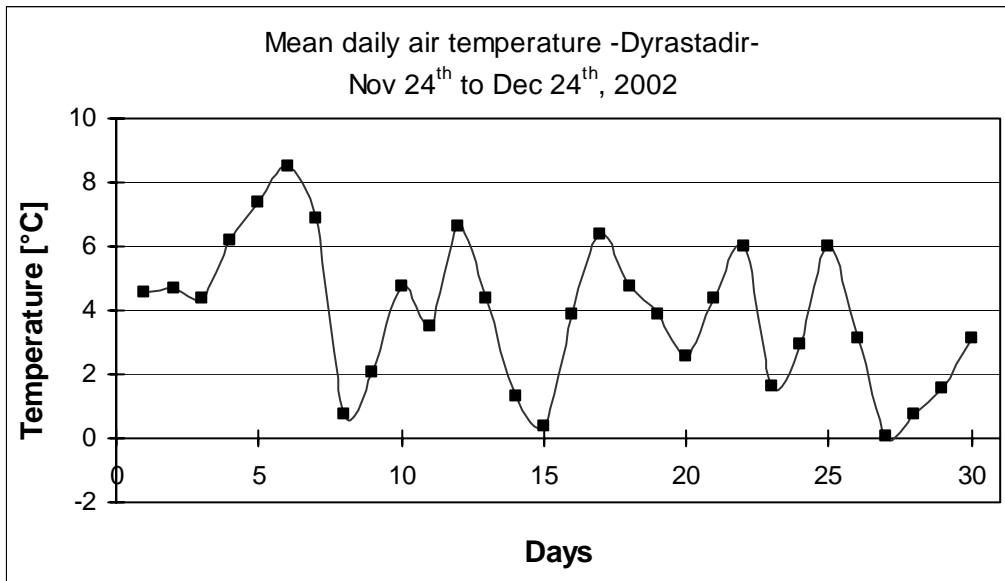


Figure 6- 1: Air temperature during the period of Case 1

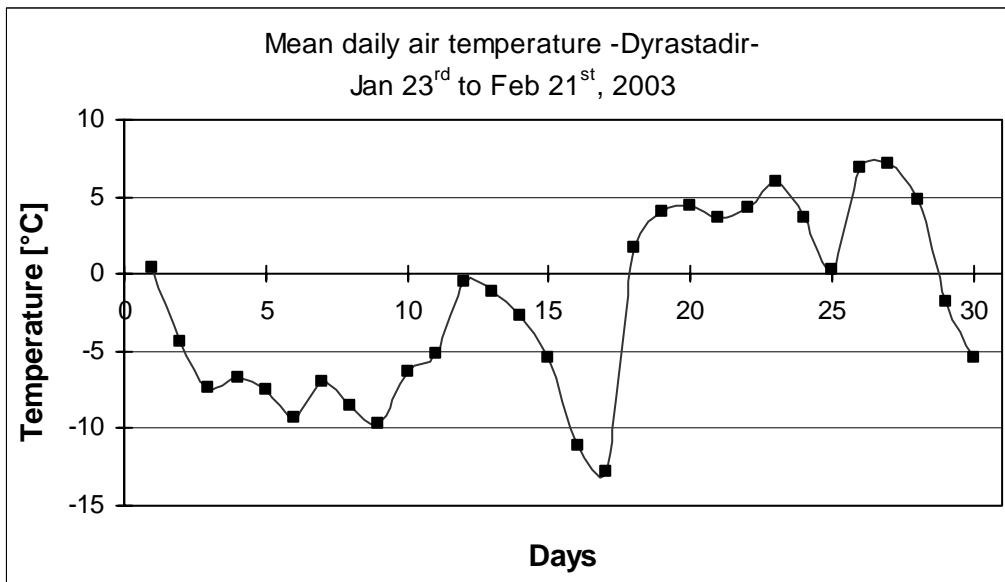


Figure 6- 2: Air temperature during the period of Case 2

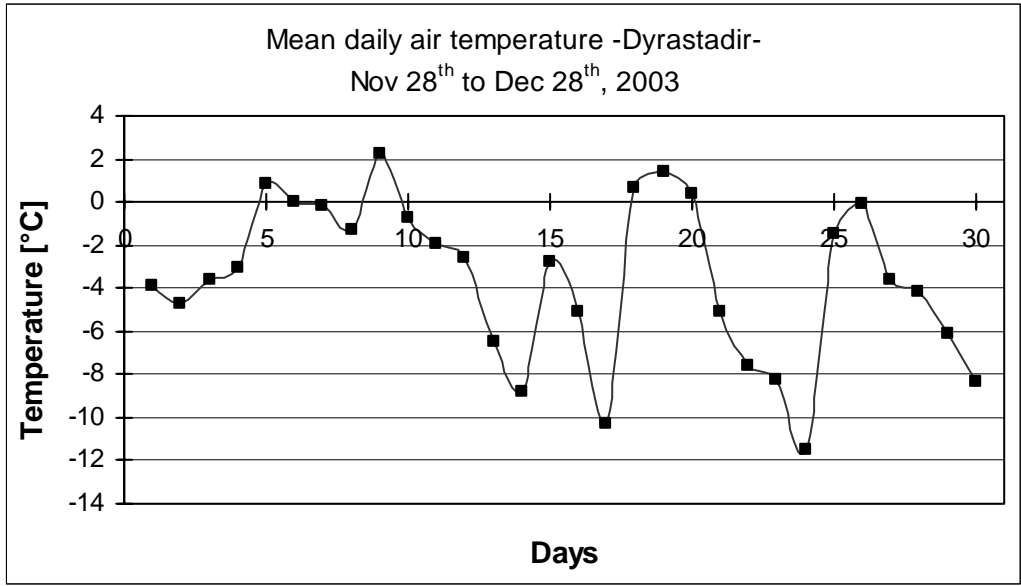


Figure 6- 3: Air temperature during the period of Case 3



Figure 6- 4: Picture taken from the section at Vatskard (photograph taken by ICERA)

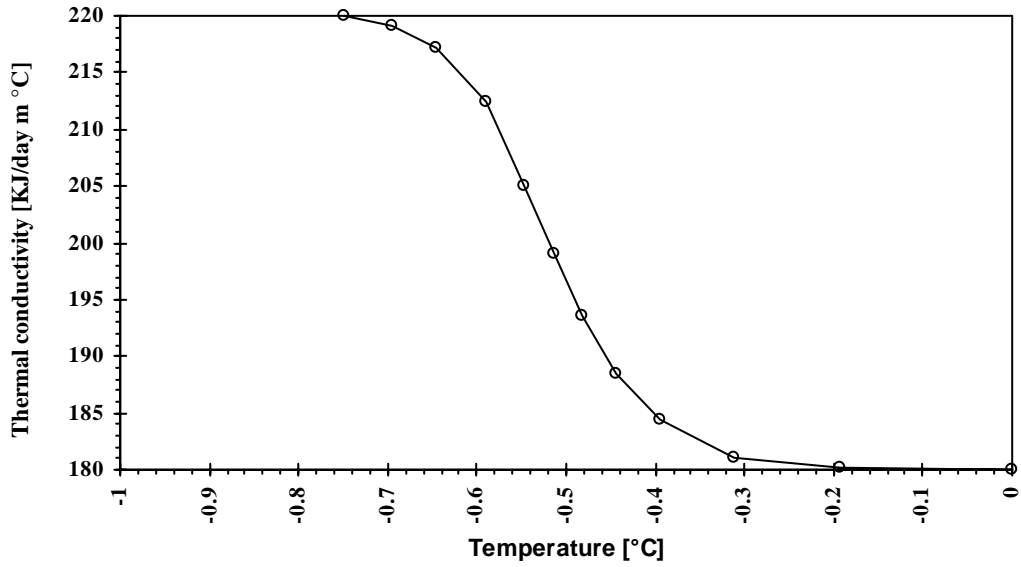


Figure 6- 5: Thermal conductivity versus temperature for gravel, graph from Temp/W

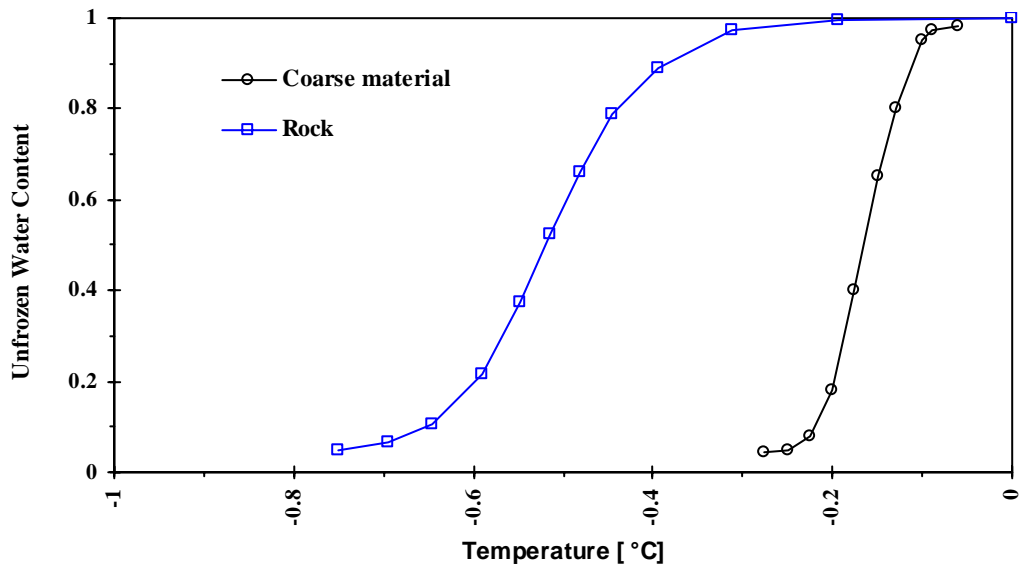
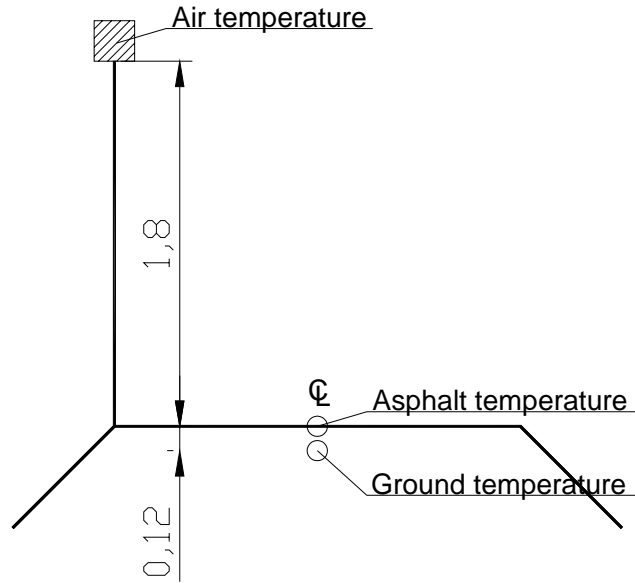


Figure 6- 6: The relationship between unfrozen water content and temperature, Coarse material was used in case 3 and rock in case 1 and 2.



All measurements in meters

Figure 6- 7: Schematic drawing of measured temperatures at a road section.

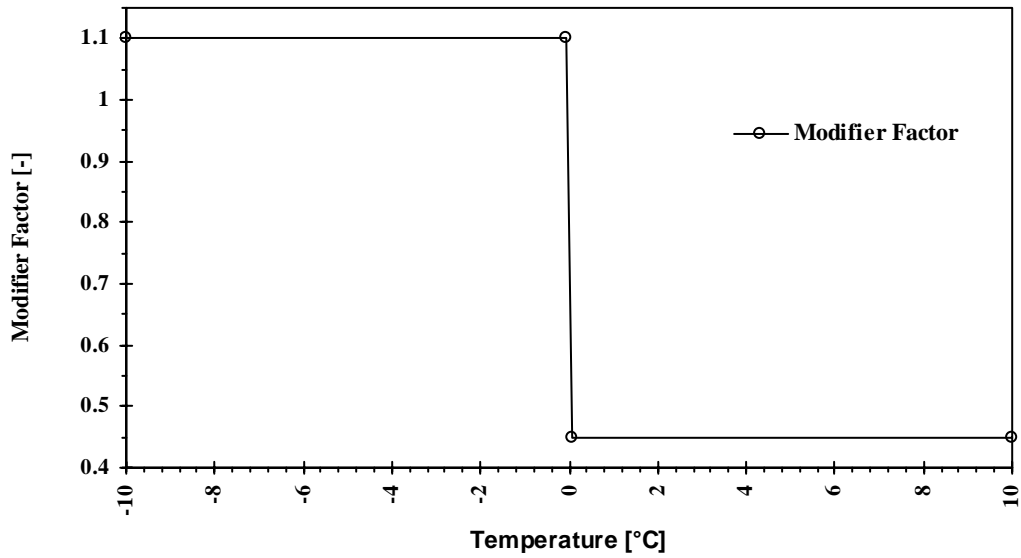


Figure 6- 8: The thermal modifier function versus temperature, graph from Temp/W.

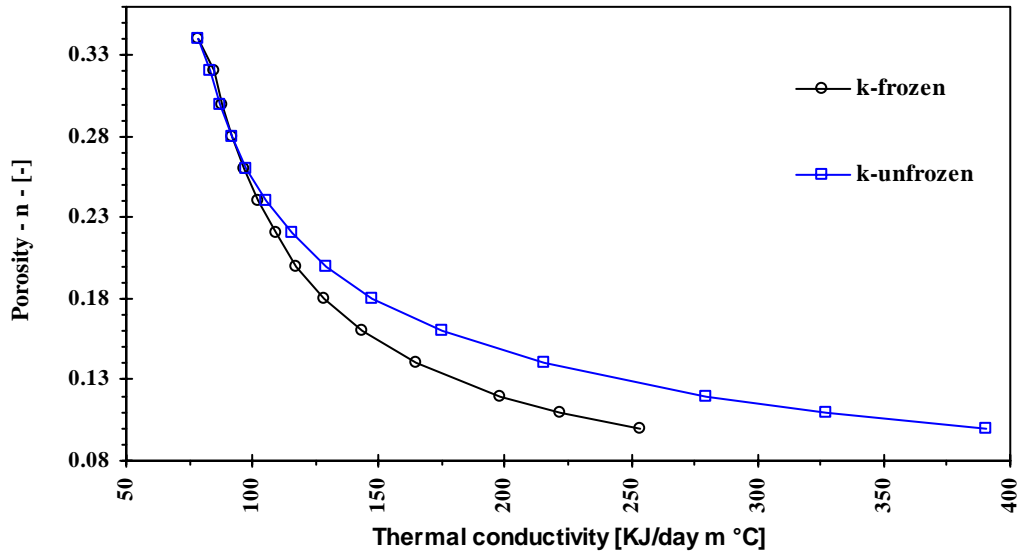


Figure 6- 9: Sensitivity analysis, showing how thermal conductivity is dependant on the porosity.

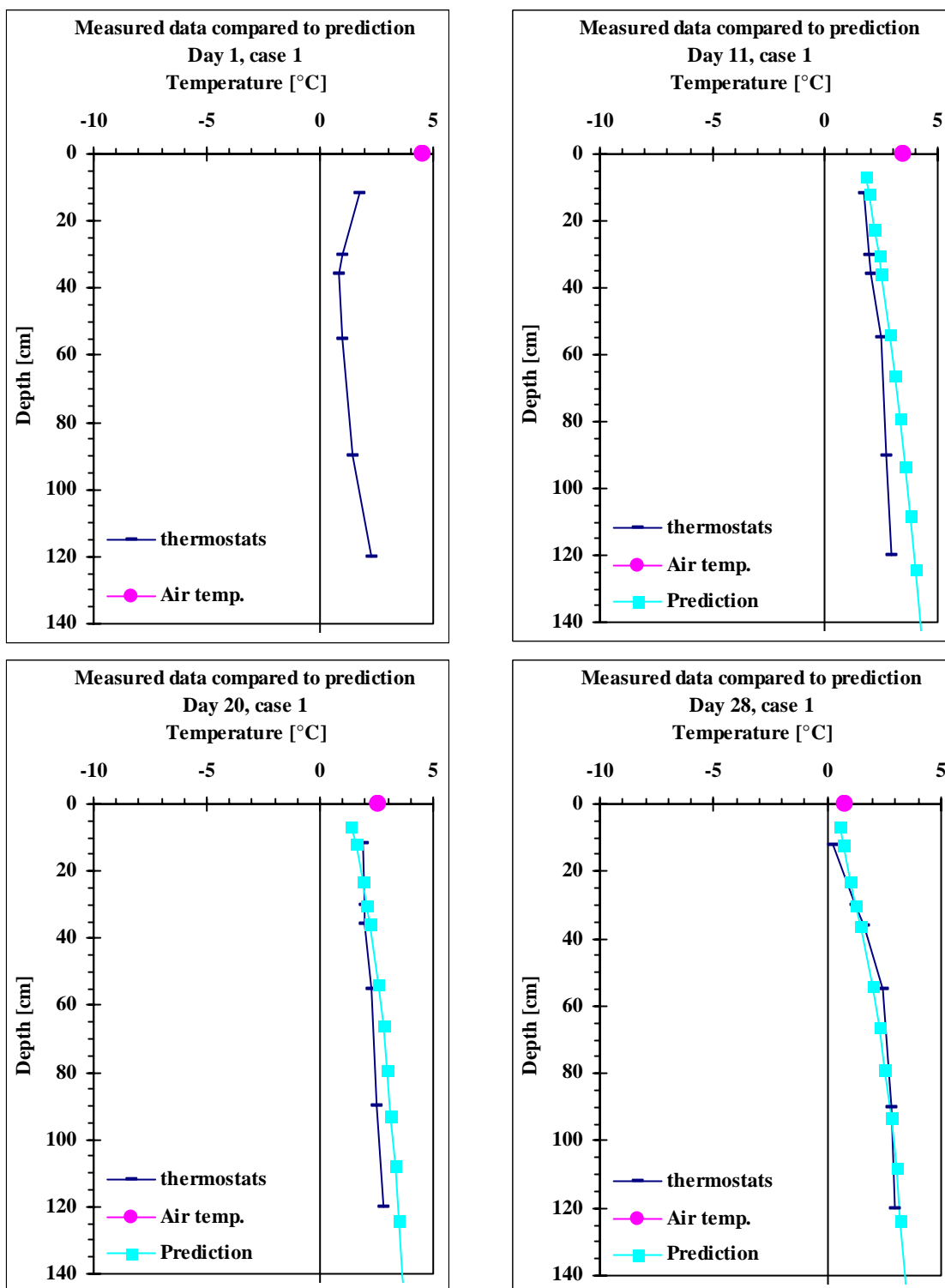


Figure 6- 10: Comparison of measured and predicted temperature profiles for case 1

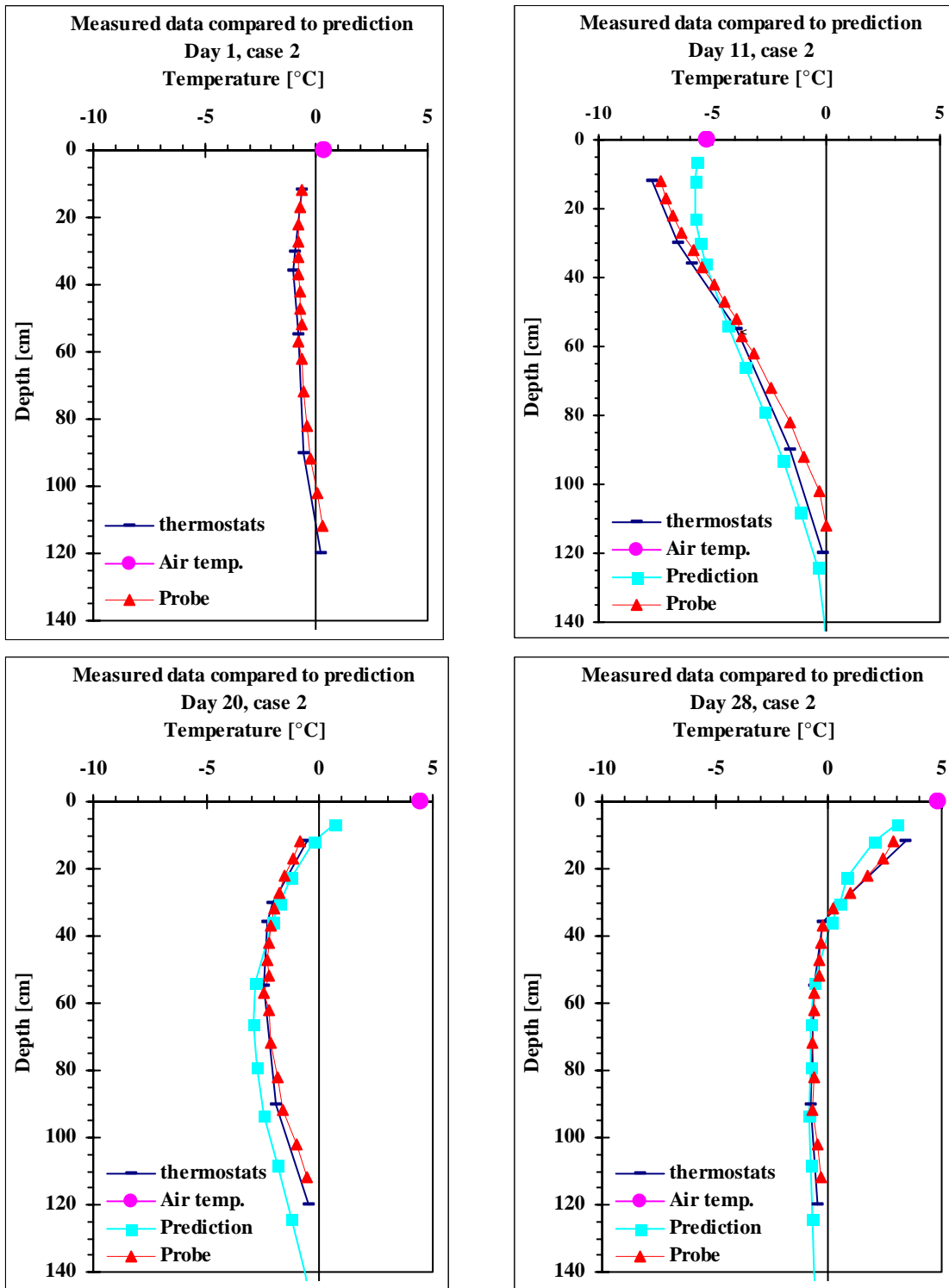


Figure 6- 11: Comparison of measured and predicted temperature profiles for case 2

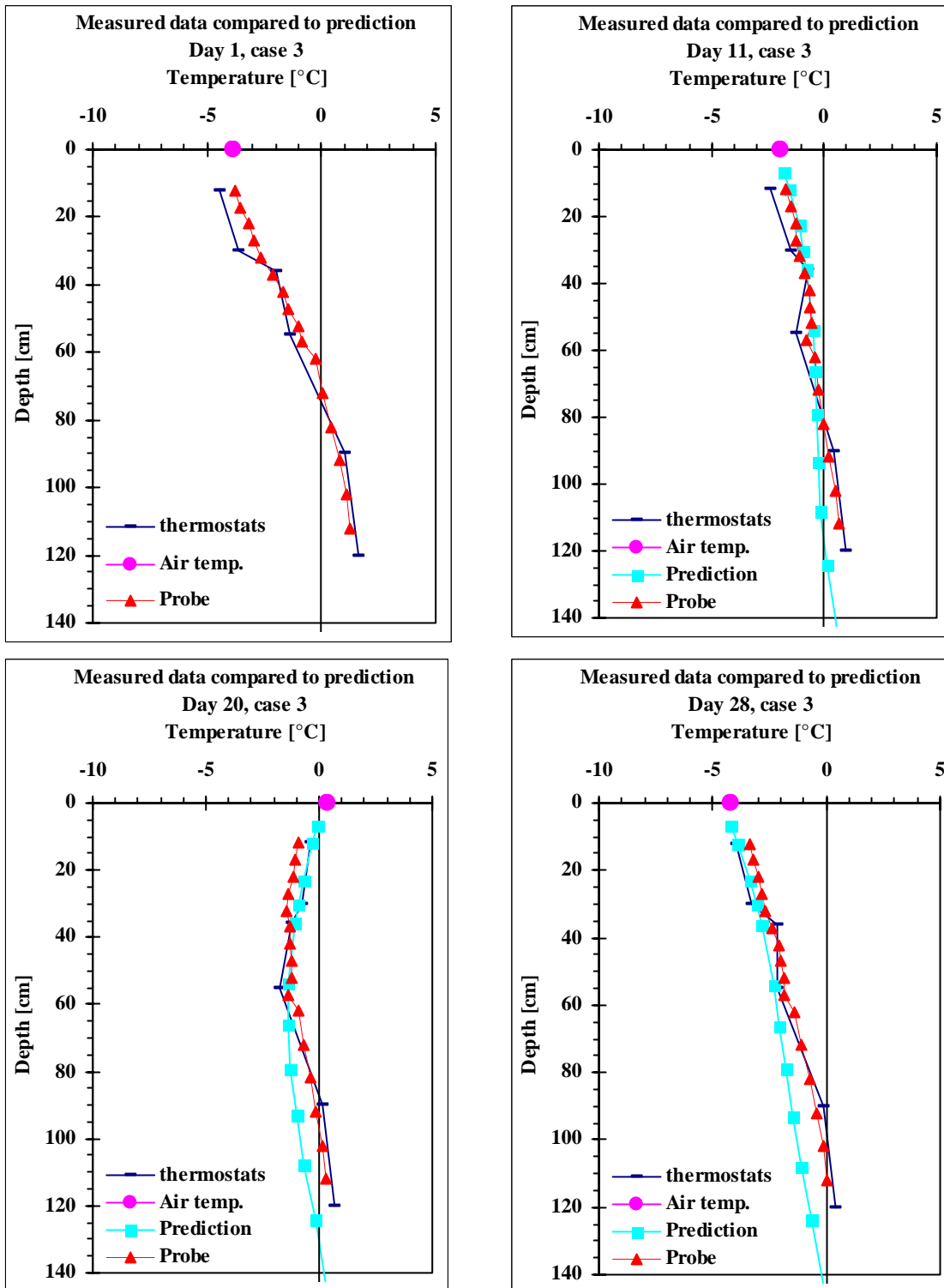


Figure 6- 12: Comparison of measured and predicted temperature profiles for case 3

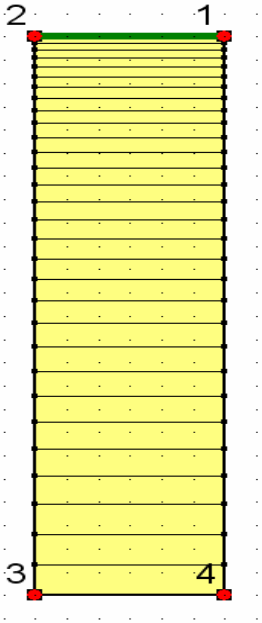


Figure 6- 13: The mesh used in the analysis, the section is 1.5m wide and the height is 6m.

## **7. Summary and Conclusions**

The objective of this thesis was to study variables associated with the determination of onset and removal of axle load limitations during thaw. The Icelandic Road Administration (ICERA) has an ongoing research project focused on improving the application of spring load restrictions and this study is a part of that research project. The ICERA has been collecting data from various test sections for several years. The database includes hourly measurements of air temperature, moisture content, and temperature profiles, and electrical conductivity measurements with depth from several test sections. The database was accessible for the purpose of this thesis. The conclusions of the study are presented later in this chapter.

A summary of the available data was presented in Chapters 4 and 5. The available database was quite comprehensive; therefore, only periods of particular interest were discussed. The following conclusions were drawn from the comparison:

- As expected, moisture content and temperature profiles in road sections are related. Temperature greatly affects the measurement of the unfrozen moisture content, and the peak moisture content clearly occurs at 0°C (Figures 5-13 to 5-15). The moisture content in the top layers of the road starts to increase around -3°C and therefore that is a more suitable benchmark to apply SLR, given continued favourable thawing conditions.
- Air temperature was compared to temperature in the top part of a road section (at 7 cm). It was observed that the air temperature can indeed be warmer or colder

than the temperature at a 7 cm depth (Figure 5-6), guiding the definition of a thermal modifier function used in the modeling of a road section (Chapter 6).

- A comparison of falling weight deflectometer (FWD)-data and moisture content in the test sections was carried out in Chapter 5 (Figures 5-16 to 5-21). The comparison showed a loss of stiffness in the section during spring thaw when moisture content was at its maximum. However, the stiffness of the section did not increase as it drained, indicating that the stiffness was not directly related to the moisture content. The road became more rigid during winter and lost that additional stiffness during spring thaw, demonstrating that the increased strength is caused mostly by cementation of the frozen water binding the soil particles together. This cohesion is lost during thaw. However, the breakdown of the soil particles in the road section due to cyclic pore-pressures occurs mainly during spring thaw, justifying the application of SLR.
- The equipment installed at the test sections, including temperature and moisture content sensors, electrical conductivity probes, and air temperature sensors functioned well. Therefore confirming the reliability of the measuring equipment installed at the test sections.

Various methods for determining the onset and removal of SLR used by various road administration agencies were summarized in Chapter 5. In most cases, these methods depend on the air temperature. These various methods were applied to the monitored test sections, where the road conditions are already known, to estimate their applicability.

- Empirical formulas using freezing and thawing indices to evaluate SLR were in general not reliable. Air temperature during thaw is often ignored, causing error in

the predicted thaw. These guidelines were tested for two locations (Dyrastadir and Thingvellir, Sections 5.2.1.3 and 5.2.1.4) where the actual conditions of the road sections were known. Therefore, an estimation of the accuracy of the guidelines could be evaluated. However, due to how easy and common it is to measure air temperature, such readings are often available when no other data about the condition of a road section are obtainable. Empirical guidelines relying on the air temperature should then be used rather than using visual inspection or a fixed date to determine SLR.

- Various road administration agencies use temperature profiles to determine the onset of axle load limitations [Kestler et al. 1999]. The applicability of this method was confirmed in Chapter 5. Kestler et al. (1999) suggest imposing axle load limitations when the road is at 0°C, however due the importance of the first few days of thaw [Ovik et al. 2000] an earlier application of the SLR is advised.
- Measurements of moisture content or electrical conductivity are more reliable than temperature measurements to evaluate the conditions of a road section. It is therefore recommended to base decisions regarding SLR on either moisture content or electrical conductivity.

While summarizing the available literature (Chapter 2) it was observed that few applications of electrical conductivity to evaluate conditions of a road sections have been reported. Measurements of electrical conductivity in various studies of permafrost are, on the other hand, commonly available. A description of the electrical conductivity probe, its installation, and calibration is provided in Chapter 4.

- A comparison of the electrical conductivity measurements and more conventional measurements of moisture content with a TDR (time domain reflectometer) contributed to the reliability of the electrical conductivity probe. Based on the graphical representation of the electrical conductivity and moisture content presented in Chapter 5, it can be concluded that measurements of electrical conductivity could successfully replace conventional measurements of moisture content for applying axle load limitations.
- When evaluating conditions of a previously existing road section, installation and monitoring with an electrical conductivity probe is less expensive than doing so with conventional TDR measurements<sup>1</sup>.
- Derivation of an empirical relationship between the electrical conductivity and TDR measurements was not successful. An approximation of the moisture content can be achieved from the electrical conductivity but it is not reliable. On the other hand an exact value of the moisture content calculated from the electrical conductivity was not found to be of particular interest. The most important information from the conductivity measurements is the time when the thaw of the road section begins, resulting in the need for onset of the spring load restrictions (SLR)

## **7.1. Modeling**

Temperature distribution in a road section was modeled in Temp/W. The practical application of the model designed in Chapter 6 is that a road administration agency requires an evaluation only of the material properties in a section and an air temperature

---

<sup>1</sup> Erlingsson, S. (personal communication 2006)

forecast to be able to predict the temperature profile in the section for the duration of the weather forecast. Road administration agencies often need to give 7 to 10 days notice before applying spring load restrictions [Ovik et al. 2000]. Since the first days of the thawing of a road section contribute most damage, it is very useful to be able to know the temperature distribution in the road section several days early in order to apply the restrictions in time.

- Predicted profiles were compared to two independent sets of measured profiles. By comparing the prediction to the actual measurements, it was possible to evaluate the accuracy of the variables used in the prediction. Variables used in the prediction were in general in accordance with the calculated or previously published values for coarse material. Values for unfrozen and frozen thermal conductivity calculated based on reasonable, approximate soil properties did not give good results when used in the model. Slightly adjusted values published in Andersland and Ladanayi (2004) were used instead. Values for rock gave better results than for sand and gravel (rock has a higher thermal conductivity), findings which might be justified due to the high density of the road section.
- Three cases were modeled, and the difference between the measured and predicted values was on average 0.5°C or about 25%. Single measurements, predominately in the top part of the road, often contributed significantly to the average difference between the measured and predicted values. The reason was mainly that the top part of the road was greatly affected by the external forces of nature, such as the sun heating up the darkened surface.

- Comparison of predicted and measured temperature profiles are presented in Chapter 6. The shape of the predicted profiles is always similar to that of the measured ones. Comparison of the depth of the 0°C isotherm according to measured and predicted temperature profiles implied that the predicted profiles were dependable.

## **7.2. Improvements and recommendations**

Determination of axle load limitations in Iceland can be improved, and the ICERA is, in fact, incorporating the information from the electrical conductivity probes into its decisions-making regarding SLR. In the beginning of 2005 and until recently, new probes were installed at various locations on Highway nr. 1 in Iceland that allowed the ICERA to base its decisions to impose axle load restrictions on the results of these measurements. Prior to 2005, the probes were located only in a limited area in northern Iceland. The reliability of the conductivity probes has been studied in this project. It is not necessary to install TDR or air temperature equipment at each test section in order to acquire necessary information to evaluate the condition of the road section; for that the electrical conductivity probes can be relied on. To the author's knowledge, it is the ICERA'S intention to increase the number of functional probes in the highway system, to improve the available information for onset or removal of spring load restrictions. Special attention should be paid to the elevation of the test locations. Test sections that are located at low elevations thaw first and are critical for onset of SLR. Test sections at higher elevations are more critically placed for evaluating the duration of the SLR.

The road system should be divided into a few routes between the large cities (Reykjavik, Akureyri, Hella, and Egilsstadir for an example), and each route should be handled separately although coordinated with the other routes. It might be acceptable to allow full axle loads at the beginning of thaw and accept the damage to the roads or to remove limitations, even before the sections have not yet fully thawed and drained. The break even point for negative social economic impacts associated with axle load limitations and repair of damage occurring during spring thaw is not well studied. An estimation of damage to Icelandic highways occurring during spring thaw and an estimation of the percentage of the damage caused by heavy trucks would improve determination of axle load limitations.

The next step in improving the decision-making concerning axle load limitations in Iceland could be to look at the methodology in more detail. The measurement equipment has proved to work well, but the data interpretation needs improving. Electrical conductivity is closely monitored, but when should the axle load limitations be applied? Certainly, it is easy to point out when ICERA should apply the SLR when the measurements from the whole year are available and studied. However, to evaluate when to apply the SLR in real time given the measurements is more challenging. Should a specific value of electrical conductivity be used or should the rate of increase in the conductivity be looked at to determine the onset of SLR? How would a specific value or the rate of increase be determined? What about removal? Should a certain percentage of drainage take place before the limitations can be removed or should the ICERA use a fixed relative conductivity? The measurements from the sensors nearest to the surface

would probably determine the onset, but what depth should be used for removal? The best way of determining a benchmark that can be referred to when applying or removing axle load limitations, would be to relate the conductivity to strain. Measuring conductivity of various samples and then testing them in a triaxial cell to measure deformations could be sufficient calibration. Weather forecasts must be included in the evaluation of when to apply the SLR. Forecasts indicating favourable conditions for continued thaw support the decision of applying SLR.

No experience has yet been acquired about the durability and long-term reliability of the electrical conductivity probe, factors that affect the suitability of using the probe for monitoring purposes.

The decision for applying SLR cannot be fully automated: some engineering judgment has to be applied. However, it should be possible to develop some guidelines for the application of SLR.

It was noticed that the moisture content in the road section started to increase when the temperature in the uppermost layers was around  $-3^{\circ}\text{C}$ . That could be caused by the sun's radiation or other external factors. It could also be caused by dissolved minerals in the water. A chemical analysis of water obtained from the road section would be useful to answer that question.

The model presented in Chapter 6 can be significantly improved. Splitting a section up into more detailed layers and including the bituminous surface should improve the predictions. A simple study of the thermal properties of the material in the road section is necessary for improving the reliability of the model. Because of the number of unknown parameters, no unique solution exists. Therefore, reducing the unknown variables would result in better predictions. To include the flow of water in a section would also improve the model; Seep/W works with Temp/W and could probably model the flow of water in a section, although it might be difficult to model the impeded drainage of the ice lenses and the subsequent transition to fully functional drainage.

The financial gain of correctly imposing SLR is very substantial. Ovik et al. (2000) states that the lifetime of a road system can be increased by 10% by accurately applying load restrictions during spring thaw. That implies that the cost of repair and preventive measurements could be decreased by 10%. In a financial report for the year 2004 from the Icelandic Road Administration published in 2005<sup>2</sup>, it is reported that the total cost of repair for the road system that year was approximately 1,811,000,000 Ikr (\$33 million CAD<sup>3</sup>). The benefits of the improved application of SLR will not be observed in the first few years since the roads have to be repaired from previous damage, however in 5-10 years ICERA should be able to save approximately 180,000,000 Ikr (3.3\$ million CAD) annually, because of increased durability of the roads.

---

<sup>2</sup>

[http://www.vegagerdin.is/vefur2.nsf/Files/Skyrslasamgonguradherra2004/\\$file/Skyrsla%20radherra%202004.pdf](http://www.vegagerdin.is/vefur2.nsf/Files/Skyrslasamgonguradherra2004/$file/Skyrsla%20radherra%202004.pdf) (accessed the 17<sup>th</sup> January 2006)

<sup>3</sup> 1\$ CAD is assumed to be equivalent of 55 Ikr

### 7.3. References

Andersland, O.B., and Ladanyi, B. 2004. Frozen ground Engineering, Second edition, John Wiley & Sons Inc., New Jersey.

Kestler, M. A., Hanek, G., Truebe, M., and Bolander, P. 1999. Removing spring thaw load restrictions from low-volume roads: development of a reliable, cost-effective method. In Proceedings, 7th International Conference on Low-Volume Roads, May 23-26, 1999, Baton Rouge, LA. In: Transportation Research Record, no. 1652, v. 2. Washington, D.C.: National Academy Press, 188-197.

Ovik, J.M., Siekmeier, J. A., and van Deusen D. 2000. Improved load restrictions guidelines using mechanistic analysis. Minnesota Road Research Project (Mn/Road Project) Available from: <http://www.lrrb.gen.mn.us/pdf/200018.pdf> [accessed 27<sup>th</sup> March 2006].

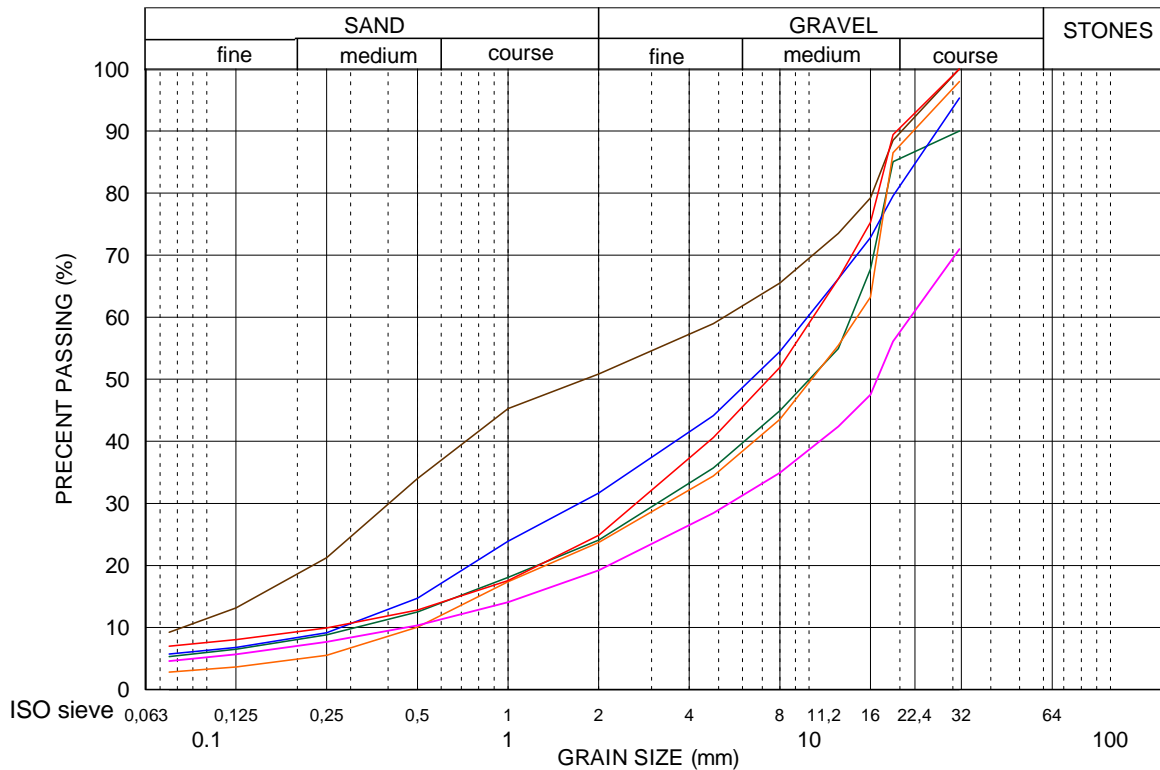
## Appendix A - Classification of Frozen Soil

(1)	Major group		Subgroup			Field identification (6)	Pertinent properties (7)	
	Description (2)	Symbol (3)	Description (4)		Symbol. (5)			
<b>Part I:</b> Description of soil phase. (independent of frozen state)	Segregated ice is not visible by eye	N	Poorly bonded or friable		Nf	Identify by visual examination. Determine presence of excess ice, use hand magnifying lens as necessary. For soils not fully saturated, estimate degree of ice saturation: medium, low. Note presence of crystals or of ice coatings around larger particles	In place temperature density and void ratio a. In froze state b. After thawing takes place Water content (total H <sub>2</sub> O including ice)	
			Well bonded	no excess ice	Nb			n
				excess ice				e
<b>Part II:</b> Description of frozen soil	Segregated ice is visible by eye (ice thickness is 1 in. or less)	V	Individual ice crystals or inclusions		Vx	For ice phase, record the following as applicable: Location Orientation Length Spacing Size Shape Pattern of arrangement Hardness (per part III) Structure (per part III) Color (per part III)	a. Average b. Distribution Strength a. Compressive b. Tensile c. Shear d. Adfreeze Elastic properties Plastic properties Thermal properties Ice crystal structure (using optical instruments) a. Orientation of axes b. Crystal size c. Pattern of arrangement	
			Ice coatings on particles		Vc			
			Random or irregularly oriented ice formations		Vr			
			Stratified or distinctly oriented ice formations		Vs			
<b>Part III:</b> Description of substantial ice strata	Ice (thickness is greater than 1 in.)	ICE	Ice with soil inclusions		ICE + soil type	Designate as ICE and use descriptive terms as follows, usually one item from each group as applicable. Hardness (of mass, not individual crystals) hard, soft Structure: clear cloudy, porous, candled, granular, stratified Color (for example): colorless, grey, blue Admixtures (for example): contains few thin silt inclusions	Same as Part II, as applicable, with special emphasis on ice crystal structure	
			Ice without soil inclusion		ICE			

Table A- 1: Classification of frozen soil, modified from Andersland and Ladanyi (2004)

# Appendix B - Grain Size Distributions

## Dýrastaðir Grain size distribution



### MEASURED VALUES:

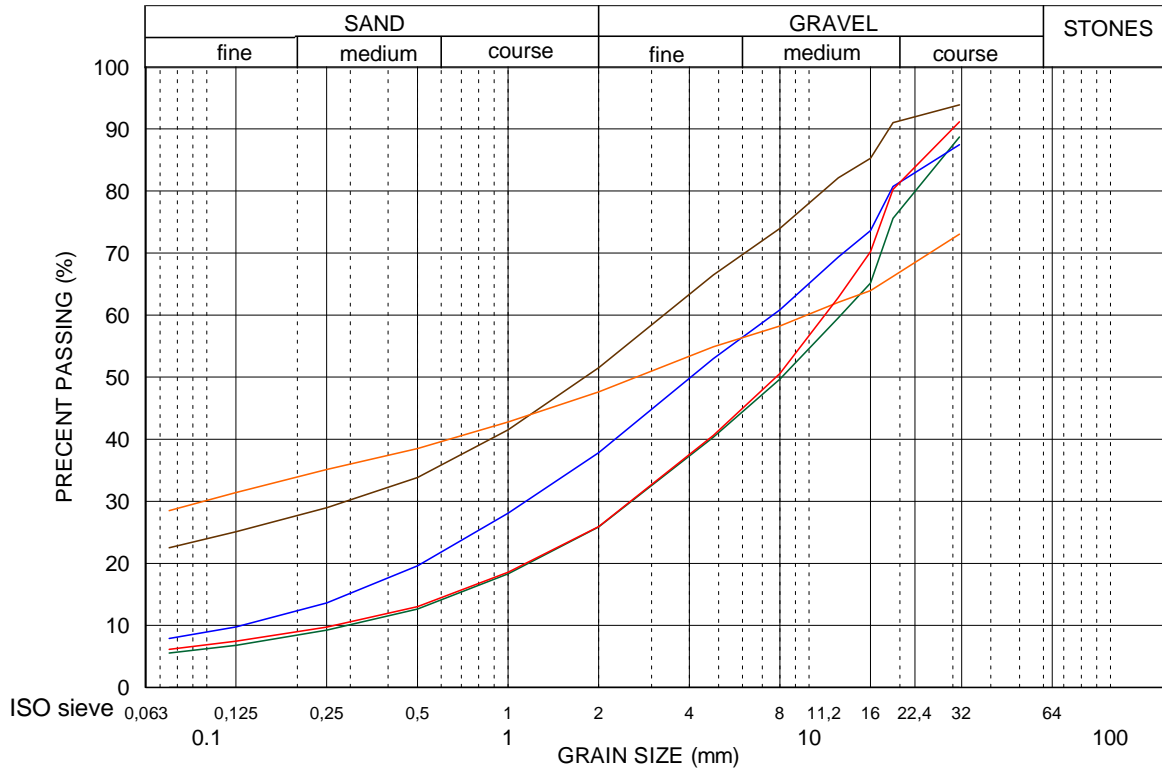
Sieve size.	0.075	0.125	0.25	0.5	1	2	5	8	13	16	19	32
Sample 1	7	8	10	13	18	25	41	52	66	75	89	100
Sample 2	5	7	9	13	18	24	36	45	55	68	85	90
Sample 3	6	7	9	15	24	32	44	54	66	73	80	95
Sample 4	9	13	21	34	45	51	59	65	74	79	89	100
Sample 5	3	4	6	10	17	24	34	44	55	63	86	98
Sample 6	5	6	8	10	14	19	28	35	42	48	56	71

### Samples:

- Sample 1: Directly under the asphalt
- Sample 2: at 3-10cm depth (upper base layer)
- Sample 3: at 16-20cm depth (upper base layer)
- Sample 4: at 33-38cm depth (lower base layer)
- Sample 5: at unknown depth (lower base layer)
- Sample 6: at 80-90cm depth (subbase)

Figure B- 1: Grain size distribution from Dyrastadir test section

## Vatnskarð Grain size distribution



**MEASURED VALUES:**

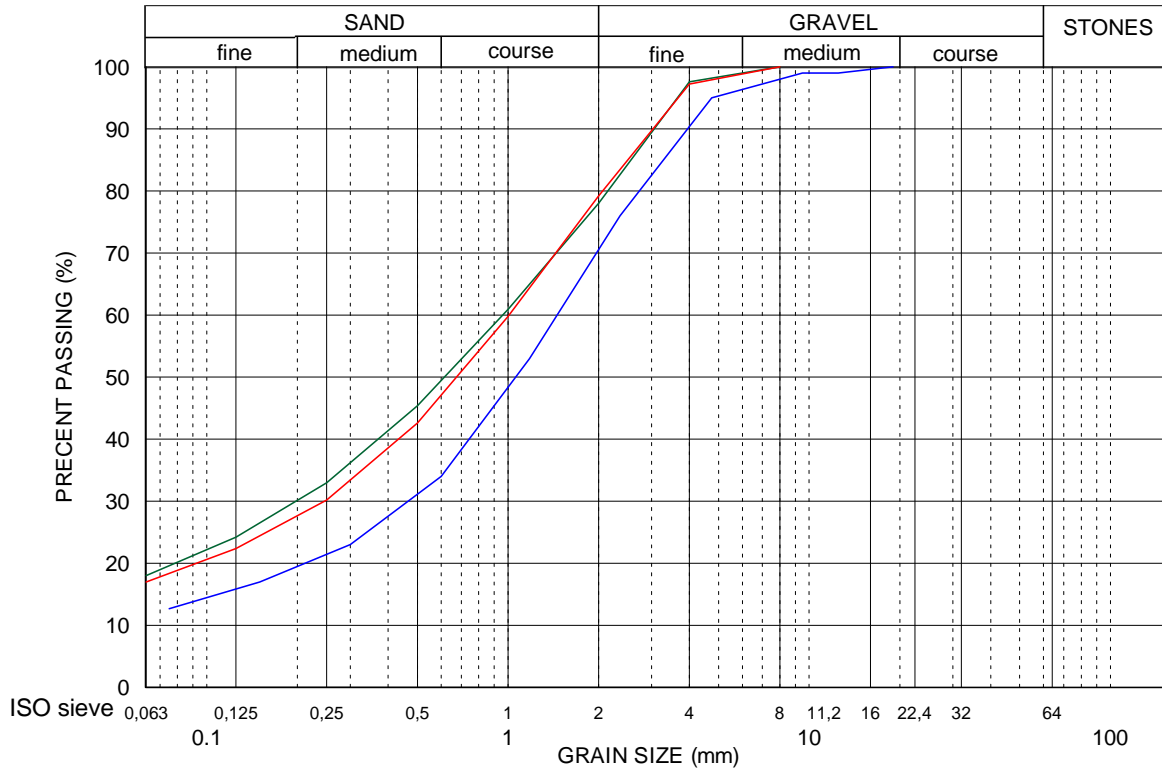
Sieve size.	0.075	0.125	0.25	0.5	1	2	5	8	13	16	19	32
Sample 1	6	7	10	13	19	26	41	51	63	70	80	91
Sample 2	6	7	9	13	18	26	40	50	60	65	76	89
Sample 3	8	10	14	20	28	38	53	61	69	74	81	87
Sample 4	23	25	29	34	42	52	66	74	82	85	91	94
Sample 5	28	31	35	38	43	48	55	58	62	64	66	73

**Samples:**

- Sample 1 at 2-8cm depth (upper base layer)
- Sample 2 at 15-20cm depth (upper base layer)
- Sample 3 at 30-40cm depth (lower base layer)
- Sample 4 at 85cm depth (subbase)
- Sample 5 at 110-120cm depth (subbase)

**Figure B- 2: Grain size distribution from Vatnskard test section**

## Moraine from quarry Grain size distribution



**MEASURED VALUES:**

Sieve size.	0.075	0.15	0.3	0.5	1.0	2.0	4.0	8.0
Sample 1	17	22	30	43	60	79	97	100
Sample 2	18	24	33	45	61	78	98	100
Sample 3	13	17	23	34	53	76	95	99 99 100

**Samples:**

- Sample 1 taken from quarry 2003
- Sample 2 taken from quarry 2003
- Sample 3 taken from quarry 2002

**Figure B- 3: Grain size distribution of the material used with the electrical conductivity probe.**

## Appendix C - Dyrastadir Freezing and Thawing indices

Date	Average temperature	0-average temp	FI	Average temp - reference	TI	Frost penetration [m]	Note
25.10.2001	4.24	-4.24		5.74			
26.10.2001	1.06	-1.06		2.56			
27.10.2001	-0.33	0.33	0.33	1.17			Early freeze
28.10.2001	-0.20	0.20	0.52	1.30			
29.10.2001	1.39	-1.39	-0.87	2.89			
30.10.2001	-0.07	0.07	-0.80	1.43			
31.10.2001	-4.19	4.19	3.39	-2.69			
1.11.2001	6.70	-6.70		8.20			
2.11.2001	2.10	-2.10		3.60			
3.11.2001	-1.87	1.87	1.87	-0.37		-0.25	
4.11.2001	-5.01	5.01	6.89	-3.51		-0.18	
5.11.2001	-3.09	3.09	9.97	-1.59		-0.15	
6.11.2001	-4.06	4.06	14.03	-2.56		-0.11	
7.11.2001	-5.34	5.34	19.37	-3.84		-0.07	
8.11.2001	-7.11	7.11	26.48	-5.61		-0.03	
9.11.2001	5.49	-5.49	20.99	6.99		-0.06	
10.11.2001	3.02	-3.02	17.98	4.52		-0.08	
11.11.2001	-2.11	2.11	20.08	-0.61		-0.07	
12.11.2001	-4.72	4.72	24.80	-3.22		-0.04	
13.11.2001	-0.07	0.07	24.86	1.43	1.43	-0.04	Early thaw
14.11.2001	4.90	-4.90		6.40	7.83		
15.11.2001	5.06	-5.06		6.56	14.40		
16.11.2001	5.95	-5.95		7.45	21.85		
17.11.2001	4.70	-4.70		6.20	28.04		
18.11.2001	6.55	-6.55		8.05	36.09		
19.11.2001	3.98	-3.98		5.48	41.57		
20.11.2001	-0.99	0.99	0.99	0.51		-0.27	Early freeze
21.11.2001	-3.57	3.57	4.55	-2.07		-0.20	
22.11.2001	-2.72	2.72	7.27	-1.22		-0.17	
23.11.2001	3.11	-3.11	4.17	4.61		-0.21	
24.11.2001	0.00	0.00	4.16	1.51		-0.21	
25.11.2001	-5.62	5.62	9.78	-4.12		-0.15	
26.11.2001	-4.16	4.16	13.94	-2.66		-0.11	
27.11.2001	-4.92	4.92	18.86	-3.42		-0.08	
28.11.2001	-10.29	10.29	29.15	-8.79		-0.02	
29.11.2001	-6.88	6.88	36.03	-5.38		0.02	
30.11.2001	-4.08	4.08	40.11	-2.58		0.04	
1.12.2001	-6.77	6.77	46.87	-5.27		0.07	

Date	Average temperature	0-average temp	FI	Average temp - reference	TI	Frost penetration [m]	Note
2.12.2001	-3.95	3.95	50.82	-2.45		0.08	
3.12.2001	-5.29	5.29	56.11	-3.79		0.10	
4.12.2001	-5.26	5.26	61.37	-3.76		0.12	
5.12.2001	-3.91	3.91	65.28	-2.41		0.14	
6.12.2001	0.75	-0.75		2.25	2.25		Early thaw
7.12.2001	2.64	-2.64		4.14	6.39		
8.12.2001	0.41	-0.41		1.91	8.30		
9.12.2001	3.91	-3.91		5.41	13.71		
10.12.2001	7.64	-7.64		9.14	22.85		
11.12.2001	5.72	-5.72		7.22	30.07		
12.12.2001	3.03	-3.03		4.53	34.60		
13.12.2001	8.26	-8.26		9.76	44.36		
14.12.2001	8.31	-8.31		9.81	54.16		
15.12.2001	8.05	-8.05		9.55	63.71		
16.12.2001	6.38	-6.38		7.88	71.59		
17.12.2001	3.74	-3.74		5.24	76.84		
18.12.2001	4.66	-4.66		6.16	83.00		
19.12.2001	1.98	-1.98		3.48	86.48		
20.12.2001	5.25	-5.25		6.75	93.23		
21.12.2001	-3.71	3.71	3.71	-2.21		-0.22	Early thaw
22.12.2001	-0.46	0.46	4.17	1.04		-0.21	
23.12.2001	1.88	-1.88	2.29	3.38		-0.24	
24.12.2001	-2.00	2.00	4.28	-0.50		-0.21	
25.12.2001	-7.96	7.96	12.25	-6.46		-0.13	
26.12.2001	-3.72	3.72	15.97	-2.22		-0.10	
27.12.2001	-8.98	8.98	24.94	-7.48		-0.04	
28.12.2001	-7.59	7.59	32.53	-6.09		0.00	
29.12.2001	-8.40	8.40	40.93	-6.90		0.04	
30.12.2001	-6.58	6.58	47.51	-5.08		0.07	
31.12.2001	1.90	-1.90		3.40	3.40		Early thaw
1.1.2002	4.69	-4.69		6.19	9.59		
2.1.2002	7.29	-7.29		8.79	18.38		
3.1.2002	-0.28	0.28		1.22	19.59		
4.1.2002	6.79	-6.79		8.29	27.89		
5.1.2002	3.30	-3.30		4.80	32.68		
6.1.2002	3.01	-3.01		4.51	37.19		
7.1.2002	0.51	-0.51		2.01	39.20		
8.1.2002	1.18	-1.18		2.68	41.87		
9.1.2002	3.12	-3.12		4.62	46.49		
10.1.2002	0.61	-0.61		2.11	48.60		
11.1.2002	-1.11	1.11		0.39	48.99		
12.1.2002	1.02	-1.02		2.52	51.51		
13.1.2002	-0.60	0.60		0.90	52.41		

Date	Average temperature	0-average temp	FI	Average temp - reference	TI	Frost penetration [m]	Note
14.1.2002	2.63	-2.63		4.13	56.54		
15.1.2002	-0.44	0.44		1.06	57.60		
16.1.2002	1.41	-1.41		2.91	60.51		
17.1.2002	1.13	-1.13		2.63	63.14		
18.1.2002	0.85	-0.85		2.35	65.49		
19.1.2002	2.17	-2.17		3.67	69.16		
20.1.2002	1.76	-1.76		3.26	72.42		
21.1.2002	0.07	-0.07		1.57	73.99		
22.1.2002	-5.46	5.46	5.46	-3.96		-0.19	START FROST
23.1.2002	-7.11	7.11	12.57	-5.61		-0.12	
24.1.2002	-9.54	9.54	22.11	-8.04		-0.06	
25.1.2002	-9.62	9.62	31.73	-8.12		0.00	
26.1.2002	-6.78	6.78	38.51	-5.28		0.03	
27.1.2002	-8.05	8.05	46.56	-6.55		0.07	
28.1.2002	-9.66	9.66	56.22	-8.16		0.11	
29.1.2002	-8.84	8.84	65.06	-7.34		0.14	
30.1.2002	-5.24	5.24	70.30	-3.74		0.16	
31.1.2002	-1.51	1.51	71.82	-0.01		0.16	
1.2.2002	1.63	-1.63	70.18	3.13		0.16	
2.2.2002	-4.39	4.39	74.57	-2.89		0.17	
3.2.2002	-5.76	5.76	80.33	-4.26		0.19	
4.2.2002	-6.11	6.11	86.44	-4.61		0.21	
5.2.2002	-7.74	7.74	94.18	-6.24		0.23	
6.2.2002	-6.82	6.82	101.01	-5.32		0.25	
7.2.2002	-8.01	8.01	109.02	-6.51		0.28	
8.2.2002	-6.00	6.00	115.02	-4.50		0.29	
9.2.2002	-3.44	3.44	118.46	-1.94		0.30	
10.2.2002	-4.60	4.60	123.06	-3.10		0.31	
11.2.2002	-4.86	4.86	127.92	-3.36		0.33	
12.2.2002	-9.67	9.67	137.59	-8.17		0.35	
13.2.2002	2.66	-2.66	134.93	4.16		0.34	
14.2.2002	-1.14	1.14	136.07	0.36		0.35	
15.2.2002	1.16	-1.16	134.91	2.66		0.34	
16.2.2002	-1.39	1.39	136.30	0.11		0.35	
17.2.2002	-2.87	2.87	139.16	-1.37		0.35	
18.2.2002	-8.20	8.20	147.37	-6.70		0.37	
19.2.2002	-6.34	6.34	153.70	-4.84		0.39	
20.2.2002	-7.84	7.84	161.54	-6.34		0.41	
21.2.2002	-3.79	3.79	165.33	-2.29		0.42	
22.2.2002	-6.66	6.66	171.99	-5.16		0.43	
23.2.2002	-10.71	10.71	182.70	-9.21		0.45	
24.2.2002	-12.99	12.99	195.69	-11.49		0.48	
25.2.2002	-7.29	7.29	202.98	-5.79		0.50	
26.2.2002	-8.27	8.27	211.25	-6.77		0.51	
27.2.2002	-10.34	10.34	221.59	-8.84		0.53	

Date	Average temperature	0-average temp	FI	Average temp - reference	TI	Frost penetration [m]	Note
28.2.2002	-11.38	11.38	232.97	-9.88		0.55	
1.3.2002	-3.09	3.09	236.06	-1.59		0.56	
2.3.2002	1.73	-1.73	234.33	3.23		0.56	
3.3.2002	-2.89	2.89	237.21	-1.39		0.56	
4.3.2002	-8.57	8.57	245.79	-7.07		0.58	
5.3.2002	-9.24	9.24	255.03	-7.74		0.60	
6.3.2002	-6.11	6.11	261.14	-4.61		0.61	
7.3.2002	-7.02	7.02	268.16	-5.52		0.62	
8.3.2002	-5.12	5.12	273.28	-3.62		0.63	
9.3.2002	-6.16	6.16	279.44	-4.66		0.64	
10.3.2002	-3.37	3.37	282.81	-1.87		0.64	
11.3.2002	-4.13	4.13	286.94	-2.63		0.65	
12.3.2002	-2.64	2.64	289.58	-1.14		0.66	
13.3.2002	0.79	-0.79	288.79	2.29		0.65	
14.3.2002	0.09	-0.09	288.70	1.59		0.65	
15.3.2002	1.51	-1.51	287.19	3.01		0.65	
16.3.2002	-2.47	2.47	289.66	-0.97		0.66	
17.3.2002	-4.59	4.59	294.24	-3.09		0.66	
18.3.2002	-7.17	7.17	301.41	-5.67		0.68	
19.3.2002	-9.42	9.42	310.83	-7.92		0.69	
20.3.2002	-4.47	4.47	315.30	-2.97		0.70	
21.3.2002	-0.90	0.90	316.20	0.60	0.60	0.70	START THAW
22.3.2002	2.76	-2.76	313.44	4.26	4.86	0.70	ONSET SLR
23.3.2002	4.36	-4.36	309.08	5.86	10.73	0.69	
24.3.2002	3.05	-3.05	306.02	4.55	15.28	0.68	
25.3.2002	0.93	-0.93	305.10	2.43	17.71	0.68	
26.3.2002	-1.24	1.24	306.33	0.27	17.97	0.68	
27.3.2002	-1.92	1.92	308.25	-0.42	17.55	0.69	$T_{ref}$ calculated
28.3.2002	-1.28	1.28	309.53	0.22	17.77	0.69	
29.3.2002	2.14	-2.14		3.64	21.41		
30.3.2002	1.86	-1.86		3.36	24.77		
31.3.2002	2.06	-2.06		3.56	28.33		
1.4.2002	0.98	-0.98		2.48	30.81		
2.4.2002	2.32	-2.32		3.82	34.63		
3.4.2002	3.43	-3.43		4.93	39.56		Minimum 2 weeks
4.4.2002	1.37	-1.37		2.87	42.43		
5.4.2002	1.68	-1.68		3.18	45.61		Eq. 5.4, remove.
6.4.2002	4.55	-4.55		6.05	51.66		
7.4.2002	2.35	-2.35		3.85	55.51		REMOVAL SLR
8.4.2002	2.73	-2.73		4.23	59.74		
9.4.2002	3.38	-3.38		4.88	64.61		
10.4.2002	-0.32	0.32		1.18	65.79		
11.4.2002	-2.54	2.54		-1.04	64.76		
12.4.2002	0.26	-0.26		1.76	66.52		
13.4.2002	0.26	-0.26		1.76	68.28		

Date	Average temperature	0-average temp	FI	Average temp - reference	TI	Frost penetration [m]	Note
14.4.2002	1.10	-1.10		2.60	70.87		
15.4.2002	4.65	-4.65		6.15	77.02		
16.4.2002	6.99	-6.99		8.49	85.51		Eq. 5.7, remove.
17.4.2002	7.61	-7.61		9.11	94.62		Eq. 5.6, remove.
18.4.2002	5.33	-5.33		6.83	101.45		
19.4.2002	4.28	-4.28		5.78	107.22		
20.4.2002	6.08	-6.08		7.58	114.80		Eq. 5.5, remove.
21.4.2002	6.68	-6.68		8.18	122.99		
22.4.2002	3.87	-3.87		5.37	128.35		
23.4.2002	3.29	-3.29		4.79	133.14		
24.4.2002	3.57	-3.57		5.07	138.21		
25.4.2002	-1.17	1.17		0.33	138.54		
26.4.2002	-3.68	3.68		-2.18	136.37		
27.4.2002	-4.14	4.14		-2.64	133.73		
28.4.2002	-3.01	3.01		-1.51	132.22		
29.4.2002	-2.54	2.54		-1.04	131.18		
30.4.2002	-0.22	0.22		1.28	132.46		
1.5.2002	1.22	-1.22		2.72	135.18		
2.5.2002	-0.08	0.08		1.42	136.60		
3.5.2002	1.39	-1.39		2.89	139.49		
4.5.2002	3.81	-3.81		5.31	144.80		
5.5.2002	5.76	-5.76		7.26	152.06		
6.5.2002	6.50	-6.50		8.00	160.07		
7.5.2002	4.44	-4.44		5.94	166.00		
8.5.2002	5.32	-5.32		6.82	172.82		
9.5.2002	4.69	-4.69		6.19	179.01		
10.5.2002	3.02	-3.02		4.52	183.53		
11.5.2002	-0.18	0.18		1.32	184.84		
12.5.2002	-0.26	0.26		1.24	186.08		
13.5.2002	-0.14	0.14		1.36	187.44		
14.5.2002	0.49	-0.49		1.99	189.43		
15.5.2002	2.50	-2.50		4.00	193.43		8 weeks, remove
16.5.2002	6.45	-6.45		7.95	201.38		
17.5.2002	7.14	-7.14		8.64	210.03		
18.5.2002	8.56	-8.56		10.06	220.09		
19.5.2002	4.53	-4.53		6.03			
20.5.2002	5.01	-5.01		6.51			
21.5.2002	6.07	-6.07		7.57			
22.5.2002	7.69	-7.69		9.19			
23.5.2002	5.44	-5.44		6.94			
24.5.2002	8.50	-8.50		10.00			
25.5.2002	6.94	-6.94		8.44			
26.5.2002	5.16	-5.16		6.66			
27.5.2002	6.34	-6.34		7.84			
28.5.2002	7.23	-7.23		8.73			

## Appendix D, Thingvellir Freezing and Thawing indices

Date	Average temperature	0-average temp	FI	Average temp - reference	TI	Frost penetration [m]	Note
1.10.1998	0.11	-0.11		1.99			
2.10.1998	3.39	-3.39		5.26			
3.10.1998	5.19	-5.19		7.06			
4.10.1998	4.81	-4.81		6.69			
5.10.1998	9.41	-9.41		11.29			
6.10.1998	9.65	-9.65		11.52			
7.10.1998	7.80	-7.80		9.67			
8.10.1998	6.45	-6.45		8.32			
9.10.1998	4.68	-4.68		6.55			
10.10.1998	2.58	-2.58		4.45			
11.10.1998	2.68	-2.68		4.55			
12.10.1998	2.79	-2.79		4.66			
13.10.1998	1.66	-1.66		3.54			
14.10.1998	-0.51	0.51	0.51	1.36		-0.29	Early freeze
15.10.1998	-2.39	2.39	2.90	-0.52		-0.23	
16.10.1998	-3.49	3.49	6.39	-1.62		-0.18	
17.10.1998	-5.58	5.58	11.96	-3.70		-0.13	
18.10.1998	-5.49	5.49	17.45	-3.62		-0.09	
19.10.1998	-1.80	1.80	19.25	0.07		-0.07	
20.10.1998	1.30	-1.30	17.95	3.17		-0.08	
21.10.1998	2.33	-2.33	15.63	4.20		-0.10	
22.10.1998	-0.49	0.49	16.11	1.39		-0.10	
23.10.1998	-2.91	2.91	19.03	-1.04		-0.08	
24.10.1998	-3.31	3.31	22.34	-1.44		-0.05	
25.10.1998	-1.95	1.95	24.29	-0.08		-0.04	
26.10.1998	-2.51	2.51	26.80	-0.64		-0.03	
27.10.1998	-0.64	0.64	27.44	1.23		-0.03	
28.10.1998	-0.23	0.23	27.67	1.64		-0.02	
29.10.1998	-1.06	1.06	28.74	0.81		-0.02	
30.10.1998	-1.16	1.16	29.90	0.71		-0.01	
31.10.1998	1.31	-1.31	28.59	3.19		-0.02	
1.11.1998	0.85	-0.85	27.74	2.72		-0.02	
2.11.1998	-0.24	0.24	27.97	1.64		-0.02	
3.11.1998	-4.55	4.55	32.52	-2.68		0.00	
4.11.1998	-2.76	2.76	35.29	-0.89		0.02	
5.11.1998	-7.24	7.24	42.52	-5.37		0.05	
6.11.1998	-4.21	4.21	46.74	-2.34		0.07	
7.11.1998	4.95	-4.95	41.79	6.82	6.82	0.05	Early thaw
8.11.1998	6.59	-6.59		8.46	15.28		
9.11.1998	5.18	-5.18		7.05	22.33		
10.11.1998	1.28	-1.28		3.15	25.48		

Date	Average temperature	0-average temp	FI	Average temp - reference	TI	Frost penetration [m]	Note
11.11.1998	0.65	-0.65		2.52	28.00		
12.11.1998	2.38	-2.38		4.25	32.25		
13.11.1998	1.59	-1.59		3.46	35.71		
14.11.1998	-5.95	5.95		-4.08	31.63		
15.11.1998	-5.54	5.54		-3.67	27.97		
16.11.1998	1.23	-1.23		3.10	31.06		
17.11.1998	4.11	-4.11		5.99	37.05		
18.11.1998	4.54	-4.54		6.41	43.46		
19.11.1998	5.78	-5.78		7.65	51.11		
20.11.1998	5.78	-5.78		7.65	58.75		
21.11.1998	4.49	-4.49		6.36	65.11		
22.11.1998	-3.05	3.05		-1.18	63.94		
23.11.1998	3.84	-3.84		5.71	69.65		
24.11.1998	2.26	-2.26		4.14	73.78		
25.11.1998	-0.55	0.55		1.32	75.10		
26.11.1998	-5.79	5.79		-3.92	71.19		
27.11.1998	4.10	-4.10		5.97	77.16		
28.11.1998	2.80	-2.80		4.67	81.83		
29.11.1998	-2.49	2.49		-0.62			
30.11.1998	4.63	-4.63		6.50			
1.12.1998	2.18	-2.18		4.05			
2.12.1998	0.71	-0.71		2.59			
3.12.1998	-6.10	6.10		-4.23			
4.12.1998	-11.88	11.88		-10.00			
5.12.1998	-0.11	0.11		1.76			
6.12.1998	7.93	-7.93		9.80			
7.12.1998	7.78	-7.78		9.65			
8.12.1998	5.23	-5.23		7.10			
9.12.1998	3.51	-3.51		5.39			
10.12.1998	3.15	-3.15		5.02			
11.12.1998	1.79	-1.79		3.66			
12.12.1998	1.01	-1.01		2.89			
13.12.1998	-2.84	2.84	2.84	-0.97		-0.23	FROST START
14.12.1998	-0.59	0.59	3.43	1.29		-0.22	
15.12.1998	-2.41	2.41	5.84	-0.54		-0.19	
16.12.1998	2.00	-2.00	3.84	3.87		-0.21	
17.12.1998	1.66	-1.66	2.18	3.54		-0.24	
18.12.1998	-4.20	4.20	6.38	-2.33		-0.18	
19.12.1998	-11.46	11.46	17.84	-9.59		-0.08	
20.12.1998	-6.14	6.14	23.98	-4.27		-0.04	
21.12.1998	2.09	-2.09	21.89	3.96		-0.06	
22.12.1998	1.84	-1.84	20.05	3.71		-0.07	
23.12.1998	1.40	-1.40	18.65	3.27		-0.08	
24.12.1998	-1.15	1.15	19.80	0.72		-0.07	
25.12.1998	0.06	-0.06	19.74	1.94		-0.07	

Date	Average temperature	0-average temp	FI	Average temp - reference	TI	Frost penetration [m]	Note
26.12.1998	-1.33	1.33	21.06	0.55		-0.06	
27.12.1998	-8.15	8.15	29.21	-6.28		-0.02	
28.12.1998	0.06	-0.06	29.15	1.94		-0.02	
29.12.1998	2.28	-2.28	26.88	4.15		-0.03	
30.12.1998	4.53	-4.53	22.35	6.40		-0.05	
31.12.1998	3.00	-3.00	19.35	4.87		-0.07	
1.1.1999	2.69	-2.69	16.66	4.56		-0.09	
2.1.1999	5.33	-5.33	11.34	7.20		-0.13	
3.1.1999	3.91	-3.91	7.43	5.79		-0.17	
4.1.1999	-1.04	1.04	8.46	0.84		-0.16	
5.1.1999	-5.36	5.36	13.83	-3.49		-0.11	
6.1.1999	-0.76	0.76	14.59	1.11		-0.11	
7.1.1999	-6.00	6.00	20.59	-4.13		-0.07	
8.1.1999	-5.86	5.86	26.45	-3.99		-0.03	
9.1.1999	-4.61	4.61	31.06	-2.74		-0.01	
10.1.1999	1.49	-1.49	29.58	3.36		-0.01	
11.1.1999	0.03	-0.03	29.55	1.90		-0.01	
12.1.1999	-0.23	0.23	29.78	1.65		-0.01	
13.1.1999	-9.00	9.00	38.78	-7.13		0.03	
14.1.1999	-9.20	9.20	47.98	-7.33		0.07	
15.1.1999	-2.15	2.15	50.13	-0.28		0.08	
16.1.1999	-2.00	2.00	52.13	-0.13		0.09	
17.1.1999	-5.20	5.20	57.33	-3.33		0.11	
18.1.1999	-4.68	4.68	62.00	-2.80		0.13	
19.1.1999	-3.88	3.88	65.88	-2.00		0.14	
20.1.1999	-4.40	4.40	70.28	-2.53		0.16	
21.1.1999	-3.24	3.24	73.51	-1.37		0.17	
22.1.1999	-0.25	0.25	73.76	1.62		0.17	
23.1.1999	1.45	-1.45	72.31	3.32		0.16	
24.1.1999	0.80	-0.80	71.51	2.67		0.16	
25.1.1999	1.24	-1.24	70.28	3.11		0.16	
26.1.1999	-5.39	5.39	75.66	-3.52		0.17	
27.1.1999	1.55	-1.55	74.11	3.42		0.17	
28.1.1999	-1.15	1.15	75.26	0.72		0.17	
29.1.1999	3.10	-3.10	72.16	4.97		0.16	
30.1.1999	1.59	-1.59	70.58	3.46		0.16	
31.1.1999	4.94	-4.94	65.64	6.81		0.14	
1.2.1999	5.06	-5.06	60.58	6.94		0.12	
2.2.1999	1.23	-1.23	59.35	3.10		0.12	
3.2.1999	-1.83	1.83	61.18	0.05		0.12	
4.2.1999	-5.45	5.45	66.63	-3.58		0.14	
5.2.1999	-8.16	8.16	74.79	-6.29		0.17	
6.2.1999	-9.70	9.70	84.49	-7.83		0.20	
7.2.1999	-10.49	10.49	94.98	-8.62		0.24	
8.2.1999	-12.75	12.75	107.73	-10.88		0.27	

Date	Average temperature	0-average temp	FI	Average temp - reference	TI	Frost penetration [m]	Note
9.2.1999	-7.25	7.25	114.98	-5.38		0.29	
10.2.1999	-0.61	0.61	115.59	1.26		0.29	
11.2.1999	3.70	-3.70	111.89	5.57		0.28	
12.2.1999	2.43	-2.43	109.46	4.30		0.28	
13.2.1999	1.10	-1.10	108.36	2.97		0.27	
14.2.1999	-0.83	0.83	109.19	1.05		0.28	
15.2.1999	-2.93	2.93	112.11	-1.05		0.28	
16.2.1999	-8.76	8.76	120.88	-6.89		0.31	
17.2.1999	-6.73	6.73	127.60	-4.85		0.32	
18.2.1999	-1.20	1.20	128.80	0.67		0.33	
19.2.1999	-6.88	6.88	135.68	-5.00		0.35	
20.2.1999	-4.71	4.71	140.39	-2.84		0.36	
21.2.1999	-3.53	3.53	143.91	-1.65		0.37	
22.2.1999	-7.04	7.04	150.95	-5.17		0.38	
23.2.1999	-0.73	0.73	151.68	1.15		0.38	
24.2.1999	3.08	-3.08	148.60	4.95		0.38	
25.2.1999	0.40	-0.40	148.20	2.27		0.38	
26.2.1999	-2.88	2.88	151.08	-1.00		0.38	
27.2.1999	-1.85	1.85	152.93	0.02		0.39	
28.2.1999	-6.51	6.51	159.44	-4.64		0.40	
1.3.1999	-9.86	9.86	169.30	-7.99		0.42	
2.3.1999	-1.65	1.65	170.95	0.22		0.43	
3.3.1999	-3.86	3.86	174.81	-1.99		0.44	
4.3.1999	-4.55	4.55	179.36	-2.68		0.45	
5.3.1999	-8.06	8.06	187.43	-6.19		0.46	
6.3.1999	-3.21	3.21	190.64	-1.34		0.47	
7.3.1999	-1.58	1.58	192.21	0.30		0.47	
8.3.1999	-8.71	8.71	200.93	-6.84		0.49	
9.3.1999	-6.85	6.85	207.78	-4.98		0.51	
10.3.1999	-7.43	7.43	215.20	-5.55		0.52	
11.3.1999	-2.13	2.13	217.33	-0.25		0.52	
12.3.1999	1.84	-1.84	215.49	3.71		0.52	
13.3.1999	-0.89	0.89	216.38	0.99		0.52	
14.3.1999	-2.76	2.76	219.14	-0.89		0.53	
15.3.1999	-2.98	2.98	222.11	-1.10		0.53	
16.3.1999	-5.86	5.86	227.98	-3.99		0.54	
17.3.1999	-0.01	0.01	227.99	1.86		0.54	
18.3.1999	-4.15	4.15	232.14	-2.28		0.55	
19.3.1999	-4.79	4.79	236.93	-2.92		0.56	
20.3.1999	0.51	-0.51	236.41	2.39		0.56	
21.3.1999	-3.31	3.31	239.73	-1.44		0.57	
22.3.1999	-2.30	2.30	242.03	-0.43		0.57	
23.3.1999	-2.09	2.09	244.11	-0.22		0.58	
24.3.1999	-2.10	2.10	246.21	-0.23		0.58	
25.3.1999	-4.41	4.41	250.63	-2.54		0.59	

Date	Average temperature	0-average temp	FI	Average temp - reference	TI	Frost penetrati. [m]	Note
26.3.1999	-0.64	0.64	251.26	1.24		0.59	
27.3.1999	-5.86	5.86	257.13	-3.99		0.60	
28.3.1999	-0.16	0.16	257.29	1.71		0.60	
29.3.1999	0.25	-0.25	257.04	2.12		0.60	
30.3.1999	-5.69	5.69	262.73	-3.82		0.61	
31.3.1999	-7.26	7.26	269.99	-5.39		0.62	
1.4.1999	-6.16	6.16	276.15	-4.29		0.63	
2.4.1999	-3.95	3.95	280.10	-2.08		0.64	
3.4.1999	1.06	-1.06	279.04	2.94	2.94	0.64	THAW STARTS
4.4.1999	5.78	-5.78	273.26	7.65	10.58	0.63	
5.4.1999	7.43	-7.43	265.84	9.30	19.88	0.61	ICERA applies SLR,
6.4.1999	5.80	-5.80	260.04	7.67	27.55	0.60	
7.4.1999	2.65	-2.65	257.39	4.52	32.08	0.60	
8.4.1999	2.88	-2.88	254.51	4.75	36.82	0.59	
9.4.1999	2.31	-2.31	252.20	4.19	41.01	0.59	Eq. 5.4, remove.
10.4.1999	2.11	-2.11	250.09	3.99	44.99	0.59	
11.4.1999	1.20	-1.20	248.89	3.07	48.07	0.58	
12.4.1999	-5.93	5.93	254.81	-4.05	44.01	0.59	
13.4.1999	-5.10	5.10	259.91	-3.23	40.79	0.60	
14.4.1999	-5.50	5.50	265.41	-3.63	37.16	0.61	
15.4.1999	-2.45	2.45	267.86	-0.58	36.58	0.62	
16.4.1999	-5.23	5.23	273.09	-3.35	33.23	0.63	Minimum 2 weeks
17.4.1999	-3.68	3.68	276.76	-1.80	31.43	0.63	Tref calculated
18.4.1999	-2.35	2.35	279.11	-0.48	30.95	0.64	
19.4.1999	4.34	-4.34	274.78	6.21	37.16		
20.4.1999	2.44	-2.44	272.34	4.31	41.47		
21.4.1999	1.00	-1.00	271.34	2.87	44.34		
22.4.1999	1.36	-1.36	269.98	3.24	47.58		
23.4.1999	1.64	-1.64	268.34	3.51	51.09		
24.4.1999	3.59	-3.59	264.75	5.46	56.55		
25.4.1999	6.60	-6.60	258.15	8.47	65.02		
26.4.1999	6.31	-6.31	251.84	8.19	73.20		
27.4.1999	7.01	-7.01	244.83	8.89	82.09		Eq. 5.6 & 5.7, remove.
28.4.1999	3.65	-3.65	241.18	5.52	87.61		
29.4.1999	3.76	-3.76	237.41	5.64	93.25		
30.4.1999	2.94	-2.94	234.48	4.81	98.06		
1.5.1999	2.39	-2.39	232.09	4.26	102.32		
2.5.1999	4.29	-4.29	227.80	6.16	108.48		Eq. 5.5, remove.
3.5.1999	4.88	-4.88	222.93	6.75	115.22		
4.5.1999	9.13	-9.13	213.80	11.00	126.22		
5.5.1999	8.83	-8.83	204.98	10.70	136.92		
6.5.1999	8.79	-8.79	196.19	10.66	147.58		

Date	Average temperature	0-average temp	FI	Average temp - reference	TI	Frost penetration [m]	Note
7.5.1999	8.55	-8.55	187.64	10.42	158.00		
8.5.1999	8.83	-8.83	178.81	10.70	168.70		
9.5.1999	5.44	-5.44	173.38	7.31	176.01		
10.5.1999	6.53	-6.53	166.85	8.40	184.41		
11.5.1999	6.61	-6.61		8.49	192.89		
12.5.1999	5.50	-5.50		7.37	200.26		
13.5.1999	5.93	-5.93		7.80	208.06		
14.5.1999	4.98	-4.98		6.85	214.91		
15.5.1999	6.00	-6.00		7.87	222.78		
16.5.1999	7.74	-7.74		9.61	232.39		
17.5.1999	5.96	-5.96		7.84	240.23		
18.5.1999	5.09	-5.09		6.96	247.19		
19.5.1999	6.49	-6.49		8.36	255.55		
20.5.1999	2.65	-2.65		4.52	260.07		
21.5.1999	4.03	-4.03		5.90	265.97		
22.5.1999	4.06	-4.06		5.94	271.90		
23.5.1999	4.06	-4.06		5.94	277.84		
24.5.1999	3.93	-3.93		5.80	283.63		
25.5.1999	5.65	-5.65		7.52	291.16		
26.5.1999	5.93	-5.93		7.80	298.95		Fixed 8 weeks

## Appendix E - Comparison of predicted and measured temperature profiles

Depth [cm]	Day 11 [°C]			Day 20 [°C]			Day 28 [°C]		
	Measured	Predicted	Difference	Measured	Predicted	Difference	Measured	Predicted	Difference
12	1.71	1.93	0.22	1.92	1.57	-0.35	0.23	0.69	0.46
30	1.94	2.38	0.44	1.94	2.08	0.14	1.27	1.25	-0.02
36	2.06	2.50	0.44	1.98	2.22	0.24	1.62	1.43	-0.19
55	2.48	2.86	0.38	2.29	2.57	0.28	2.43	1.94	-0.49
90	2.69	3.56	0.87	2.46	3.12	0.66	2.79	2.78	-0.01
120	2.97	4.01	1.04	2.81	3.47	0.66	2.99	3.20	0.21
	Aver. absolute error		0.57	Aver. absolute error		0.39	Aver. absolute error		0.23
<b>Average error for case 1</b>			<b>0.395 °C</b>	<b>Difference between measured data sets</b>				<b>NA</b>	

Table E- 1: Calculations for average error in case 1 at Dyrastadir

Depth [cm]	Day 11[°C]			Day 20 [°C]			Day 28 [°C]		
	Measured	Predicted	Difference	Measured	Predicted	Difference	Measured	Predicted	Difference
12	-7.62	-5.78	1.84	-0.52	-0.18	0.34	3.41	1.29	-2.12
30	-6.50	-5.55	0.95	-2.05	-1.71	0.34	0.50	0.48	-0.02
36	-5.93	-5.31	0.62	-2.32	-2.07	0.25	-0.27	0.16	0.43
55	-3.95	-4.34	-0.39	-2.44	-2.77	-0.33	-0.61	-0.66	-0.05
90	-1.63	-1.92	-0.29	-1.90	-2.43	-0.53	-0.79	-0.82	-0.03
120	-0.11	-0.43	-0.32	-0.48	-1.28	-0.8	-0.45	-0.74	-0.29
	Aver. absolute error		0.73	Aver. absolute error		0.43	Aver. absolute error		0.49
<b>Average error for case 2</b>			<b>0.55 °C</b>	<b>Difference between measured data sets</b>				<b>0.25 °C</b>	

Table E- 2: Calculations for average error in case 2 at Dyrastadir

Depth [cm]	Day 11 [°C]			Day 20 [°C]			Day 28 [°C]		
	Measured	Predicted	Difference	Measured	Predicted	Difference	Measured	Predicted	Difference
12	-2.40	-1.43	0.97	-0.40	-0.55	-0.15	-3.99	-3.85	0.14
30	-1.47	-0.84	0.63	-0.78	-1.55	-0.77	-3.26	-3.07	0.19
36	-0.74	-0.74	0	-1.22	-1.76	-0.54	-2.17	-2.88	-0.71
55	-1.21	-0.64	0.57	-1.76	-1.97	-0.21	-2.16	-2.41	-0.25
90	0.46	-0.39	-0.85	0.12	-0.89	-1.01	-0.15	-1.23	-1.08
120	1.00	0.15	-0.85	0.68	0.14	-0.54	0.38	-0.06	-0.44
	Aver. absolute error		0.64	Aver. absolute error		0.54	Aver. absolute error		0.47
<b>Average error for case 3</b>			<b>0.55 °C</b>	<b>Difference between measured data sets</b>			<b>0.37 °C</b>		

Table E- 3: Calculations for average error in case 3 at Vatnskard

The Average Absolute error for each day for each case is calculated as following

$$Aver. absolute error = \frac{\sum |\Delta T|}{n} \quad [E- 1]$$

Where:

$\Delta T$  is the difference between predicted and measured temperature value for a certain depth  
n is the number of measured sets, in this case 6 measurements were available.

## Appendix F – various formulas

Basic formulas in geotechnical engineering, the specific gravity and the dry density are relatively well known for gravel and therefore the porosity and void ratio can be calculated from Equations F-1 and F-2.

$$e = \frac{G_s \gamma_w}{\gamma_d} - 1 \quad \text{[F- 2]}$$

$$n = \frac{e}{e+1} \quad \text{[F- 3]}$$

The moisture content for gravel is relatively low, values around 4% are common, if that moisture content is used in Equation F-3 the degree of saturation is 37%.

$$S_r e = G_s w \quad \text{[F- 4]}$$